University of Alberta

Interactions of Dnr1 with the *Drosophila* Initiator Caspases Dredd and Dronc

by

David Alan Primrose ©

A thesis submitted to the Faculty of Graduate Studies and Research
in partial fulfillment of the requirements for the degree of

Master of Science

in

Immunology

Department of *Medical Microbiology and Immunology*

Edmonton, Alberta
Fall 2008

Library and
Archives Canada

Published Heritage
Branch

395 Wellington Street
Ottawa ON K1A 0N4
Canada

Bibliothèque et
Archives Canada

Direction du
Patrimoine de l'édition

395, rue Wellington
Ottawa ON K1A 0N4
Canada

Canada

Abstract

Caspases are essential for metazoan development and survival. Disruptions to caspase regulation can have severe effects ranging from immunological disorders to cancer. Recently, we identified an E3 ubiquitin ligase, Defense Repressor 1 (Dnr1) that impinges on the Imd pathway by regulating Dredd activity. In this study, I characterized Dnr1 regulation of the *Drosophila* initiator caspases Dredd and Dronc. Dredd is critical for an innate immune response to gram-negative bacterial infection through the Immune Deficiency (Imd) pathway and Dronc is critical in the apoptotic cascade. I demonstrate that Dnr1 regulates Dredd activity, at least partially, by mediating Dredd depletion in *Drosophila* S2 cells. Additionally, I show that the overexpression of Dnr1 inhibits signaling downstream of Dredd in the Imd pathway, which results in decreased antimicrobial peptide induction and decreased JNK phosphorylation. Furthermore, I demonstrate that depletion of Dnr1 results in elevated Dronc protein levels and increased caspase activation upon induction of apoptosis. Conversely, the overexpression of Dnr1 inhibited the apoptotic pathway by mediating the destruction of Dronc.

Acknowledgements

I am truly grateful to all those who have supported me throughout my Master's program.

First and foremost, I would like to thank my supervisor, Dr. Edan Foley, who shared with me his expertise and research insight. It was his guidance and support that shaped my research project from initial conception to the completion of my thesis.

I would like to thank my committee members, Dr. Hanne Ostergaard and Dr. Andrew Simmonds for taking the time to work with me during this endeavor. I did my best to draw on their constructive criticisms and guidance at my committee meetings.

I would like to thank all the members of the Foley lab for their help. David Bond, Sidharth Chaudhry, Silvia Guntermann, Tanja Hinck, George Johnson, Brendon Parsons, and Anja Schindler who provided me with good conversation. These conservations that ranged from scientific discussions and problems with experiments to life in general helped me survive the journey through grad school and come out the other end with an MSc. I would also like to thank Derly Benitez our lab technician.

I am tempted to individually thank all of my friends, who gave me their support and encouragement during these last three years. However, because the list might be too long and I fear leaving someone out, I will simply say thanks very much to all, from those I just meet to those I have known since the T5E.

Finally, I would like to thank my family; Mom, Dad, Nanny, Jacquelyn, Stuart, Lindsay and Morgan. Your love, understanding and encouragement has been an invaluable asset to me over the last three years. To Tessa, I want to thank-you for coming into my life and being there for me as I finished up my Master's program. Your love and support has helped me complete this journey and maintain my sanity.

Table of Contents

1   **Introduction**

2   <u>Materials and Methods</u>

3   <u>Results</u>

List of Tables

List of Figures

Abbreviations

ATP	Adenosine triphosphate
att	*attacin*
BIR	Baculovirus IAP Repeat
Bsk	Basket
CARD	Caspase Activation and Recruitment Domain
Caspase	Cysteinyl aspartate-specific proteinase
CyO	Curly Oster
DAP	diaminopimelic acid
DDAB	Dimethyl dioctadecyl ammonium bromide
DED	Death Effector Domain
dIAP1	Drosophila Inhibitor of Apoptosis 1
DID	Death Inducing Domain
dipt	*diptericin*
DNA	Deoxyribonucleic acid
Dnr1	Defense repressor 1
dsRNA	double stranded RNA
ey	*eyeless*
FADD	Fas-associated Death Domain
FERM	4.1, Ezrin, Radixin, Moesin
g	Gravity
HA	Hemagglutinin

Hid	Head involution Defective
IAP	Inhibitor of Apoptosis
ICE	Interleukin-1β-converting enzyme
I-kB	Inhibitor of κB
I-kK	Inhibitor of κB Kinase
Imd	Immune deficiency
JNK	Jun N-terminal Kinase
Jra	Jun related antigen
LPS	Lipopolysaccharides
LR	Left Right
mg	Milligram
MIR	Myosin Regulatory Light Chain Interacting protein
mL	Milliliter
mM	Millimolar
NF-κB	Nuclear Factor Kappa B
ng	nanogram
NGS	Normal Goat Serum
NLS	Nuclear Localization Signal
PAMP	Pathogen Associated Molecular Pattern
PBS	Phosphate Buffered Saline
PGN	Peptidoglycan
PGRP	Peptidoglycan Recognition Protein
PRR	Pathogen Recognition Receptors

Rel	Relish
RING	Really Interesting New Gene
RIP	Receptor Interacting Protein
RNA	Ribonucleic acid
RNAi	Ribonucleic acid interference
Rpr	Reaper
Sco	Scutoid
SDS-PAGE	Sodium dodecyl sulfate polyacrylamide gel electrophoresis
TNF	Tumor Necrosis Factor
TNFR	Tumor Necrosis Factor Receptor
TRADD	TNFR1-Associated Death Domain protein
TRAF2	TNFR Associated Factor 2
UAS	Upstream Activation Sequence
μg	Microgram
μL	Microliter
μM	Micromolar

Chapter 1

Introduction

1.1 Innate Immune Signaling and *Drosophila*

All metazoans rely on elaborate immune systems to counter the numerous microbial assaults that threaten their survival. Immune systems are comprised of two distinct parts; the innate immune system and the adaptive immune system.

The innate immune system relies on a limited number of non-rearranging, germ-line encoded genes to activate antimicrobial defenses. It is the first line of defense against invading microorganisms in higher eukaryotes and is the only recognizable immune system in most metazoans[1-3]. In contrast to the innate immune system, the adaptive immune system is characterized by clonal selection of a large repertoire of immunoglobulins and T-cell receptors that are produced through the random rearrangement of gene segments. The numerous immunoglobulins and T-cell receptors recognize a vast array of microbial antigens and small molecules and elicit an appropriate immune response. The adaptive immune system is involved in the elimination of pathogens in the late phase of infection and is capable of immunological memory, which results in faster responses to secondary infections from the same organism.

The study of adaptive immunity has been at the forefront of immunological research for many years. However, adaptive immune systems are restricted to jawed vertebrates. In contrast, there is an estimated five to ten million species of metazoans that rely solely on an innate immune system to cope with invading microorganisms[4].

In addition, innate immune signaling plays a critical instructive role in the progression of adaptive immune responses in higher organisms by orientating the effector mechanisms of the adaptive responses[5, 6]. Thus, there is a clear need to understand innate immune signaling pathways.

Innate immune signaling involves three distinct steps: detection of a pathogen, activation of a signal transduction cascade, and the mounting of an appropriate response. In the first step, pathogen recognition receptors (PRR) recognize conserved pathogen associated molecular patterns (PAMPs) such as lipopolysaccharides (LPS), petidoglycans, and β-1,3-glucans, which are absent in the host but present in the pathogens[4, 7, 8]. Recognition of a PAMP by a PRR results in the rapid activation of appropriate signaling modules. The activation of the signaling modules leads to the transcription of a wide rage of host defense genes, including various cytokines and anti-microbial peptides.

Drosophila has evolved as a highly attractive model for the study of innate immunity over the past decade[9]. *Drosophila* lacks an adaptive immune response and relies solely on innate immune signaling pathways. Discoveries in *Drosophila* innate immune signaling are directly relevant to human medicine as these pathways share significant homology with higher vertebrates. In addition, the fully sequenced genome and the availability of powerful molecular genetic techniques makes *Drosophila* an ideal organism to study innate immune signaling[10]. In *Drosophila,* microbial infections induce the synthesis of seven antimicrobial peptides by cells in the fat body, which is functionally similar to the mammalian liver[11-15]. The production of antimicrobial peptides is controlled by two distinct signaling pathways, the Toll pathway and the Immune

2

Deficiency (Imd) pathway, which are activated in response to different classes of microbes[16].

The Toll pathway mediates appropriate cellular responses to infection with fungi and gram-positive bacteria[17]. It was the discovery of the Toll pathways involvement in antifungal defense in *Drosophila* that raised interest in *Drosophila* as a model for the study of innate immune signaling. The Toll pathway was originally identified and characterized for its role in the establishment of dorsal-ventral polarity in the *Drosophila* embryo[18]. However, similarities of pathway components to genes involved in mammalian immunity prompted the hallmark studies that determined the Toll pathway is a central mediator of antifungal and gram-positive bacterial defenses in *Drosophila*[19-21]. The results of these studies prompted the search for and subsequent identification of mammalian Toll homologs, which was a major advancement in our understanding of innate immunity in mammals[22-24]. Numerous studies have now identified similarities between *Drosophila* and mammals at the level of signal transduction[25, 26].

1.2 Imd/TNF Pathways

The Imd pathway of *Drosophila* is primarily involved in defense against gram-negative bacteria[27]. The Imd pathway shares similarities to the mammalian Tumor Necrosis Factor (TNF) pathway (Figure 1.1). However, there are several differences between these two pathways, particularly at the level of receptor/ligand interaction and the downstream transcriptional response. The TNF pathway is activated through binding of the TNF cytokine to the TNF receptor (TNFR), resulting in TNFR trimerization. The TNFR then recruits the TNFR1-Associated Death Domain protein (TRADD),

which subsequently recruits the Receptor Interacting Protein (RIP) and TNFR Associated Factor 2 (TRAF2).

Formation of the TNFR/TRADD/RIP/TRAF2 complex at the membrane subsequently leads to the activation of the c-Jun N-terminal Kinase (JNK) signaling cassette and activation of the Inhibitor of Kappa B Kinase (I-κK) complex. JNK phosphorylates specific subunits, including c-Jun, JunB, JunD, and ATF-2, of the AP-1 transcription factor, turning on genes that control diverse cellular functions including proliferation, differentiation, and apoptosis[28]. The active I-κK complex is required to activate the transcription factor Nuclear Factor Kappa B (NF-κB). In unstimulated cells, the Inhibitor of κB (I-κB) proteins bind to NF-κB dimers and mask its Nuclear Localization Signal (NLS), thus retaining NF-κB in the cytoplasm[29]. Active I-κK phosphorylates I-κB, which results in the subsequent ubiquitination and proteasomal degradation of I-κB[30, 31]. Degradation of I-κB unmasks the NF-κB NLS, allowing NF-κB to translocate to the nucleus where it promotes the transcription of various pro-survival genes, which include transcripts that block apoptosis[32-35]. The balance between JNK signaling and NF-κB signaling determines the fate of the cell. Prolonged activation of the JNK pathway induces apoptosis, whereas a robust NF-κB response commits a cell to survival[36]. In cells committed to die, caspase-8 is the central mediator of apoptosis. Pro-caspase-8 is recruited by Fas-associated Death Domain (FADD) into a complex with RIP/TRAF2/TRADD/FADD[37-39]. Aggregation of pro-caspase-8 leads to its auto-activation and subsequent activation of effector caspases such as caspase-3, resulting in apoptosis[40]. However, dominant NF-κB-responsive transcripts that block apoptosis normally inhibit caspase-8 activation and the induction of apoptosis.

4

In contrast to the mammalian TNF pathway, the Imd pathway is activated by peptidoglycan recognition proteins (PGRP)[41-44]. Imd signaling is initiated by the recognition of diaminopimelic acid-type (DAP-type) peptidoglycan derived from gram-negative bacteria[45-47]. Two *Drosophila* PGRPs, PGRP-LC and PGRP-LE are involved in DAP-type peptidoglycan recognition[48, 49]. PGRP-LC encodes a protein with an N-terminal cytoplasmic domain, a transmembrane domain and a C-terminal extracellular domain that contains three PGRP domains[43]. In contrast, PGRP-LE does not contain a transmembrane domain and is predicted to be an intracellular PGRP[50]. Additionally, the PGRP domain of endogenous PRGP-LE (PGRP-LE[pg]) resides outside the cell in the hemolymph (insect blood). PGRP-LE[pg] activates Imd signaling in a non-cell-autonomous way, however this activation is dependent on the surface expression of PGRP-LC[51]. Further studies suggested that PGRP-LE[pg] functions in a CD14-like way by binding DAP-type peptidoglycan and carrying it to the cell surface where it interacts with PGRP-LC to induce signal transduction[51, 52].

Although the exact mechanisms by which signaling occurs downstream of PGRP-LC and –LE are not fully understood, genetic experiments suggest that the *Drosophila* Imd (mammalian RIP homolog) protein is immediately downstream of PGRP-LC and –LE [27, 52-54]. Imd serves as a platform to initiate intracellular signaling and contains an apparent 80-residue death domain that shares marked sequence similarity to the death domain of the mouse and human RIPs[54]. Upon immune challenge, Imd recruits the death domain containing adaptor dFADD (FADD homolog) which in turn interacts with the initiator caspase Dredd (caspase-8 homolog)[55-58]. The receptor proximal complex of Imd, dFADD and Dredd are required to activate the map kinase kinase kinase

(MAP3K) dTAK1 (TAK1 homolog)[59]. Two additional genes, dTAB2 (TAB2 homolog) and dIAP2, are also involved in dTAK1 activation. dTAB2 is a required component of the Imd pathway and binds dTAK1 and may regulate dTAK1 activity[60-62]. dIAP2 is required for a sustained Imd response and acts downstream of Imd, but upstream of or at the same level of dTAK1[61, 63, 64]. The Imd pathway bifurcates at the level of dTAK1 resulting in the activation of the JNK signaling cassette and the I-κK complex[59, 65-67].

Activation of the JNK pathway by dTAK1 results in immediate and transient phosphorylation of Basket (Bsk, JNK ortholog)[68]. Bsk, in turn, phosphorylates and triggers the nuclear translocation of Jra (Jun ortholog), which forms a heterodimer with Kayak (Fos ortholog) in the nucleus[69]. The Jra/Kayak heterodimer constitute the AP-1 transcription factor that initiates the transcription of a subset of immune response genes, primarily thought to be involved in wound repair and stress responses[65, 69-71].

The active IKK complex, which is comprised of Immune Response Deficient 5 (Ird5, IKKβ homologue) and *kenny* (IKKγ homolog) phosphorylates the p105 homolog Relish (Rel)[72-75]. Rel is a dual-domain protein that contains an N-terminal Rel homology domain and a C-terminal Iκ-B domain with six ankyrin repeats[76]. Phosphorylated Relish is a substrate for protelytic cleavage, which results in the separation of the Iκ-B domain from the N-terminal Rel domain[74]. While the exact mechanism of Relish cleavage remains to be determined, the *Drosophila* initiator caspase Dredd is require for Relish cleavage and cleavage occurs at a classical caspase consensus sequence [75, 77]. Upon proteolytic cleavage, the Iκ-B domain remains in the cytoplasm and the N-terminal Rel domain translocates to the nucleus[77]. Nuclear Rel is involved in the transcription of

numerous genes, including those that encode the anti-microbial peptides *attacin* (*att*) and *diptericin* (*dipt*)[77].

The initiator caspase Dredd is a key regulator of the Imd pathway. Dredd is involved both upstream of dTAK1 activation and downstream of IKK in the cleavage of Relish[75, 77, 78]. While the exact mechanism of Dredd activity in the Imd pathway remains to be elucidated, loss of Dredd results in the loss of JNK phosphorylation and the loss of anti-microbial peptide transcription by Relish[58, 78]. The role of caspases in immune signaling is not unique to *Drosophila,* as caspase-8 is required for lymphocyte activation in humans and mice[79, 80].
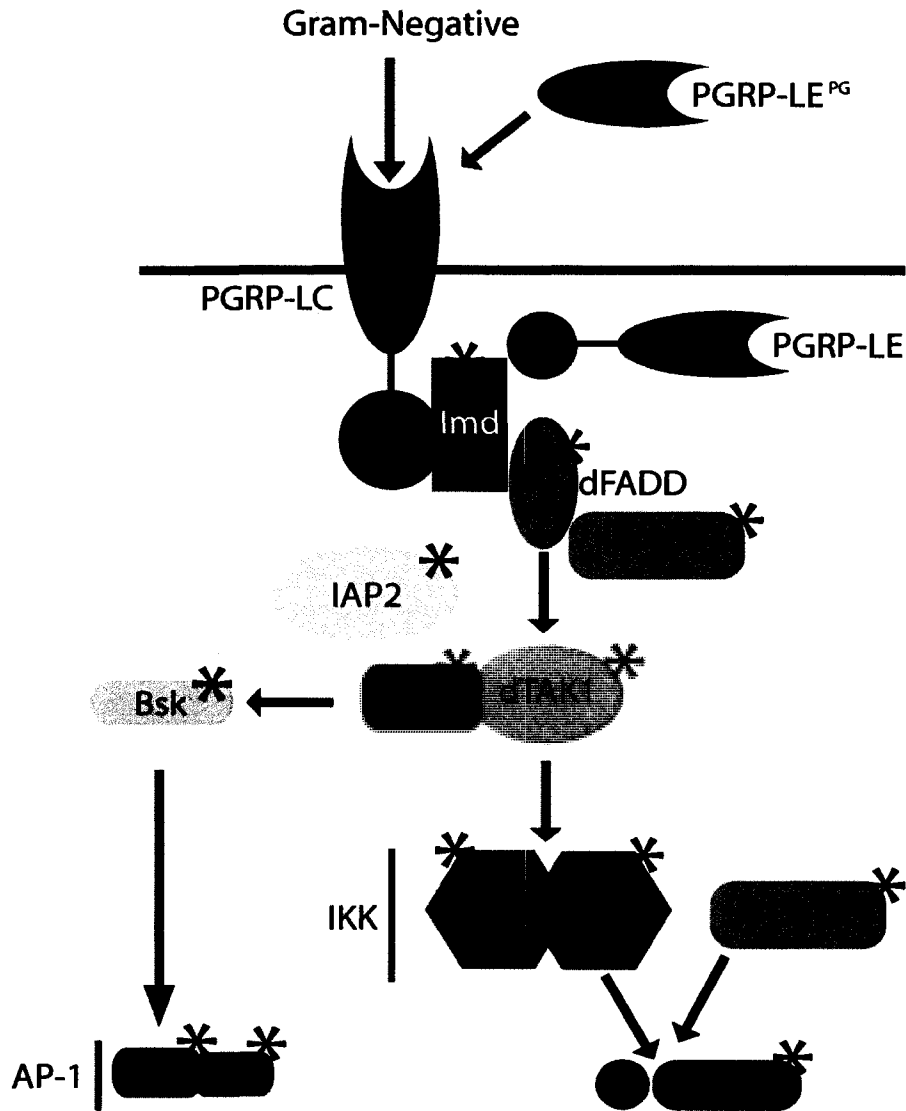
Figure 1.1: Schematic representation of the *Drosophila* Imd pathway. Activation of the Imd pathway is initiated by the recognition of DAP-type peptidoglycan by PGRP-LC or PGRP-LE. Signaling proceeds through the receptor proximal complex of Imd / dFADD / Dredd, which activates dTAK1. At the level of dTAK1 the Imd pathway bifurcates with the activation of the JNK signaling cassette and the IκK-complex. Activation of JNK signaling results in JNK (Basket) dependent phosphorylation of Jra, which partners with Kayak in the nucleus to initiate transcription of a subset of immune response genes. The active I-κK complex phosphorylates Relish, which results in the cleavage and concomitant nuclear translocation of Rel. Nuclear Rel drives the transcription of genes encoding anti-microbial peptides. * represents homologs of genes involved in the mammalian TNF pathway.

1.3 Caspases

Caspases derive their name from their function as cysteinyl aspartate-specific proteinases, which cleave their target proteins after an aspartic acid residue[81, 82]. Most identified caspases contain the active site consensus sequence, QACR/QG, where the cysteine residue is required for caspase proteolytic activity. The first known caspase family member was caspase-1, originally know as interleukin-1β-converting enzyme (ICE), which functions in monocytes as a mediator of inflammation[83, 84]. However, work in the model organism *Caenorhabditis elegans* revealed a role for caspases in apoptosis[83, 84]. Caspases are now recognized as essential mediators of apoptosis across a wide range of organisms[85].

Caspases are synthesized as inactive zymogen precursors (referred to as procaspase) comprised of a prodomain, followed by a large (p20) and small (p10) catalytic subunit[86]. Typically, caspases are divided into two general classes: initiator and effector. Initiator caspases are characterized by the presence of long N-terminal prodomains that typically contain death domains or Caspase Activation and Recruitment Domains (CARD), whereas effector caspases are characterized by short or absent N-terminal prodomains. Activation of initiator caspases occurs through autoprocessing after their recruitment into large protein complexes, such as the apoptosome. Activated initiator caspases in turn activate effector caspases through a cleavage that separates the large and small subunit of the effector caspase[87]. Upon cleavage caspases reassemble as active heterotetramers, which consists of two large and two small catalytic subunits. Once active, effector caspases are responsible for the proteolytic cleavage of a wide range of cellular substrates[88].

1.4 *Drosophila* Caspases

The *Drosophila* genome encodes three putative initiator caspases, Dredd, Strica and Dronc and four putative effector caspases, Drice, Dcp-1, Decay and Damm[89-95] (Figure 1.2). Dredd is typically considered a caspase-8 homolog, due to mild similarities to mammalian caspase-8 (25% identity)[91]. However, unlike other caspase-8 homologs, Dredd does not contain Death Effector Domains (DED) that mediate caspase-8-FADD interactions[96]. Instead Dredd interacts with dFADD via uncharacterized N-terminal Death-Inducing Domains (DID)[56]. Additionally, the sequence surrounding the catalytic cysteine of Dredd does not conform to the established caspase active site consensus sequence. Unlike all caspase-8 homologs described so far, Dredd bears a glutamic acid residue (QACQ*E*) at a position normally occupied by glycine[91]. While mammalian caspase-8 has dual roles in apoptosis and NF-κB activation, Dredd is essential for innate immune responses through the Imd pathway[97, 98].

Dredd mutants fail to express Imd-responsive antimicrobial gene products and display reduced viability upon infection with gram-negative bacteria[58]. Conversely, overexpression of Dredd in uninfected flies mimics activation of the Imd pathway, as characterized by the ectopic production of signature antimicrobial peptides[59]. Thus, Dredd activity is critical for Imd-dependent gram-negative bacterial defenses.

Strica bears a long N-terminal pro-domain, however it does not contain any known protein-protein interaction motifs but instead has a novel, serine/threonine-rich prodomain[90]. A phylogenetic analysis also revealed Strica clusters with effector caspases[99]. Strica is required for Hid induced apoptosis and is involved in several facets of developmental apoptosis, however the proteins that might mediate Strica activation

have not been identified[100, 101]. In contrast to Dredd and Strica, the initiator caspase Dronc

appears to be a classical apical caspase and is the key upstream caspase in the *Drosophila*

apoptotic cascade[89, 102, 103]. The Dronc prodomain contains caspase activation and

recruitment domains (CARD) which mediate the formation of the Dronc-Dark

(Apaf1 homolog) complex required for Dronc activation[104, 105]. Active Dronc substrates

include the effector caspases Drice and Dcp-1, both of which function in the apoptotic

cascade[106, 107]. In addition to Drice and Dcp-1, there is some evidence the other two

Drosophila effector caspases Decay and Damm may play a role in apoptosis [94, 108].
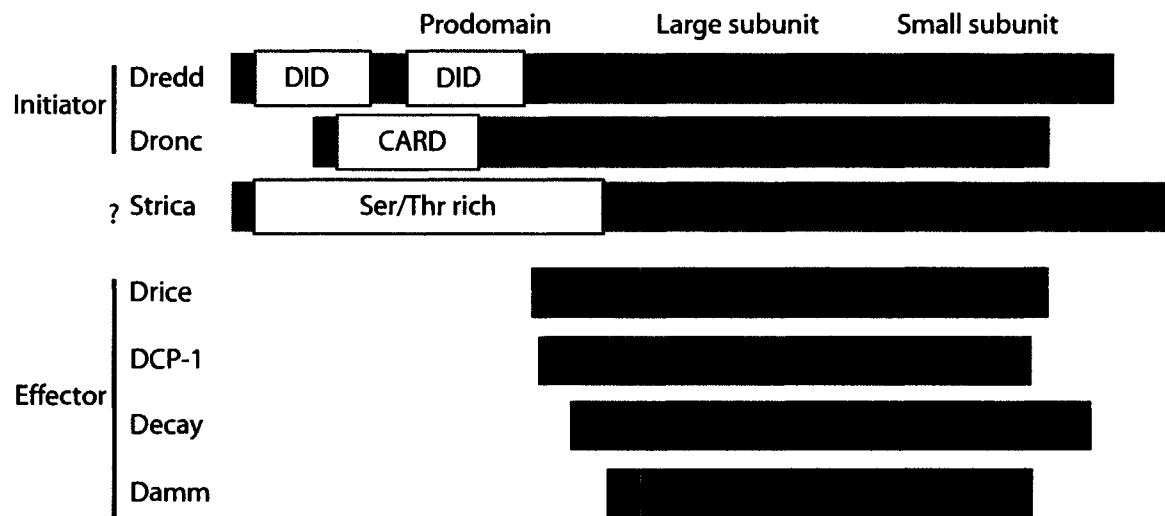
Figure 1.2: Schematic representation of the *Drosophila* caspases. All *Drosophila* caspases are composed of a pro-domain and a large and small catalytic subunit of variable size. The pro-domains of the initiator caspases are longer than the effector caspases and contain domains required for protein-protein interactions. Dredd contains two Death inducing domains (DID), Dronc contains a Caspase Activation and Recruitment domain (CARD) and Strica has a Ser/Thr-rich pro-domain.

1.5 Caspase-Dependent Apoptosis

Apoptosis is a genetically controlled form of cell death that is an important feature of animal development and homeostasis[109]. Apoptosis contributes to the formation of adult structures during development and is essential for the removal of pre-cancerous or virally infected cells and the negative selection of self-reactive lymphocytes[110, 111]. Loss of apoptotic regulation is also linked to debilitating disorders such as Cancer and Alzheimer's[112, 113].

In mammals, the intrinsic apoptotic cascade is initiated by the release of Cytochrome c from mitochondria into the cytoplasm (Figure 1.3 a). In the cytoplasm, Cytochrome c acts as a co-factor and promotes the oligomerization of the adaptor protein Apaf-1[114, 115]. Apaf-1 in turn recruits the proCaspase-9 to form the apoptosome, which promotes caspase-9 dimerization and activation[116]. Active caspase-9 is a target for XIAP, which inhibits caspase-9 through binding. XIAP-dependent caspase-9 inhibition is relieved by the pro-apoptotic molecule Smac, which is released from mitochondria[117]. Released from XIAP, active Caspase-9 propagates a proteolytic cascade, leading to the cleavage and activation of the effector caspases 3 and 7[118]. The effector caspases cleave cellular targets, ultimately leading to cell death[119].

The canonical *Drosophila* apoptotic pathway shares overt similarities with the mammalian intrinsic apoptotic cascade (Figure 1.3 b). Activation of the initiator caspase, Dronc (caspase-9 homolog) is a central step in the induction of apoptosis in *Drosophila*. Dronc activation is regulated by DIAP1 and the H99 cell death locus genes Reaper (Rpr), Head involution Defective (Hid) and Grim[120-124]. DIAP1 is a member of the Inhibitor of Apoptosis family (discussed below) and in the absence of cell death signals, dIAP1 binds

Dronc and prevents Dronc activation[125]. Upon receiving an apoptotic stimulus, *Drosophila* cells up-regulate the transcription of Rpr, Hid and Grim[126]. Rpr, Hid and Grim activate apoptosis through their N-terminal RHG motif[127]. The RHG motif promotes a high affinity interaction with DIAP1, thus relieving DIAP1 inhibition of Dronc[125]. Released from DIAP1 inhibition, Dronc forms a high-molecular-weight complex with the Apaf-1 homolog Dark[128-130]. Formation of the Dark/Dronc apoptosome-like complex results in Dronc auto-processing and activation[104, 105]. Active Dronc cleaves and concomitantly activates the effector caspases Drice and Dcp-1 (caspase-3 and -7 homologs)[106]. The effector caspases usher in apoptosis by the cleavage of downstream target substrates such as nuclear lamins, ICAD and PARP, which results in DNA fragmentation, nuclear contraction, condensation of the cytosol and membrane blebbing[131, 132].
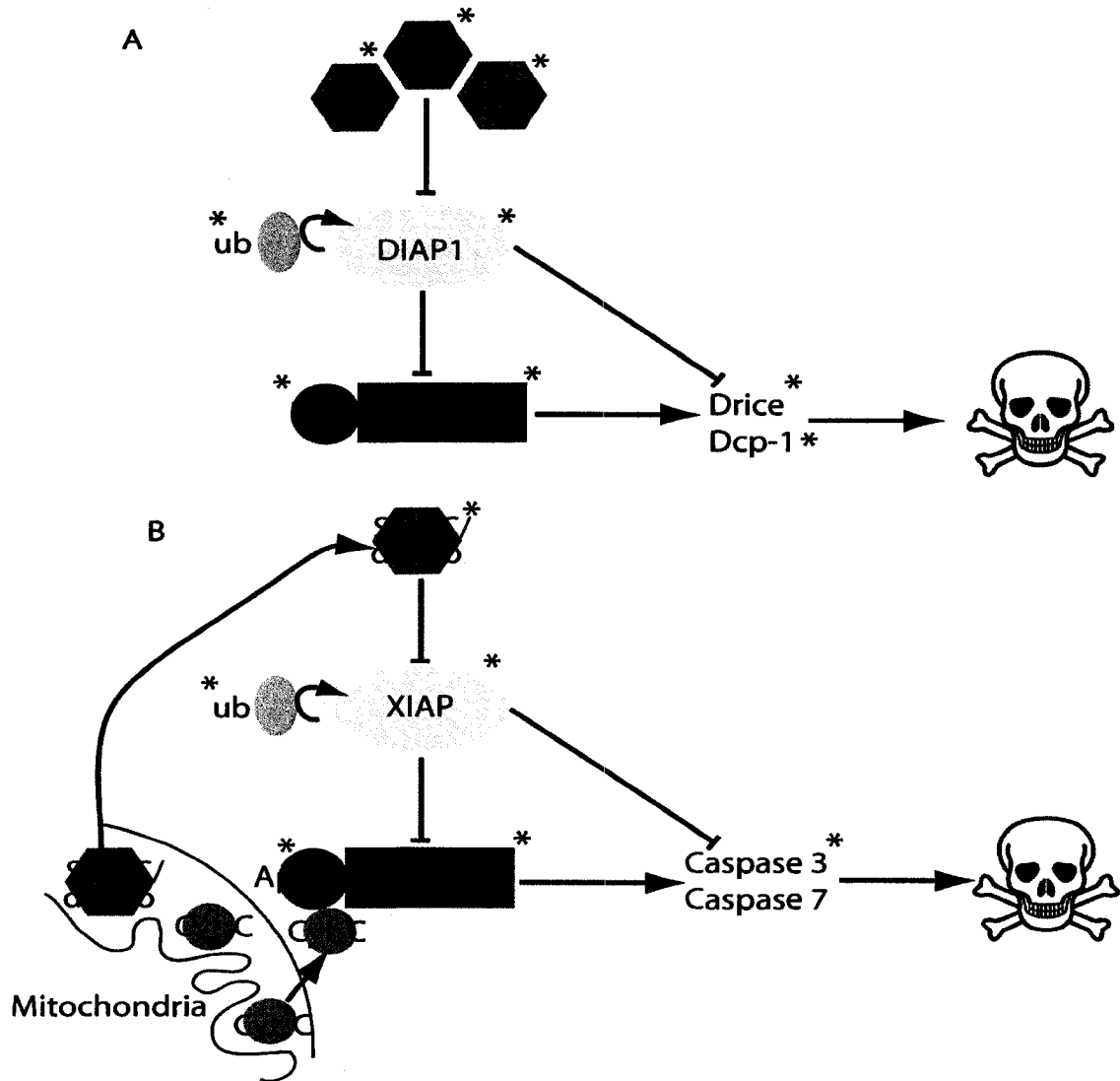
Figure 1.3: Schematic representation of the *Drosophila* and intrinsic mammalian apoptotic cascades. (A) In *Drosophila*, the IAP antagonists Rpr, Hid, and Grim release Dronc from dIAP1 inhibition. Free Dronc then associates with the adaptor protein Dark resulting in Dronc autoprocessing and activation. Active Dronc cleaves and activates the effector caspases Drice and Dcp-1, which cleave downstream cellular targets ushering in apoptosis. (B) In mammals, release of Cytochrome c from the mitochondria initiates apoptosis resulting in caspase-9 activation. Active caspase-9 propagates a proteolytic cascade, leading to the cleavage and activation of the effector caspases 3 and 7 and the induction of apoptosis. * represents conserved genes in these two pathways and homologs are indicated with identical colors. Ubiquitin is indicated with ub.

1.6 Inhibitor of Apoptosis Protein Family

Regulation of caspase activation is crucial to prevent the induction of apoptosis in the absence of a stimulus. The inhibitor of apoptosis protein (IAP) family is a critical regulator of caspase-induced cell death. IAPs were first identified in baculoviruses as novel cell death inhibitors and homologous proteins have since been identified in numerous organisms ranging from yeast to humans[121, 133-135]. The IAP family is defined by the presence of one or more baculovirus IAP repeat (BIR) that mediates IAP-Caspase interactions[86]. However, not all proteins that contain BIR domains are caspase regulators[136]. In addition to the BIR domain, many IAPs contain a C-terminal RING domain, which contributes to caspase inhibition. RING domains are E3 ubiquitin ligases that target substrates for proteasomal degradation via polyubiquitination. RING domain proteins also regulate their own stability through auto-ubiquitination[137]. One of the best-characterized IAPs is *Drosophila* IAP1 (dIAP1), which is an essential regulator of apoptosis[97, 138]. Loss of dIAP1 results in massive apoptosis in both cell culture and the whole animal context[121, 139-142]. DIAP1 inhibits Dronc through the binding and ubiquitination of procaspase-Dronc[143]. DIAP1 also physically interacts with active Drice and Dcp-1 to inhibit their caspase activity[139, 140]. In addition to DIAP1, three other BIR domain proteins (DIAP2, Deterin, and dBRUCE) have been identified in *Drosophila*[121, 138, 144, 145]. Deterin and dBRUCE have both been ascribed roles in the suppression of apoptosis in *Drosophila*[144, 146]. DIAP2, which has three N-terminal BIR domains and a C-terminal RING finger was initially identified as an inhibitor of apoptosis however, the primary role for DIAP2 now appears to be in activation of the Imd pathway[61, 64, 121, 147].

15

1.7 Defense repressor 1

Recently, a genome wide screen identified Defense repressor 1 (Dnr1) as a regulator of the Imd pathway[148] (Figure 1.4). In particular, Dnr1 acted as an inhibitor of Dredd activity in the absence of a microbial insult in S2 cells. Dnr1 depletion in S2 cells resulted in the ectopic expression of a Relish-dependent reporter. The ectopic expression of the Relish reporter was Dredd-dependent, as depletion of Dredd in conjunction with Dnr1 suppressed Relish reporter expression. The genomic sequence for Dnr1 encodes a protein that is 677 amino acids long and has a molecular weight of 73.2 kDa. Analysis of the primary sequence of Dnr1 revealed that Dnr1 has an N-terminal FERM domain, followed by a glutamine/serine-rich region, a FERM_C motif, and a C-terminal RING domain (Figure 1.5).

FERM domains are plasma membrane-binding domains, involved in the linkage of cytoplasmic proteins to the membrane[149]. RING domains are protein interaction domains associated with a wide range of biological activities[150]. One group of RING domain proteins, which feature a set of cysteine and histidine residues that have a distinctive spacing, function as E3 ubiquitin ligases that target a variety of substrates for proteasomal degradation[151]. Analysis of the Dnr1 RING domain revealed extensive similarities to the E3 RING domain found in the IAP family of proteins (Figure 1.6). Similar to E3 RING domain IAPs, Dnr1 is an unstable protein and mutation of a cysteine residue critical for RING domain E3 activity greatly stabilized Dnr1 in S2 cells. Additionally, Imd pathway activity affects Dnr1 protein levels; Dredd activation causes increased Dnr1 levels, whereas inactivation of Dredd resulted in diminished Dnr1 levels.

These data are consistent with a negative feedback loop, where Dredd activation results in the accumulation of its own inhibitor, Dnr1[148].
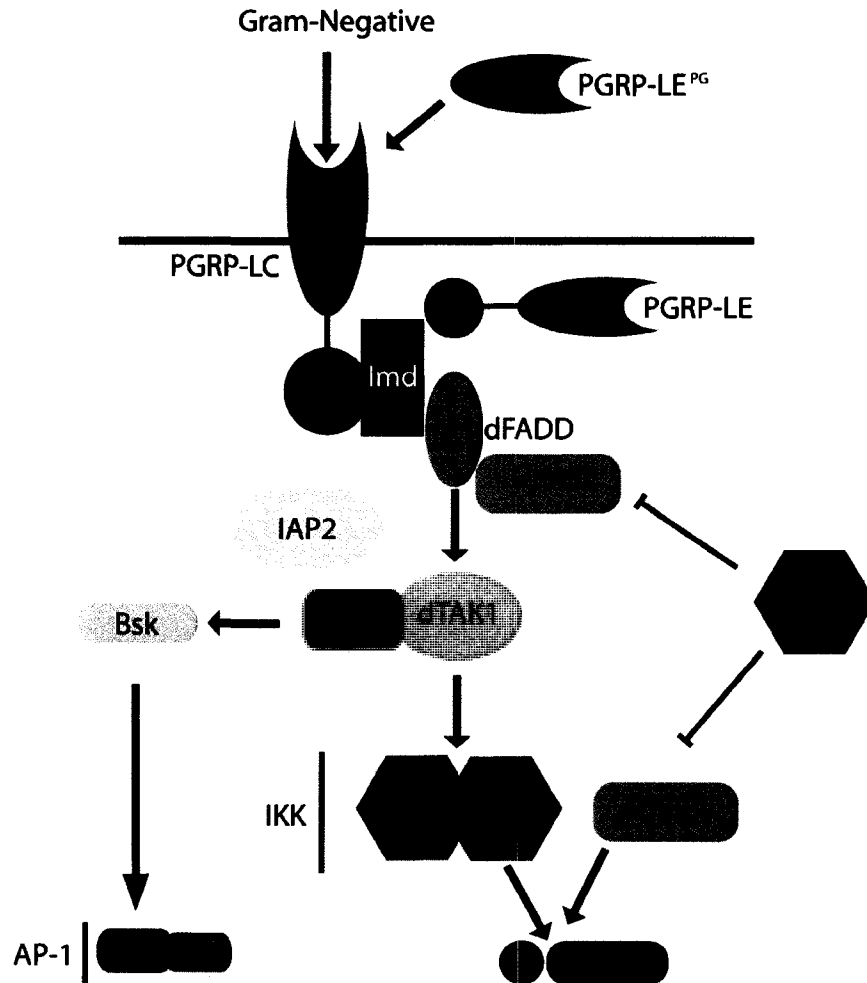
Figure 1.4: Schematic representation of Dnr1 regulation of the *Drosophila* Imd pathway. Dnr1 is proposed to inhibit the Imd pathway at the level of the initiator caspase Dredd. Dnr1 protein levels are regulated by a negative feedback loop, where Dredd activation results in the accumulation of Dnr1.

Figure 1.5: Schematic representation of the domain structure of Dnr1. Dnr1 contains an N-terminal FERM domain, followed by a glutamine/serine-rich regions, a FERM_C motif and a C-terminal RING domain.


```
  **  *    *******  **  ** **  *** *  **      *** **  *   ** **
RISEAMQCKICMDRAINTVFNPCCHVIACAQCAARCSNCPNCRVKITSVVKIYL    CG12489(Dnr1)
RLQEERTCKVVMDREVSIVFIPCGHLVVCRECAPSLRKCPICRGTIKGTVRTFL    DIAP1
RLQEERTCKVCMDREVSIVFIPCGHLVVCRECAPSLRKCPICRGTIKGTVRTFL    IAP2 (RAT)
RLQEERTCKVCMDRAINTVFNPCGHLVVCKECAPSLRKCPICRGMVKGTVRTFL    IAP (FISH)
RLPEERTCKVCMDKEVSIVFIPCGHVVACKDCAPSLRKCPICRSTIKGTVRTFL    IAP-1 (HUMAN)
RLQEERTCKVCMDKEVSIVFIPCGHLVVCKECAPSLRKCPICRGTIKGTVRTFL    IAP-LIKE (CHICKEN)
        CX2C    X9-39   CXH3  CX2C X4-48CX2C               CONSENSUS
```

Figure 1.6: The RING domain of Dnr1 shares similarities to the RING domains of IAP proteins. The RING domain consensus motif is indicated by shading and conserved residues by an asterisk. The arrowhead indicates the catalytic cysteine of the RING domain.

18

HYPOTHESIS

Based on the observations that Dnr1 inhibits the initiator caspase Dredd and contains a RING domain similar to the RING domain of dIAP1, I hypothesized that Dnr1 regulates Dredd activity through the depletion of Dredd protein levels. Additionally, I hypothesized that Dnr1 inhibits the apoptotic cascade by mediating the depletion of Dronc. To test these hypotheses, I determined the role of Dnr1 in regulation of the initiator caspases Dredd and Dronc in the Imd and apoptotic pathways, respectively. Therefore, the research objectives of the work described in this thesis were as follows:

1.8 Research Objectives

1. **Analysis of Dnr1 Regulation of the Imd Signaling Pathway.** To characterize the involvement of Dnr1-dependent regulation of Dredd activity in the Imd pathway, I examined the consequences of Dnr1 overexpression on Imd pathway signaling in S2 cell culture.

2. **Analysis of Dnr1 Regulation of Caspase-Dependent Apoptosis.** To characterize the involvement of Dnr1-dependent regulation of Dronc activity in the apoptotic pathway, I examined the consequences of Dnr1 depletion or overexpression on apoptotic progression in S2 cell culture.

3. **Functional Analysis of Dnr1 Regulation of Dnr1, Dredd and Dronc protein levels.** To elucidate the mechanisms by which Dnr1 regulates Dredd/Dronc protein levels, I examined the requirement of the pro-domain of Dredd/Dronc for Dnr1 mediated-depletion of Dredd/Dronc. I will identify the domains of Dnr1 required for Dnr1-mediated Dronc depletion. Furthermore, I will identify the domains of Dnr1 which contributes to its stability in S2 cells.

Chapter 2

MATERIALS AND METHODS

2.1 S2 Cell Culture

2.1.1 S2 Cell Culture Maintenance

S2 cells were maintained at 25°C in HyQ TNM-FH medium (Gibco) supplemented with 10% heat inactivated fetal calf serum, penicillin and streptomycin in 25 cm^2 flasks. S2 cells were split into new flasks at a 1:5 dilution every 4 or 5 days.

2.1.2 Expression Constructs for S2 cells

The HADnr1 and HADnr1C563Y expression plasmids have been described previously[148]. The Flag-HA-Dredd-myc and Flag-HA-DreddΔPD-myc were generated by David Tran and Edan Foley, respectively. I generated the myc-Dnr1, myc-Dnr1C563Y, myc-Dronc and myc-DroncΔPD expression constructs using the Gateway recombination system. Edan Foley and George Johnson generated all other tagged expression constructs using the Gateway recombination system. Briefly, primer pairs were designed to amplify the gene of interest with the sequence CACC on the 5' end of the forward primer followed by the gene specific sequence in the correct reading frame. The CACC sequence is required to facilitate the directional cloning of the gene of interest into pENTR/D-TOPO vectors (Invitrogen). After PCR amplification of the gene of interest, a TOPO cloning reaction was set up according to the manufacturer's instructions (Invitrogen). The

pENTR/D-TOPO vector is an entry vector that is used to flank the gene of interest with the attL1 and attL2 recombination sites required for recombination into Gateway vectors (Invitrogen, *Drosophila* Gateway vectors purchased from the DGRC). The *Drosophila* Gateway vector collection is a set of Gateway-based vectors designed to express epitope-tagged proteins in *Drosophila* cell culture or flies. The gene of interest in the pENTR/D-TOPO entry vector was recombined into the *Drosophila* Gateway vectors through a LR recombination reaction that was set up according to the manufacturer's instructions (Invitrogen, Gateway LR Clonase II Enzyme Mix). Table 2.1 lists the primers used to generate the individual pENTR/D-TOPO constructs. Table 2.2 lists the Gateway LR recombination reactions, all Gateway vectors had the pA (Actin5c) promoter.

Construct	Forward Primer	Reverse Primer
Dronc	CACCATGCAGCCGCCGGAGCT	TTCGTTGAAAAACCCGGG
DroncΔPD	CACCGTTCTATTGGAATCCGTCG	TTCGTTGAAAAACCCGGG
Dnr1	CACCATGTGGTGCATTGTCAACCTGCC	CTAGGCGGCCGTCGTAACCTTCG
Dnr1$^{142-677}$	CACCGAGTCGTCGCTGAAGGCCGACTGC	CTAGGCGGCCGTCGTAACCTTCG
Dnr1$^{1-531}$	CACCATGTGGTGCATTGTCAACCTGCC	CTACTCACGCGCCTCCTTCTCGC
Dnr1$^{1-433}$	CACCATGTGGTGCATTGTCAACCTGCC	CTACTTGAGATCCCGGGTAAACTG
Dnr1$^{1-397}$	CACCATGTGGTGCATTGTCAACCTGCC	CTACTTGGGCAGCTTGATCTCCAGC
Dnr1$^{324-677}$	CACCTACGGCGAGGAGCTCTTTAGC	CTAGGCGGCCGTCGTAACCTTCG
Dnr1$^{397-677}$	CACCCAGCCGATCGCCGCGGGCC	CTAGGCGGCCGTCGTAACCTTCG
Dredd	CACCATGTCAGCGAGTGCAATTTATCG	TCACAGACGAGGTGG
DreddΔPD	CACCGTGGATAAAGAACGACTAATCG	TCACAGACGAGGTGG

Table 2.1 Primer sequences for TOPO cloning

pENTR/D-TOPO Insert	Gateway Vector	Expression Construct
Dronc	pAMW- N-terminal 6xMyc	6xMyc-Dronc
DroncΔPD	pAMW- N-terminal 6xMyc	6xDroncΔPD
Dnr1	pAMW- N-terminal 6xMyc	6xDnr1
Dnr1C563Y	pAMW- N-terminal 6xMyc	6xDnr1C563Y
Dnr1	pAGW- N-terminal EGFP	GFP-Dnr1
Dnr1$^{142\text{-}677}$	pAGW- N-terminal EGFP	GFP-Dnr1$^{142\text{-}677}$
Dnr1$^{1\text{-}531}$	pAGW- N-terminal EGFP	GFP-Dnr1$^{1\text{-}531}$
Dnr1$^{1\text{-}433}$	pAGW- N-terminal EGFP	GFP-Dnr1$^{1\text{-}433}$
Dnr1$^{1\text{-}397}$	pAGW- N-terminal EGFP	GFP-Dnr1$^{1\text{-}397}$
Dnr1$^{324\text{-}677}$	pAGW- N-terminal EGFP	GFP-Dnr1$^{324\text{-}677}$
Dnr1$^{397\text{-}677}$	pAGW- N-terminal EGFP	GFP-Dnr1$^{397\text{-}677}$
Dredd-Myc	pAFHW-N-terminal 3xFLAG-3xHA	3xFLAG-3xHA-Dredd-Myc
DreddΔPD-Myc	pAFHW-N-terminal 3xFLAG-3xHA	3x-FLAG-3x-HA-DreddΔPD-Myc

Table 2.2 Gateway LR recombination reactions

2.1.3 DDAB Transfection Reagent

Dimethyl Dioctadecyl Ammonium Bromide (DDAB) transfection reagent was prepared as follows. To produce a stock solution, DDAB (Sigma) was suspended in ddH$_2$O at a final concentration of 2.5mg/ml. To bring DDAB into solution, the suspension was sonicated for ten one-minute pulses. However, additional sonication may be required to get DDAB into solution. For a working stock, the stock solution was

diluted to 250µg/ml with ddH$_2$O and sonicated for five one-minute pulses. The working solution is stable for 1 year at 4°C, but the solution should not be frozen.

2.1.4 Stable S2 Cell Line Generation

S2 cells that stably express GFP-tagged Dnr1, Dnr1$^{1-397}$, Dnr1$^{1-433}$, Dnr1$^{1-531}$, Dnr1$^{142-677}$, Dnr1$^{397-677}$, Dnr1$^{324-677}$ were established as follows. S2 cells were plated out in a six well plate with 3ml of cells per well at one million cells per ml. A DDAB transfection solution was then prepared by the addition of 2.85µg of DNA for each Dnr1 expression-construct and 0.15µg of a pCoHygro expression plasmid (Invitrogen) to 60µl of HyQ SFX-Insect Serum free medium (Gibco) and 120µl of DDAB reagent in a 1.5ml microcentrifuge tube. The mixture was incubated for 20 minutes at room temperature and then added to the cells drop wise. After incubating at 25°C for 3 days, cells that stably express the Dnr1 constructs were selected for by adding 300µg per ml of Hygromycin B. The cells were then centrifuged and resuspended in fresh HyQ TNM-FH medium with 300µg per ml Hygromycin B every four days thereafter until resistant cells started growing. Cells were then transferred into 25cm^2 flasks and maintained as stable stocks by continual selection with Hygromycin B.

2.1.5 Transient Transfection of S2 Cells

Transient transfections were performed as follows. S2 cells were plated out in a twelve well plate with 1ml of cells per well at one million cells per ml. A DDAB transfection solution was prepared by the addition of 1.5µg of DNA for the various expression-constructs to 20µl of HyQ SFX-Insect Serum free medium (Gibco) and 40µl

of DDAB reagent in a 1.5ml microcentrifuge tube. The mixture was incubated for 20 minutes at room temperature then added to the cells drop wise. Cells were incubated for ~24 hours and used in the various experiments as described.

2.1.6 RNAi

dsRNA was generated in an *in vitro* transcription reaction[148]. Briefly, template DNA was amplified from genomic DNA using gene-specific primers with a GGGCGGGT anchor sequence at the 5' end. The template DNA was amplified in a second round of PCR with a universal primer bearing the T7 RNA polymerase promoter sequence followed by the anchor sequence (TAATACGACTCACTATAGGGAGACCACGGGCGGGT) dsRNA was generated from second round PCR products in an *in vitro* reaction with T7 RNA polymerase with the T7 RiboMAX Express RNAi system (Promega). dsRNA was heated to 90°C and cooled slowly to room temperature to allow annealing. 10µg per ml dsRNA was then added directly to S2 cells plated out in a 12-well plate at one million cells per ml. The cells were then incubated for three days at 25°C to allow for depletion of the respective transcripts prior to phenotypic analysis.

2.2 Coimmunoprecipitation Assays

Immunoprecipitations were carried out as follows. S2 cells that stably express HA-DreddC408A were plated in a six well plate with 3ml of cells per well at one million cells per ml. The cells were transiently transfected as described above with expression plasmids for 6xmyc-tagged Dnr1 or Dnr1C563Y. Twenty-four hours after transfection,

cells were collect by centrifugation at 1000xg for 3 minutes and were lysed in 1ml lysis buffer (50mM HEPES (pH 7.5), 10mM EDTA (pH 8.0), 50mM KCl, 50mM NaCl, 1mM MgCl$_2$, 0.1% NP40, Protease inhibitors (Roche Inhibitor cocktail tablets), Phosphatase inhibitors (Sigma, Phosphatase inhibitor cocktail 1) for 10 minutes at 4°C. The cellular debris was removed by centrifugation at 21000xg for 10 minutes at 4°C. 2μl of rabbit anti-myc antibody (Sigma) was added to the supernatant and the samples were incubated overnight at 4°C. Samples were then centrifuged at 21000xg for 10 minutes at 4°C and the supernatant was collected. 40μl of Protein G Sepharose 4 fast flow (Amersham Biosciences) was added and samples were rocked for 1 hour at 4°C. Beads were pelleted at 300xg for 30 seconds and washed in lysis buffer 4 times for 10 minutes. 40μl of loading buffer (6.2mM Tris (pH 6.8), 10% Glycerol, 2% SDS, 3.5mM Beta-Mercaptoethanol, 0.05% Bromophenol blue) was added to the beads, which were then vortexed for 30 seconds and boiled for 10 minutes. Input lysates of approximately 100,000 cells and immunoprecipitates from approximately 500,000 cells were run on a Western blot as described below.

2.3 Western Blot Analysis

Unless otherwise indicated, one million cells were lysed directly in 100μl of Loading buffer and boiled for 10 minutes. The protein from 10μl of cell lysates (~100 000 cells) were separated on a 10% SDS-PAGE gel, except for the anti-active-caspase-3 blots, which were separated on a 12% SDS-PAGE gel. The gels were then transferred onto a nitrocellulose membrane using the Bio-Rad Trans-Blot Semi-Dry Electrophoretic Transfer Cell as per the manufacturers directions. The membranes were

blocked with Odyssey blocking buffer (Licor), diluted 1:1 in PBS for 3-5 hours at room temperature. The membranes were then incubated O/N at 4°C with the primary antibodies in Odyssey blocking buffer, diluted 1:1 in PBS with 0.1% Tween-20. Membranes were then washed 4 times for 5 minutes in PBS with 0.1% Tween-20. The membranes were then incubated with secondary antibodies in PBS with 0.1% Tween-20 for 1 hour at room temperature. Secondary antibodies were alexa fluor 680 Goat anti-rabbit and alexa fluor 750 goat anti-mouse (Invitrogen). Membranes were washed 4 times for 5 minutes in PBS + 0.1% Tween-20, then washed for 5 minutes in PBS. Membrane scanning and Protein quantification was performed using a Licor Aerius automated infrared imaging system according to manufacturer's instructions. The primary antibodies used for the Western blots are listed in table 2.3.

Antibody	Manufacturer	Concentration	Figures
Mouse anti-Actin	Sigma	1 in 1000	1.1b, 1.2, 2.1b, 2.2a,b, 2.4a, 3.1a,b, 3.2c, 3.3a
Mouse anti-HA	Sigma	1 in 10000	1.1a, 1.2, 3.1a
Mouse anti-myc	Sigma	1 in 2500	1.1a
Mouse anti-GFP	BabCO	1 in 5000	3.2b,c
Mouse anti-phospho-JNK	Cell Signaling	1 in 2000	1.4a-c
Rabbit anti-myc	Sigma	1 in 2500	1.1b, 2.4a, 3.1b, 3.3a
Rabbit anti-ubiquitin	Sigma	1 in 1000	3.4
Rabbit anti-active caspase-3	Cell Signaling	1 in 1000	2.2a,b
Rabbit anti-Dronc	Muro et al. 2002[141]		2.1b
Rabbit anti-JNK	Santa Cruz biotechnology	1 in 4000	1.4a-c

Table 2.3 Primary antibodies for Western blotting

2.4 Quantitative real-time PCR

For real-time PCR analysis total RNA was purified from 1 million cells at the times indicated for the various experiments using Trizol (Invitrogen) according to the manufacturers instructions. Purified RNA was then incubated with amplification grade DNase 1 at 37°C for 30 minutes to eliminate any DNA contamination. cDNA was prepared from purified RNA using oligonucleotode dT primers. Briefly, 5μg of RNA template, 1μl Oligo dT (50μM, Invitrogen) and 1μl dNTPs (10mM, Invitrogen) were added to a PCR tube. The Oligo dT primer was allowed to anneal to the RNA template by incubating the tubes at 65°C for 5 minutes. Then 4μl of 5x first strand buffer (Invitrogen), 1μl 0.1M DTT and 0.5ul SuperScript III (Invitrogen) was added. The tubes were then incubated at 50°C for 45 minutes to allow cDNA synthesis and 70°C for 15 minutes to terminate the reaction. Real-time PCR analysis was run with 2.5ul cDNA, 2.5ul primer mix that contains 1.6mM of the forward and reverse primer and 5ul 2X SYBR green mix (20mM Tris (pH 8.3), 100mM KCl, 6mM $MgCl_2$, 1.6% Glycerol, 0.02% Tween20, 4% DMSO, 0.4mM dNTPs, 0.06U per μl Platinum taq (Invitrogen), 1x SYBR Green). Realtime PCR was performed in an Eppendorf realplex2 PCR machine with a 2 step cycle and a melting curve. Samples were initially denatured at 95°C for 2 minutes; this was followed by 40 cycles of 95°C for 15 sec and 60°C for 1 minute. SyBr green incorporation was measured at the end of each extension step. After completion of the 40 cycles, a melting curve analysis was used to determine the specificity of the PCR. All samples were normalized to actin expression levels and comparison between samples was performed using the $\Delta\Delta C_T$ method[152]. The primers used to detect their respective transcripts are listed in table 2.4.

Primer	Sequence
actin forward	5`-TGCCTCATCGCCGACATAA-3`
actin reverse	5`-CACGTCACCAGGGCGTAA-3`
attacin forward	5`-AGTCACAACTGGCGGAAC-3`
attacin reverse	5`-TGTTGAATAAATTGGCATGG-3`
diptericin forward	5`-ACCGCAGTACCCACTCAATC-3`
diptericin reverse	5`-ACTTTCCAGCTCGGTTCTGA-3`
Dnr1 forward	5`-ATTCAATGAGTCGTCGCT-3`
Dnr1 reverse	5`-AGCACATGCTCCTTCTCCTT-3`

Table 2.4 real-time PCR primer sequences

2.5 Caspase Activity Assays

Caspase activity was measured using a fluorogenic AMC-labeled caspase peptide substrate (AMC-DEVD). After the indicated treatments, S2 cells were pelleted at 1000xg for 3 minutes at 4°C. Pellets were washed in ice cold PBS and then lysed in cell lysis buffer [10 mM Tris (pH 7.4), 10 mM $NaH2PO4$, 150 mM NaCl, 1% Triton X-100] on ice for 10 minutes. 100 µg cell lysates were then incubated with 50 µM AMC-labeled DEVD caspase substrate in a final volume of 100 µl reaction buffer [10 mM HEPES (pH 7.5), 50 mM NaCl, 0.5 mM EDTA (pH 8.0), 0.1% CHAPS, 10% glycerol, 10 mM DTT] and incubated at 37°C for 1 hour. We determined caspase activity by measuring AMC liberation from DEVD with a Wallac Victor 2 multilable counter.

2.6 Apoptotic Index

The apoptotic index of S2 cells was determined as follows. After the indicated treatments, S2 cells were incubated with various concentrations of actinomycin D. At the indicted times after actinomycin D treatment, a population of approximately two hundred S2 cells was captured in a series of DIC images on a Zeiss Invertoskop 40C microscope using a Canon Powershot S2 IS camera. The total S2 cell population captured was

counted, and cells were defined as apoptotic if membrane blebbing was visible. The apoptotic index was calculated by dividing the number of apoptotic cells by the total number of cells in a given population.

2.7 Microscopy, Immunofluorescence and Image Processing

For Immunofluorescence analysis of the GFP-Dnr1 variants in S2 cells, a 100μl suspension of approximately one-hundred thousand cells were deposited onto a Superfrost Gold Plus Slide (Fisher). Cells were allowed to adhere to the slide by incubating at room temperature for 5 minutes. Cells were then fixed for 5 minutes at room temperature in 4% formaldehyde in PBS + 0.1% TritonX-100 (Sigma). Cells were then washed three times for 5 minutes with PBS + 0.1% TritonX-100. The cells were blocked with 5% Normal Goat Serum (NGS) in PBS + 0.1% Tween20 for 1 hour at room temperature. Cells were then incubated with Hoechst (to visualize DNA) and Alexa-Fluor-568-phallodin (to visualize filamentous Actin) or Alexa-Fluor-568 wheat germ agglutinin (to visualize the nuclear envelope) (All from Molecular Probes) in PBS + 0.1% Tween20 for 10 minutes at room temperature in the dark. Cells were then washed once with PBS + 0.1% Tween20. Cells were then mounted in Pro-Long Gold mounting medium (Invitrogen) and covered with a coverslip. Confocal images were captured on a Zeiss LSM 510 confocal microscope using LSM 5 software. Images were processed with Adobe Photoshop 8.0, and figures were assembled with Adobe Illustrator 11.0.

2.8 Ubiquitination·Assay

The ubiquitination assay was performed with commercially available E1, E2 and ubiquitin and bacterially purified, recombinant Dnr1 or Dnr1C563Y (Edan Foley). The indicated amount of bacterially purified, recombinant Dnr1 or Dnr1C563Y was incubated with 100ng E1 (Sigma), 2μg E2 (UbcH5a, BioMol) and 2μg of ubiquitin (Sigma) in 10μl assay buffer [25mM Tris (pH 7.5), 5mM MgCl$_2$ 2mM ATP, 0.5mM DTT 0.05% NP-40]. Reactions were incubated at 37°C for 30 minutes. Then 15μl of sample buffer was added and the reactions were boiled for 10 minutes. 20μl from each reaction were separated on a 10% SDS-PAGE gel and transferred onto a nitrocellulose membrane. The membrane was then autoclaved in PBS for 20 minutes. Autoclaving the membrane exposes latent antigenic sites on the extremely stable, mostly globular ubiquitin molecule, causing those sites to be exposed and enabling them to be recognized by anti-ubiquitin antibodies generated against denatured ubiquitin[153]. Once autoclaved, the analysis of the blot continued as described in the Western blot analysis protocol. The blot was probed with a primary rabbit anti-ubiquitin antibody (Sigma).

2.9 Fly culture

2.9.1 Handling of *Drosophila*

Fly stocks were handled according to "Basic Methods of Culturing *Drosophila*" (http://flystocks.bio.indiana.edu/flywork/culturing) by the Bloomington *Drosophila* Stock Centre at Indiana University. All *Drosophila* stocks were maintained on standard cornmeal medium and kept at 25°C.

2.9.2 UAS/GAL4 Bipartite Expression System

The UAS/GAL4 system is a yeast derived expression system that consists of the GAL4 transcription faction, which binds to UAS sequences to promote gene transcription. In *Drosophila*, GAL4 can be placed under the control of various promoters to drive its expression in specific tissues or at specific stages of development. Transgenes under the control of a UAS element are transcriptionally induced by GAL4 in the specific tissue or at the specific stage of development. Because transcription of genes under control of a UAS element requires the presence of GAL4, the absence of GAL4 maintains these genes in a transcriptionally silent state. For the *in vivo* studies, I used flies carrying *eyeless(ey)*-GAL4, which express GAL4 under the control of the eye specific *ey* promoter, which is expressed early in eye morphogenesis prior to the expression of GMR. When these flies are crossed to flies carrying the UAS-*Dnr1* transgene, Dnr1 is expressed in the developing eye in the same pattern as the GAL4 transcription factor.

2.9.3 *Drosophila* Crosses

To determine the effect of Dnr1 expression in the developing eye on Hid induced apoptosis, I set up a series of crosses (Figure 2.1) to establish flies that express one or two copies of the Dnr1 transgene in conjunction with Hid expression. For the crosses, I used GMR-*Hid*;*ey*GAL4 flies (Bloomington Stock Center) that express Hid under the control of the GMR promoter, which results in Hid expression in cells behind the mophogenetic furrow of the developing eye. Additionally, these flies express GAL4 under control of the *ey* promoter, which is expressed throughout the developing eye prior to activation of the

GMR promoter. I also used UAS-*Dnr1* flies (George Johnson and Edan Foley), which contain a Dnr1 transgene under control of UAS. The *w;Sco/Cyo;TM6B/MKRS* *Drosophila* (Dr. Sarah Hughes) line was used to help in selection of the progeny from the crosses. Oregon R fly (Bloomington Stock Center) eyes were used as a wild type control.

♀ GMR-*Hid;ey*GAL4   X   *w;* $\dfrac{Sco}{Cyo}; \dfrac{TM6B}{MKRS}$ X   UAS-*Dnr1* ♀ F_0

♀ GMR-*Hid; Cyo;* $\dfrac{ey\text{GAL4}}{TM6B}$ X $\dfrac{UAS\text{-}Dnr1}{Sco}; \dfrac{MKRS}{+}$ ♂ F_1

(F$_1$ Progeny)

♀ $\dfrac{UAS\text{-}Dnr1}{Cyo}; \dfrac{TM6B}{+}$ X $\dfrac{GMR\text{-}Hid}{Y}; \dfrac{UAS\text{-}Dnr1}{Cyo}; \dfrac{ey\text{GAL4}}{MKRS}$ ♂ F_2

♀ $\dfrac{GMR\text{-}Hid}{X}; \dfrac{UAS\text{-}Dnr1}{UAS\text{-}Dnr1}; \dfrac{ey\text{GAL4}}{TM6B}$

F_3

♀ $\dfrac{GMR\text{-}Hid}{X}; \dfrac{UAS\text{-}Dnr1}{Cyo}; \dfrac{ey\text{GAL4}}{TM6B}$
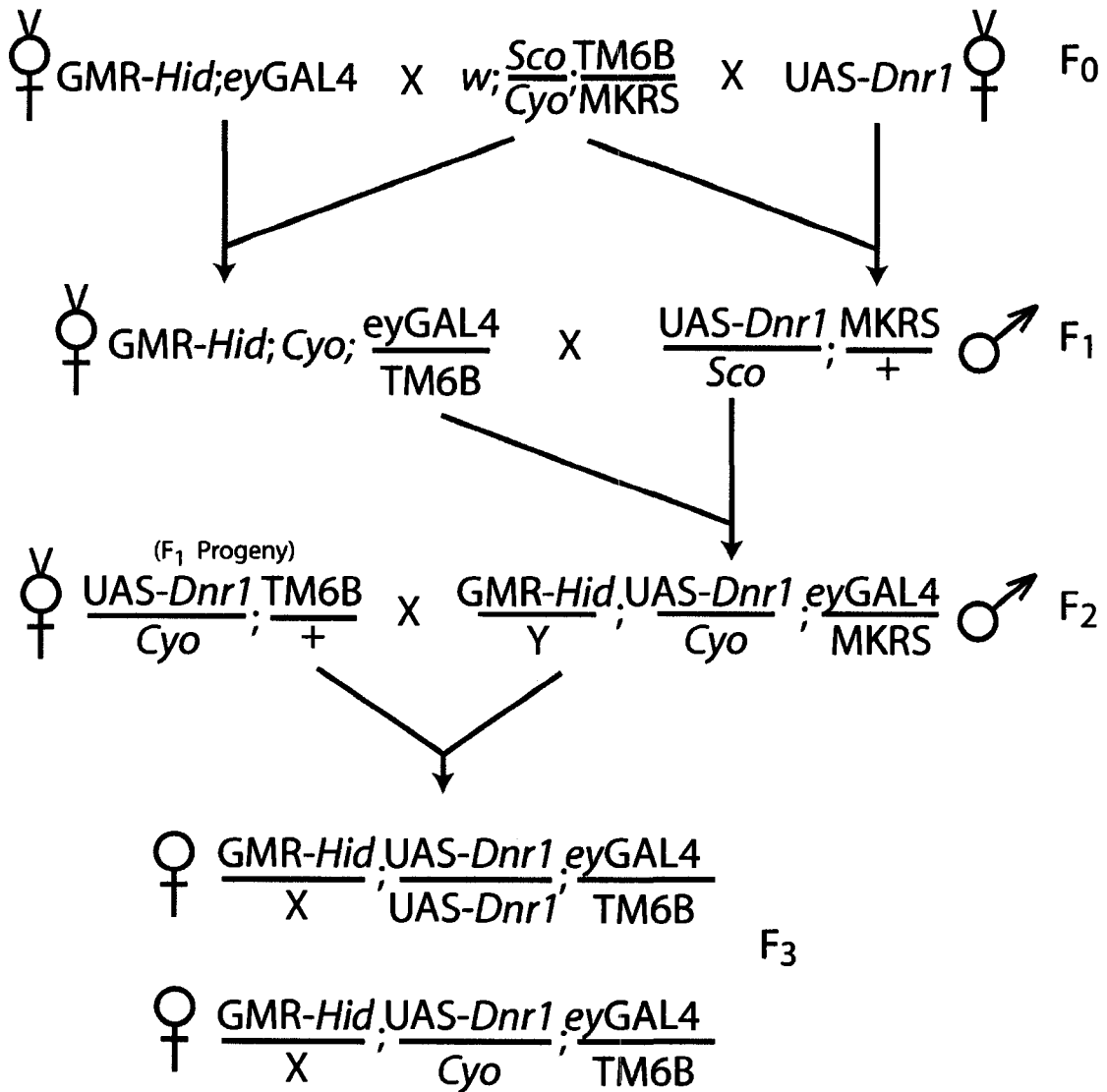
Figure 2.1 Schematic representation of *Drosophila* crosses

Chapter 3

RESULTS

3.1 Dnr1 Regulation of Imd Signaling

3.1.1 Dnr1 and Dnr1C563Y Complex with DreddC408A in S2 Cells

Dnr1 impinges on the Imd signaling pathway by the regulation of the initiator caspase Dredd. To determine if Dnr1 interacts with Dredd, I performed an *in vitro* co-immunoprecipitation experiment using inputs of embryonic macrophage-like *Drosophila* S2 cell line. In particular, I used S2 cells that stably express an inactive variant of Dredd, where the crucial catalytic cysteine residue has been inactivated by site-directed mutagenesis (DreddC408A). I used the catalytically inactive DreddC408A to prevent the possibility of Dredd-mediated cleavage of Dnr1, which could affect the immunoprecipitation experiment. I transfected S2 cells that stably express HA-DreddC408A with a plasmid that drives the constitutive expression of N-terminally 6Xmyc-tagged Dnr1 (myc-Dnr1) or a Dnr1 variant where the RING domain has been inactivated by site-directed mutagenesis of a crucial cysteine residue (myc-Dnr1C563Y). Twenty-four hours after transfection, I collected cell lysates and immunoprecipitated Dnr1 with an anti-myc antibody. I analyzed the input cell lysates and myc immunoprecipitates with anti-myc and anti-HA antibodies by Western blot analysis (Figure 3.1 a). The anti-myc antibody did not precipitate HA-DreddC408A from control cells, which did not express a myc-tagged protein (Figure 3.1 a lane 5), although

33

HA-DreddC408 was readily detected in the control input cell lysate (Figure 3.1 a lane 3). This result demonstrates that the anti-myc antibody does not bind and precipitate HA-DreddC408A in a non-specific manner. As expected, the anti-myc antibody precipitated myc-Dnr1 and myc-Dnr1C563Y from the respective S2 cell lysates (fig. 1.1 a lanes 6&7). Analysis of the myc precipitates revealed that both myc-Dnr1 and myc-Dnr1C563Y formed complexes with HA-DreddC408A (Figure 3.1 a lanes 6&7). This result also indicates that the formation of a complex between DreddC408A and HA-Dnr1 is independent of a functional RING domain, as HA-Dnr1C563Y complexes with DreddC408A in S2 cell lysates.

While I readily detected myc-Dnr1C563Y in the input cell lysate and the immunoprecipitate (Figure 3.1 a lanes 3&7), I was unable to detect myc-Dnr1 in the input cell lysate and myc-Dnr1 was barely detectable in the immunoprecipitate (Figure 3.1 lanes 2&6). I consistently observed that Dnr1 that lacks a functional RING domain is more stable in S2 cells than Dnr1 with an intact RING domain. To confirm this observation, I transiently transfected S2 cells with equal amounts of plasmids that drive the constitutive expression of N-terminally 6Xmyc-tagged Dnr1 or Dnr1C563Y. Twenty-four hours after transfection, I performed Western blot analysis of cell lysates with an anti-myc antibody and an anti-actin antibody, which served as a loading control. Consistent with the results from the immunoprecipitations, I readily detected myc-Dnr1C563Y on the Western blot, whereas myc-Dnr1 was barely visible (Figure 3.1 b, results consistent over three independent experiments). The result of the Western blot analysis indicates the RING domain contributes to the stability of Dnr1 in S2 cells.
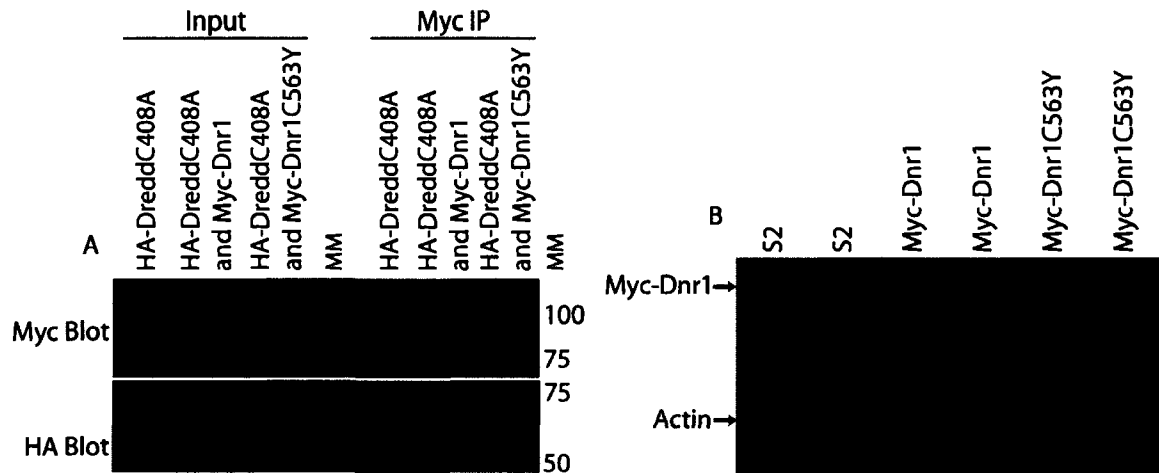
Figure 3.1 Dnr1 and Dnr1C563Y complex with DreddC408A. (A) Western blot analysis of a Dnr1/Dredd co-immunoprecipitation. S2 cells that stably express HA-DreddC408A were transfected with equal amounts of a plasmid that drives the expression of myc-Dnr1 (Lanes 2 and 6) or myc-Dnr1C563Y (Lanes 3 and 7). Twenty-four hours after transfection, cell lysates were immunoprecipitated with an anti-myc antibody. The immunoprecipitates were probed with an anti-myc antibody to detect myc-Dnr1 and myc-Dnr1C563Y (lanes 5-7, top blot) and an anti-HA antibody to detect HA-DreddC408A (lanes 5-7, bottom blot). Inputs are in lanes 1-3 and Immunoprecipitations are in lanes 5-7. Molecular mass markers are in lane four and the sizes of the bands are indicated on the right. Dnr1 co-immunoprecipitates DreddC408A from S2 cells lysates, the co-immunoprecipitation is not dependent on a functional RING domain as Dnr1C563Y also co-immunoprecipitated DreddC408A from S2 cell lysates. (B) Western blot analysis of S2 cell lysates. S2 cells were transfected with equal amounts of a plasmid that drives the expression of myc-Dnr1 (lanes 3&4) or myc-Dnr1C563Y (lanes 5&6). Twenty-four hours after transfection, cell lysates were probed with anti-myc and anti-Actin antibodies.

3.1.2 Dnr1 Mediates Dredd Depletion in a RING Domain-Dependent Manner

Dnr1 contains a C-terminal RING domain that has greatest similarity to the RING domains of IAPs (Figure 1.6). RING domains are E3 ubiquitin ligases that polyubiquitinate their target substrates to mark them for proteasomal degradation. Based on these observations, and the demonstration that Dnr1 interacts with DreddC408A, I hypothesized that Dnr1 inhibits Dredd activity by regulation of Dredd levels in a RING domain-dependent manner. To test this hypothesis, I established an assay to quantify the ability of Dnr1 and Dnr1C563Y to decrease Dredd protein levels in S2 cells. To this end, I transfected S2 cells, S2 cells that stably express HA-Dnr1 and S2 cells that stably express HA-Dnr1C563Y with equal amounts of a plasmid that drives the constitutive expression of Flag-HA-Dredd-myc (F-H-Dredd-M). Twenty-four hours after transfection, I performed Western blot analysis of cell lysates with an anti-HA antibody and an anti-actin antibody, which served as a loading control for quantification purposes. I detected a single band corresponding to F-H-Dredd-M in the individual transfected cell lines (Figure 3.2, lanes 2-4). The F-H-Dredd-M band appeared diminished in the S2 cells that stably express HA-Dnr1 compared to both S2 cells and S2 cells that stably express HA-Dnr1C563Y. I then quantified the F-H-Dredd-M protein levels relative to a control protein (actin) in the individual transfected cell lines (Figure 3.2). The F-H-Dredd-M:actin ratio was significantly reduced in S2 cells that stably express HA-Dnr1 compared to control S2 cells. The F-H-Dredd-M:actin ratio in control S2 cells was almost double that observed in S2 cells that stably express HA-Dnr1. Expression of HA-Dnr1C563Y did not have a significant impact on F-H-Dredd-M protein levels, as the F-H-Dredd-M:actin ratio was similar in S2 and S2 cells that stably express HA-Dnr1C563Y. The

results of the above assay indicate that Dnr1 regulates Dredd protein levels in S2 cells by mediating the depletion of Dredd in a RING domain-dependent manner.
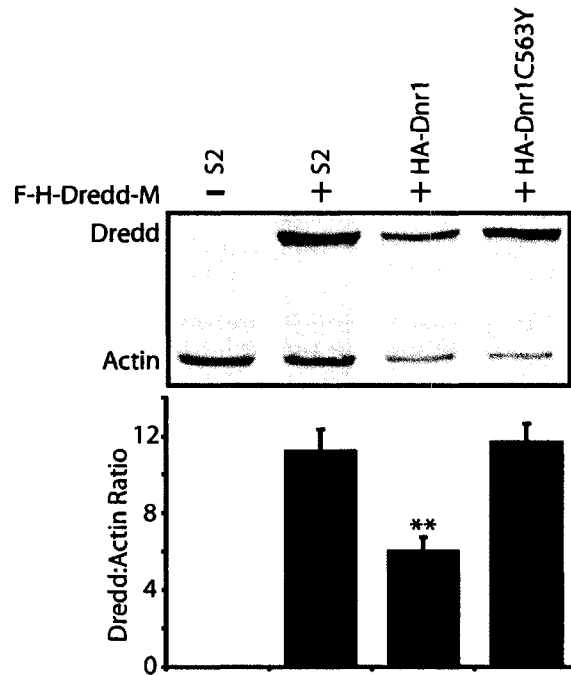
Figure 3.2   Dnr1-dependent Dredd destruction is dependent on an intact RING domain. Western blot analysis of lysates from S2 cells (lanes 1 and 2) and S2 cells that stably express HA-Dnr1 (lane 3) or HA-Dnr1C563Y (lane 4). The individual lines were transfected with equal amounts of a plasmid that drives the expression of 3XFlag-3XHA-Dredd-myc (F-H-Dredd-M) where indicated. Twenty-four hours after transfection, cell lysates were probed with anti-HA and anti-Actin antibodies (top panel, bands where indicated). F-H-Dredd-M was quantified relative to a control protein (Actin) (bottom panel). Results are the mean of three independent experiments and error bars indicate standard error. ** indicates values that differ significantly from S2 cells with a p<0.01. Overexpression of Dnr1 in S2 cells depletes the levels of F-H-Dredd-M, whereas overexpression of the RING domain mutant Dnr1C563Y in S2 cells has no significant impact on F-H-Dredd-M levels.

3.1.3 Dnr1 Inhibits Imd-Dependent Antimicrobial Peptide Production in S2 Cells

Overexpression of HA-Dnr1 led to the depletion of F-H-Dredd-M protein levels in S2 cells. As Dredd activity is required for the production of antimicrobial peptides by the Imd pathway, I hypothesized that overexpression of Dnr1 would result in downstream loss of antimicrobial peptide production upon activation of the Imd pathway. To test this hypothesis, I establish a quantitative real-time PCR assay to monitor the transcription of genes that encode the antimicrobial peptides *att* and *dipt,* whose expression relies solely on activation of the Imd pathway. Specifically, I incubated S2 cells, S2 cells that stably express HA-Dnr1 and S2 cells that stably express HA-Dnr1C563Y with Lipopolysaccharides (LPS). Commercial preparations of LPS are contaminated with peptidoglycan and strongly induces the Imd signaling pathway[44]. I isolated total RNA at zero and six hours after LPS treatment from the individual cell lines. I used real-time PCR quantification to determine the induction of *att* and *dipt* transcription at the six hour time point relative to the zero hour time point for each cell line. S2 cells had a hundred fold increase in *att* transcript levels and a ten fold increase in *dipt* transcript levels at the six hour time point compared to the zero hour time point.(Figure 3.3 a,b column 1). The ten fold increase in *dipt* and the hundred fold increase in *att* transcription are consistent with the increases observed in *Drosophila* after they are infected with *E. coli*[154].

Analysis of S2 cells that stably express HA-Dnr1 revealed they had a significant reduction in Imd-dependent antimicrobial peptide transcription compared to control S2 cells, with no detectable increase in either *att* or *dipt* transcription at the six hour time point (Figure 3.3 a,b column 2). These data indicate that Dnr1-mediated depletion of

F-H-Dredd-M observed in Figure 3.2, results in the downstream loss of Imd-dependent antimicrobial peptide transcription in S2 cells.

Interestingly, compared to control S2 cells, S2 cells that stably express HA-Dnr1C563Y had a significantly lower increase in *att* and *dipt* transcription (10 fold and 2 fold, respectively) at the six hour time point compared to the zero hour time point (Figure 3.3 a,b column 3). A possible mechanism for the inhibition of antimicrobial peptide transcription by HA-Dnr1C563Y is the physical interaction with F-H-Dredd-M observed in the co-immunoprecipitation experiment (Figure 3.1 a). The interaction between Dnr1C563Y and Dredd may inhibit Dredd activity and cause a loss of Imd-dependent antimicrobial peptide transcription.

The level of *att* and *dipt* transcription in S2 cells that stably express HA-Dnr1C563Y was inhibited to a lesser extent then in S2 cells that stably express HA-Dnr1. It is likely that this result is an artifact of HA-Dnr1C563Yoverexpression, which results in the sequestration of Dredd, thus inhibiting antimicrobial peptide production.
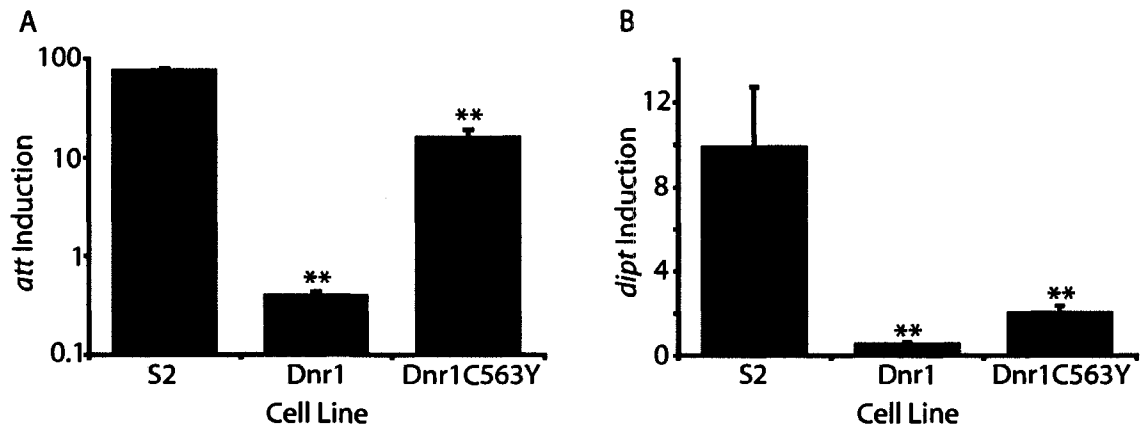
Figure 3.3 Overexpression of Dnr1 inhibits antimicrobial peptide transcription. Real-time PCR quantification of *att* (a) and *dipt* (b) transcript levels in S2 cells and S2 cells that stably express HA-Dnr1 or HA-Dnr1C563Y. Total RNA was isolated at zero and six hours after LPS treatment from the individual cell lines. Real-time PCR quantification was used to determine the induction of *att* (a) and *dipt* (b) transcription at the six hour time point relative to the zero hour time point for each cell line. Results are the mean of three experiments and error bars indicate standard deviations. ** indicates values that differ significantly from S2 cells with a p<0.01. The overexpression of Dnr1 or Dnr1C563Y significantly inhibits *att* and *dipt* transcription in S2 cells.

3.1.4 Dnr1 and Dnr1C563Y Inhibit Imd-Dependent JNK Phosphorylation

In addition to antimicrobial peptide transcription, signaling through the Imd pathway results in the Dredd-dependent activation of the JNK signaling cassette, which results in transient phosphorylation of JNK. As Dnr1 overexpression led to the depletion of Dredd in S2 cells, I hypothesized that Dnr1 overexpression would result in decreased JNK phosphorylation in response to the activation of the Imd pathway. To test this hypothesis, I stimulated S2 cells, S2 cells that stably express HA-Dnr1 and S2 cells that stably express HA-Dnr1C563Y with LPS. I collected cell lysates at various times after exposure to LPS and probed for phospho-JNK (p-JNK) and total JNK on a single Western blot for each individual cell line. Total JNK levels remained constant in each individual cell line over the entire two·hour time period (Figure 3.4 a,b,c). In contrast, there was a transitory increase in JNK phosphorylation that began five minutes after exposure to LPS in each of the individual cell lines (Figure 3.4 a,b,c). Quantification of p-JNK to total JNK revealed a maximal eighteen-fold increase in p-JNK:total JNK ratio in S2 cells within fifteen minutes of LPS exposure and the ratio returned to background levels by ninety minutes (Figure 3.4). This result is consistent with previous reports that JNK is transiently phosphorylated through the Imd pathway upon PGN exposure[68].

Compared to control S2 cells, S2 cells that stably express HA-Dnr1 had a significantly lower maximal increase in the p-JNK:total JNK ratio. The p-JNK:total JNK ratio had a maximal 5.7 fold increase in S2 cells that stably express HA-Dnr1 at the fifteen minute time point. Additionally, the p-JNK: total JNK ratio remained significantly lower throughout the entire time course and returned to background levels faster in S2 cells that stably express HA-Dnr1 compared to control S2 cells (Figure 3.4 d). The results

of the Western blot analysis provide further evidence that Dnr1 impacts on the Imd signaling pathway. Similar to the reduction in antimicrobial peptide production, the stable expression of HA-Dnr1 in S2 cells results in decrease Imd pathway-dependent JNK phosphorylation.

Analysis of S2 cells that stably express HA-Dnr1C563Y revealed they had significantly reduced JNK phosphorylation compared to control S2 cells, with a maximal twelve fold increase in the p-JNK:total JNK ratio at the fifteen minute time point (Figure 3.4 d). The p-JNK:total JNK ratio remained significantly lower compared to control S2 cells throughout the entire time course, however, similar to S2 cells the p-JNK:total JNK ratio returned to background levels at the ninety minute time point in S2 cells that stably express HA-Dnr1C563Y. The results of the Western blot analysis lend further support to the idea that HA-Dnr1C563Y inhibits the Imd signaling pathway by binding and sequestering Dredd.

In summary, overexpression of Dnr1 or Dnr1C563Y in S2 cells results in decreased antimicrobial peptide production and abbreviated and diminished JNK phosphorylation in response to stimulation of the Imd signaling pathway. The observations that Dnr1C563Y inhibit Imd signaling to a lesser extent than Dnr1 indicates that the Dnr1 RING domain is required to fully inhibit Dredd activity.
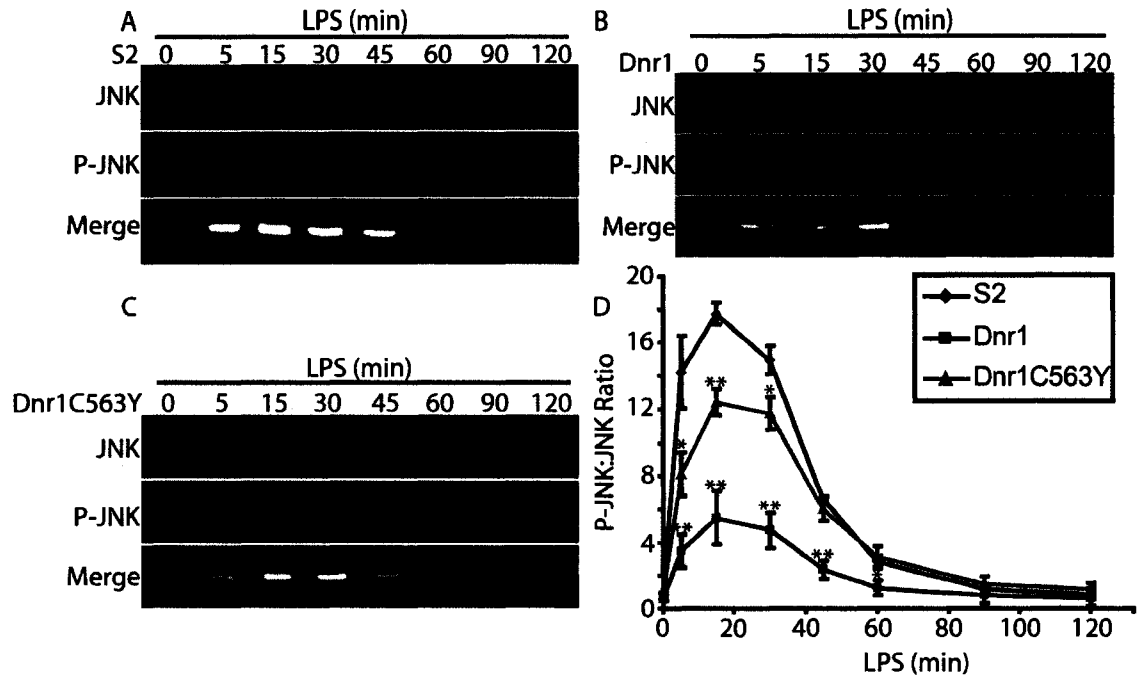
Figure 3.4 Overexpression of Dnr1 inhibits JNK phosphorylation. Western blot analysis of total and phospho-JNK protein in S2 cells (A), S2 cells that stably express HA-Dnr1 (B) and S2 cells that stably express HA-Dnr1C563Y (C). Cells were stimulated with LPS for the indicated time periods and lysates were collected for each individual cell line and   probed with anti-total JNK (top blot) and anti-phospho-JNK (middle blot) antibodies. The top and middle blot are false colored and merged in the bottom panel with Total JNK in red and phospho-JNK in green. (D) phospho-JNK protein levels were quantified and normalized relative to total-JNK protein levels for each time point for the three cell lines. Results are the mean of three independent experiments and error bars indicate standard error. ** and * indicates values that differ significantly from S2 cells with a p<0.01 and p<0.05 respectively. The overexpression of Dnr1 or Dnr1C563Y significantly inhibits JNK-phosphorylation in S2 cells.

3.2 Dnr1 Regulation of the *Drosophila* Apoptotic Cascade

3.2.1 Dnr1 Regulates Dronc Protein Levels in S2 Cells

The RING domain of Dnr1 shares greatest similarity with the RING domains of the IAP family of proteins, a group that includes the *Drosophila* caspase inhibitor, dIAP1. While not all IAPs function as caspase inhibitors, the presence of the C-terminal RING domain is generally associated with their ability to inhibit caspase activity. Additionally, I demonstrated that Dnr1 mediates the depletion of the initiator caspase Dredd in S2 cells. Based on these observations, we tested if Dnr1 regulates the protein levels of another *Drosophila* initiator caspase, Dronc, which functions in the apoptotic cascade. To this end, I treated S2 cells with dsRNA to target Dnr1 for destruction. Seventy-two hours after incubation with Dnr1 dsRNA, I used quantitative real-time PCR to measure Dnr1 transcript levels. Real-time PCR analysis confirmed a greater than 99% depletion of Dnr1 transcript levels in Dnr1 dsRNA treated S2 cells compared to control S2 cells (Figure 3.5 a).

After confirmation of the Dnr1 knockdown, we determined the consequence of Dnr1 loss on the levels of the initiator caspase Dronc. To this end, we treated Dnr1 depleted S2 cells with the transcriptional inhibitor actinomycin D, which is a potent inducer of apoptosis in S2 cells. We collected cell lysates from control S2 cells (Figure 3.5 b lanes 2-5) or S2 cells treated with Dnr1 dsRNA (Figure 3.5 b lanes 7-10) at various times after actinomycin D exposure and probed them with an anti-Dronc antibody by Western blot analysis. We detected three Dronc isoforms from the S2 cell lysates with the anti-Dronc antibody (Figure 3.5 b). The three isoforms correspond to full length

Dronc, and two additional Dronc cleavage products that are associated with entry into apoptosis. The two Dronc cleavage products detected correspond to the large Dronc catalytic subunit (L) and active Dronc, which lacks a prodomain (Pr2).

Prior to actinomycin D exposure, we detected elevated levels of full length Dronc in S2 cells treated with Dnr1 dsRNA compared to control S2 cells (Figure 3.5 b lanes 2 and 7). Quantification of full length Dronc relative to a control protein (actin) prior to actinomycin D exposure revealed that full length Dronc protein levels were significantly elevated in S2 cells treated with Dnr1 dsRNA compared to control S2 cells (Figure 3.5 c). There was approximately 60% more full length Dronc in Dnr1 dsRNA treated S2 cells than in control S2 cells. The elevated Dronc protein levels suggest that Dnr1 plays a role in the regulation of Dronc protein levels in S2 cells.

As expected, upon exposure of S2 cells to actinomycin D, we observed the disappearance of full length Dronc in both Dnr1 dsRNA treated and control S2 cells (Figure 3.5 b). The disappearance of full length Dronc corresponded to the appearance of the Pr2 and L Dronc isoforms (Figure 3.5 b lanes 3-5 and 8-10). We then quantified the Pr2 and L Dronc isoforms relative to a control protein (actin). Quantification of the Pr2 Dronc isoform revealed a significant elevation of Pr2 in S2 cells treated with Dnr1 dsRNA compared to control S2 cells over the entire actinomycin D time course (Figure 3.5 d). The levels of the L Dronc isoform were also mildly elevated in Dnr1 dsRNA treated S2 cells compared to control S2 cells (Figure 3.5 d). The results of this section demonstrate that loss of Dnr1 results in elevated Dronc protein levels in S2 cells. Corresponding to the elevated full length Dronc protein levels, we detected elevated active Dronc protein levels after apoptotic stimulation.
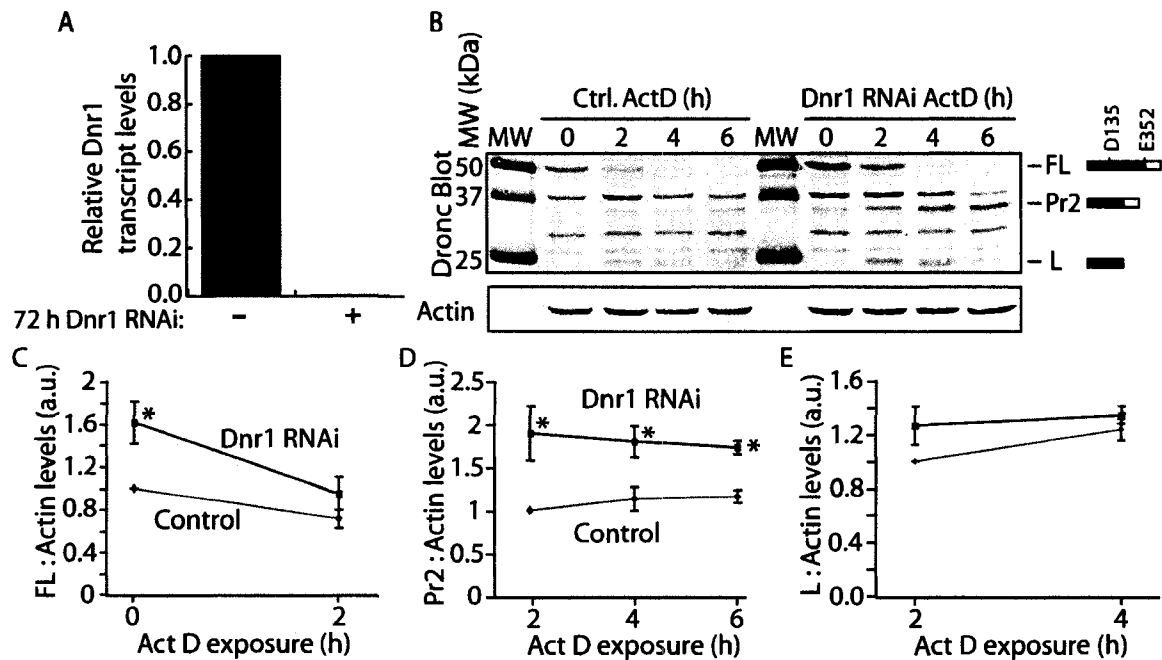
Figure 3.5 Dnr1 affects Dronc protein levels (A) Real-time PCR quantification of *dnr1* transcript levels in S2 cells and S2 cells treated with Dnr1 dsRNA. Total RNA was isolated from S2 cells (column 1) and S2 cells treated with Dnr1 dsRNA for 72 hours to deplete Dnr1 (column 2). Real-time PCR measurement of *dnr1* transcript levels revealed a greater than 99% decrease in *dnr1* in Dnr1 dsRNA treated S2 cells. *dnr1* transcript levels were normalized to actin transcript levels in both samples. (B) Western blot analysis of lysates from S2 cells (lanes 2-5) and S2 cells treated with Dnr1 dsRNA for 72 hours (lanes 7-10). Cells were treated with actinomycin D for the indicated time period and lysates were probed with an anti-Dronc antibody (top blot) and an anti-actin antibody (bottom blot), which serves as a loading control. Three distinct Dronc isoforms were detected corresponding to full-length (FL), Pr2 and L Dronc isoforms. (C-E) Quantification of (C) Full length Dronc, (D) the Pr2 Dronc isoform and (E) the L Dronc isoform relative to the level of a control protein (actin). The Dronc:actin levels in control S2 cells at 0 hours actinomycin D treatment were assigned a value of 1 in (C) and the remaining Dronc:actin values are reported relative to this value. We detected a significant increase in full-length Dronc in S2 cells incubated with Dnr1 dsRNA compared to control S2 cells in the absence of actinomycin D treatment. Results are the mean of three independent experiments and error bars indicate standard error. * indicates values that differ significantly from S2 cells with a p<0.03. We also detected elevated levels of the Pr2 and L Dronc isoforms in cells treated with Dnr1 dsRNA (D and E, respectively). Results are the mean of three independent experiments and error bars indicate standard error. * indicates values that differ significantly from S2 cells with a p<0.01. The depletion of Dnr1 significantly increased Dronc protein levels in S2 cells. (E. Foley contributed panels B-E)

46

3.2.2 Depletion of Dnr1 Sensitizes S2 Cells to the Induction of Caspase Activity

Depletion of Dnr1 from S2 cells results in the accumulation of the full length Dronc protein, which corresponds to elevated active Dronc protein levels after apoptotic stimulation. Based on these observations, we determined the consequences of Dnr1 depletion on apoptotic progression in S2 cells. To this end, we used a commercially available anti-active caspase-3 antibody to monitor actinomycin D induced apoptosis. The anti-active caspase-3 antibody is routinely used in *Drosophila* as a reliable indicator of apoptotic progression; however the exact antigen recognized by the antibody is unknown. To determine the antigen recognized by the anti-active caspase-3 antibody, I treated S2 cells with dsRNA to deplete the *Drosophila* caspases; Decay, Dredd, Drice or Dronc. Seventy-two hours after incubation with the various dsRNAs, I treated the S2 cells with actinomycin D to induce apoptosis. I collected cell lysates at zero and six hours after actinomycin D treatment and probed the lysates with the anti-active caspase-3 antibody by Western blot analysis. Prior to incubation with actinomycin D, I did not detect an active caspase-3 signal in the control S2 cells or any of the S2 cells treated with the various dsRNAs. (Figure 3.6 a lanes 1,3,5,7,9). After actinomycin D treatment, I detected an active caspase-3 signal in control S2 cells and S2 cells treated with either Decay or Dredd dsRNA (Figure 3.6 a lanes 2,4,6). In contrast, I failed to detect an active caspase-3 signal after actinomycin D exposure in S2 cells treated with either Drice or Dronc dsRNA (Figure 3.6 a lanes 8,10). Because the caspase signal requires Drice activity, which lies downstream of Dronc, I propose that the anti-active-caspase-3 antibody recognizes an antigen downstream of Dronc in the apoptotic cascade and

requires the presence of Drice. However, Dcp-1 is highly similar to Drice and may contribute to the active caspase-3 signal.

To determine the effect of Dnr1 depletion on the accumulation of the active caspase-3 signal upon apoptotic induction, we incubated S2 cells with Dnr1 dsRNA to deplete endogenous Dnr1. Seventy-two hours after incubation with Dnr1 dsRNA, we incubated the S2 cells with actinomycin D to induce apoptosis. We collected cell lysates at various times after actinomycin D exposure and probed the lysates with the anti-active capsase-3 antibody by Western blot analysis. We detected the appearance of the active caspase-3 signal in control S2 cells four hours after actinomycin D exposure and the signal continued to accumulate for the remainder of the time course (Figure 3.6 b). In comparison, we detected the active caspase-3 signal within one hour of actinomycin D exposure in S2 cells treated with Dnr1 dsRNA. The accumulation of the active caspase-3 signal was more intense at all time points measured after actinomycin D exposure in Dnr1 dsRNA treated S2 cells compared to control S2 cells (Figure 3.6 b). The results of the Western blot analysis indicate that loss of Dnr1 results in elevated caspase activation in S2 cells treated with actinomycin D.

To determine if the increased active caspase-3 signal corresponds to increased caspase activity, we performed a DEVDase caspase activity assay. The DEVDase assay uses the fluorogenic AMC-labeled caspase peptide substrate DEVD to monitor caspase activity. When a caspase cleaves AMC-DEVD, the fluorogenic AMC label is liberated and we measure the total AMC fluorescence to determine the amount of caspase activity. To monitor caspase activity, we incubated S2 cells and S2 cells treated with Dnr1 dsRNA with actinomycin D to induce apoptosis. We collected cell lysates at various time after

Act D exposure and performed a DEVDase assay. Prior to actinomycin D exposure, Dnr1 dsRNA treated and control S2 cells had similar basal levels of caspase activity (Figure 3.6 c). After actinomycin D exposure, we detected significantly elevated caspase activity in S2 cell treated with Dnr1 dsRNA compared to control S2 cells (Figure 3.6 c). The results of this section demonstrate that Dnr1 depletion results in increased caspase activity in S2 cells after apoptotic induction.
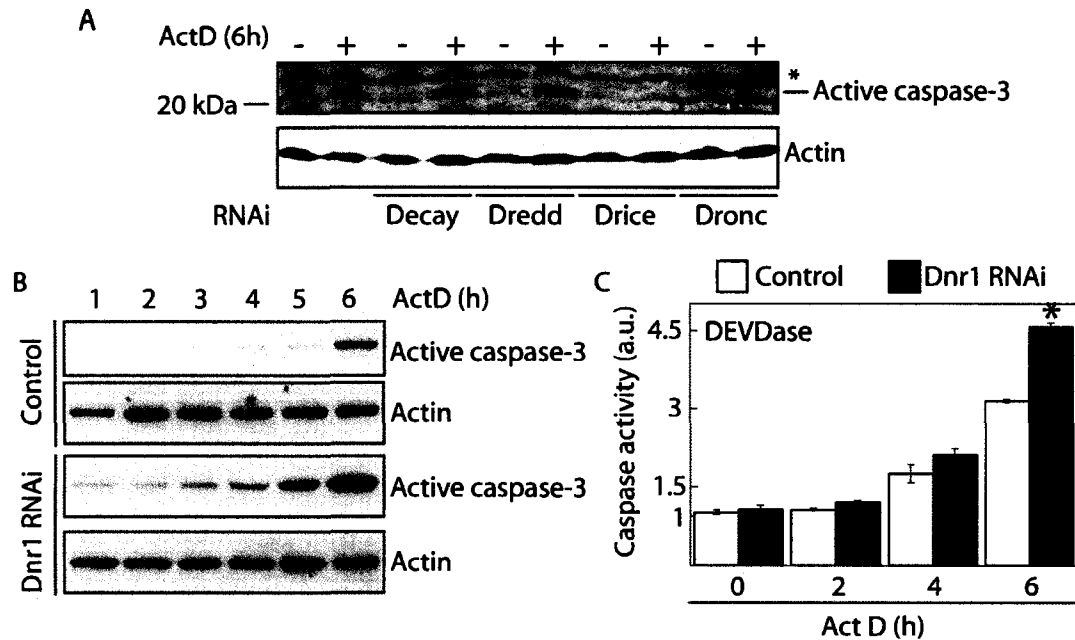
Figure 3.6 Depletion of Dnr1 enhances actinomycin D induced caspase activation and activity (A) Western blot analysis of lysates from control S2 cells (lanes 1&2), S2 cells incubated with Decay dsRNA (lanes 3&4), S2 cells incubated with Dredd dsRNA (lanes 5&6), S2 cells incubated with Drice dsRNA (lanes 7&8) and S2 cells incubated with Dronc dsRNA (lanes 9&10). Cells were incubated with actinomycin D for 6 hours where indicated. Lysates were probed with an anti-active-caspase-3 antibody (top blot) and an anti-actin antibody (bottom blot), which served as a loading control. An anti-active-caspase-3 signal was detected after actinomycin D in control S2 cells and S2 cells treated with Decay or Dredd dsRNA, whereas the signal is abrogated in S2 cells treated with Drice or Dronc dsRNA after actinomycin D exposure. * indicates a cross reactive band. (B) Western blot analysis of lysates from control S2 cells (top two blots) and S2 cells treated with Dnr1 dsRNA (bottom two blots). Cells were incubated with actinomycin D for the indicated times and lysates were probed with an anti-active-caspase-3 antibody (first and third blot) and an anti-actin antibody (second and forth blot), which served as a loading control. We detected an earlier and more intense anti-active-caspase-3 signal in S2 cells treated with Dnr1 dsRNA compared to control S2 cells. (C) DEVDase caspase activity assay. S2 cells and S2 cells treated with Dnr1 dsRNA were incubated with actinomycin D for the indicated times and DEVDase activity was measured. We detected a significant increase in DEVDase activity in S2 cells treated with Dnr1 dsRNA compared to control S2 cells. Results are the mean of three independent experiments and error bars indicate standard error. * indicates values that differ significantly from S2 cells with a p<0.01. Dnr1 depletion results in increased caspase activation and activity in S2 cells. (E. Foley contributed panels B and C)

50

3.2.3 Depletion of Dnr1 Sensitizes S2 Cells to Apoptotic Induction

Dnr1 depletion in S2 cells led to increased Dronc protein levels and increased actinomycin D induced caspase activity compared to control S2 cells. Based on these results, I hypothesized that depletion of Dnr1 would sensitize S2 cells to the induction of apoptosis. To test this hypothesis, I incubated S2 cells with Dnr1 dsRNA to deplete endogenous Dnr1 and I incubated a second group of S2 cells with GFP dsRNA to serve as a control. Seventy-two hours after incubation with their respective dsRNAs, I induced apoptosis in the respective S2 cells with various concentrations of actinomycin D. To monitor apoptosis, I measured the apoptotic index of the S2 cells over the six hour actinomycin D time course. At all three concentrations of actinomycin D, control and GFP dsRNA treated S2 cells had similar apoptotic indices (Figure 3.7 a-c). In contrast, I detected a significant increase in the apoptotic index of Dnr1 dsRNA treated S2 cells compared to control S2 cells within four hours of incubation with 0.1 or 1μm of actinomycin D. The apoptotic index of the Dnr1 dsRNA treated S2 cells remained significantly elevated at the six hour time point (Figure 3.7 b,c). At lower concentrations of actinomycin D (0.01μm), I detected a significant increase in the apoptotic index of Dnr1 dsRNA treated S2 cells compared to control S2 cells within two hours of actinomycin D exposure. Additionally, the apoptotic index of Dnr1 dsRNA treated S2 cells was more than double that of control S2 cells at both the four and six hour time point after exposure to 0.01μm of actinomycin D (Figure 3.7 a). The results of this section demonstrate that the depletion of Dnr1 sensitizes S2 cells to the actinomycin D induced apoptosis. The sensitization to apoptosis is more dramatic at lower concentrations of actinomycin D, which barely induced apoptosis in control S2 cells.
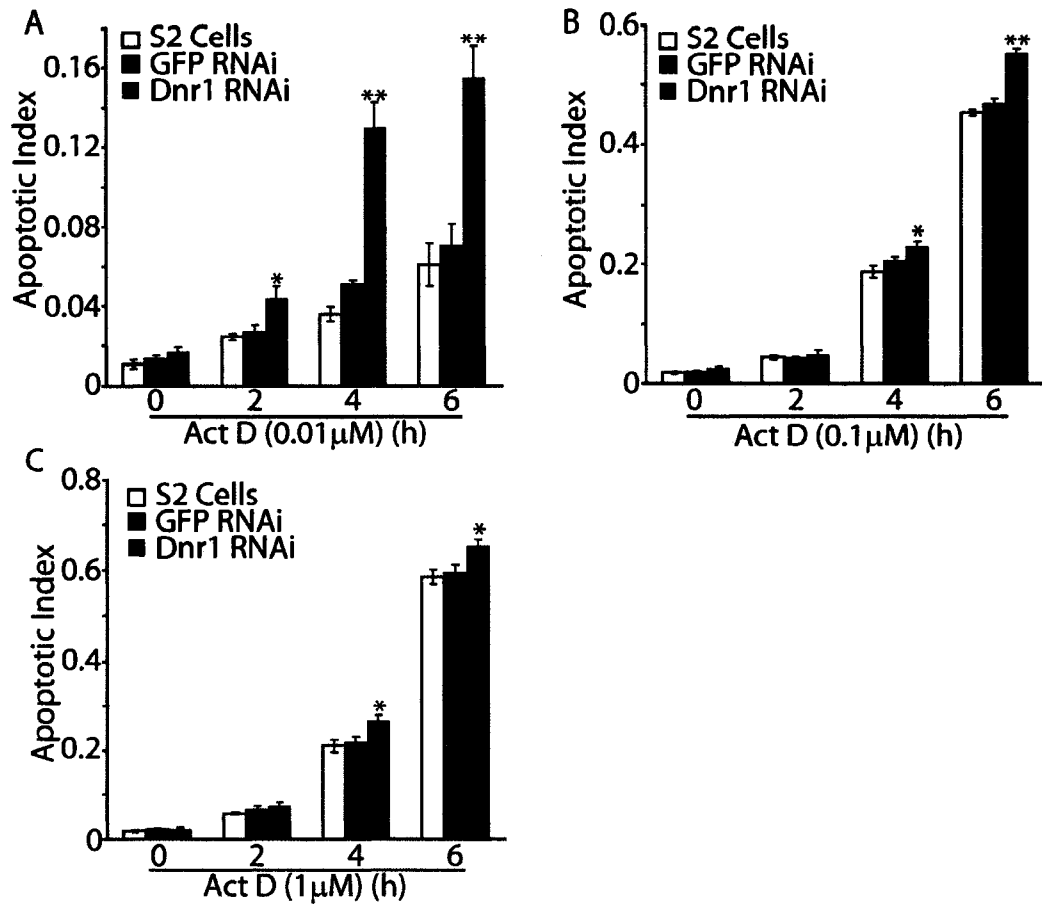
Figure 3.7 Depletion of Dnr1 sensitizes S2 cells to actinomycin D induced apoptosis. (A-C) The apoptotic indexes of S2 cells, GFP dsRNA-treated S2 cells or Dnr1 dsRNA-treated S2 cells. The individual cell lines were incubated with 0.01 (A), 0.1 (B) or 1μM (C) actinomycin D and the apoptotic indexes of were determined at the indicated time points. Results are the mean of three independent experiments and error bars indicate standard error. ** and * indicates values that differ significantly from S2 cells with a $p<0.01$ and $p<0.05$, respectively. Depletion of Dnr1 from S2 cells results in elevated apoptosis in response to actinomycin D treatment.

3.2.4 Dnr1 Mediates Depletion of Dronc in a RING Domain-Dependent Manner

As depletion of Dnr1 in S2 cells led to increased Dronc protein levels, I tested whether overexpression of Dnr1 had the converse effect. Specifically, I monitored the ability of Dnr1 to diminish myc-Dronc protein levels in S2 cells. To this end, I transfected S2 cells and S2 cells that stably express HA-Dnr1 or HA-Dnr1C563Y with a plasmid that drives constitutive expression of N-terminally, 6xmyc-tagged Dronc (myc-Dronc). Twenty-four hours after transfection, I performed Western blot analysis of cell lysates with an anti-myc antibody and an anti-actin antibody, which served as a loading control for quantification purposes. I detected three distinct myc-Dronc signals in the transfected cell lines (Figure 3.8 a lanes 2-4). The signals correspond to full length myc-Dronc (FL) and two previously described Dronc isoforms, cleaved at aspartate residue 113 or 135 (D113 and D135, respectively). The signals of all three myc-Dronc isoforms appeared diminished in S2 cells stably expressing HA-Dnr1 compared to both the control S2 cells and the S2 cells that stably express HA-Dnr1C563Y. To confirm this observation, I quantified the individual levels of the three myc-Dronc isoforms relative to a control protein (actin) for each transfected cell line. The quantifications revealed a significant reduction in the myc-Dronc:actin ratio, for all three myc-Dronc isofroms, in S2 cells that stably express HA-Dnr1 compared to control S2 cells (Figure 3.8 b). The myc-Dronc:actin ratio for all three Dronc isoforms in control S2 cells was more than double that observed in S2 cells that stably express HA-Dnr1. Interestingly, expression of HA-Dnr1C563Y did not have an effect on the protein levels of the three Dronc isoforms, as I detected similar myc-Dronc:actin ratios in S2 cells that stably express HA-Dnr1C563Y and in control S2 cells. The results of this section are consistent with a

role for Dnr1 in the regulation of Dronc protein levels. Overexpression of HA-Dnr1 resulted in diminished myc-Dronc protein levels in S2 cells, which is in agreement with the increased Dronc protein levels observed in Dnr1 depleted S2 cells (Figure 3.2). Furthermore, consistent with the observations for Dredd (Figure 3.6), Dnr1 requires an intact RING domain to mediate the depletion of myc-Dronc protein levels in S2 cells.
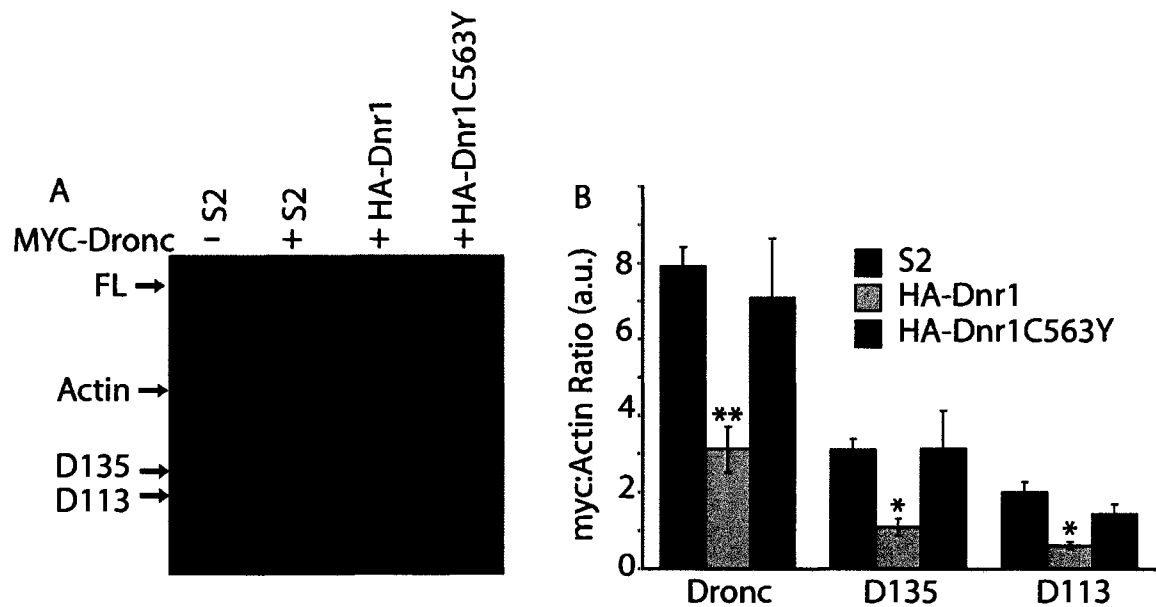
Figure 3.8 Dnr1 depletes Dronc protein levels in S2 cells. (A) Western blot analysis of S2 cells, S2 cells that stably express HA-Dnr1 and S2 cells that stably express HA-Dnr1C563Y. The individual cell lines were transfected with equal amounts of a plasmid that drives the expression of 6xmycDronc. Twenty-four hours after transfection, cell lysates were probed with anti-myc (red) and anti-actin (green) antibodies. Three distinct Dronc isoforms were detected corresponding to full-length (FL), D135 and D113 isoforms. (B) Serial dilutions of lysates from S2 cells, S2 cells that stably express HA-Dnr1 and S2 cells that stably express HA-Dnr1C563Y transfected with 6xmycDronc expression plasmid were analyzed by Western blot analysis. The levels of FL, D135 and D113 isoforms of Dronc were quantified relative to the level of a control protein (actin). The levels of all three Dronc isoforms is significantly reduced in S2 cells that stably express HA-Dnr1 compared to control S2 cells, whereas the stable expression of HA-Drn1C563Y in S2 cells fails to impact Dronc protein levels. Results are the mean of three independent experiments and error bars indicate standard error. ** and * indicates values that differ significantly from S2 cells with a p<0.01 and p<0.05 respectively. Dnr1 mediates the depletion of myc-Dronc in S2 cells in a RING domain dependent manner.

3.2.5 Dnr1 Overexpression in S2 Cells Prevents the Induction of Apoptosis

Overexpression of Dnr1 led to the depletion of myc-tagged Dronc protein levels in S2 cells. As Dronc is the critical initiator caspase in the *Drosophila* apoptotic cascade, I hypothesized that overexpression of Dnr1 would protect S2 cells from induction of apoptosis. To test this hypothesis, I exposed S2 cells and S2 cells that stably express HA-Dnr1 or HA-Dnr1C563Y to actinomycin D for six hours. We then collected cell lysates and performed a DEVDase assay to measure caspase activity. We detected more than a six fold increase in DEVDase activity in both control S2 cells and S2 cells that stably express HA-Dnr1C563Y after exposure to actinomycin D (Figure 3.9 a, columns 2 and 4). In contrast, S2 cells that stably express HA-Dnr1 had no detectable increase in DEVDase activity after actinomycin D exposure (Figure 3.9 a, column 3).

We also measured the apoptotic index of control S2 cells and S2 cells that stably express HA-Dnr1 or HA-Dnr1C563Y after exposure to actinomycin D. The three cell lines had similar basal levels of apoptosis (Figure 3.9 b, column 1-3). After a six hour incubation period with actinomycin D, both S2 cells and S2 cells that stably express HA-Dnr1C563Y had more than a four fold increase in their apoptotic indexes (Figure 3.9 b, column 4 and 5). In contrast, the apoptotic index of S2 cells that stably express HA-Dnr1 remained at background levels (Figure 3.9 b, column 6). The inhibition of apoptosis in S2 cells that stably express HA-Dnr1 corresponded to the lack of caspase activity detected in the DEVDase assay. The results of this section demonstrate that overexpression of Dnr1 protects S2 cells from actinomycin D induced apoptosis.
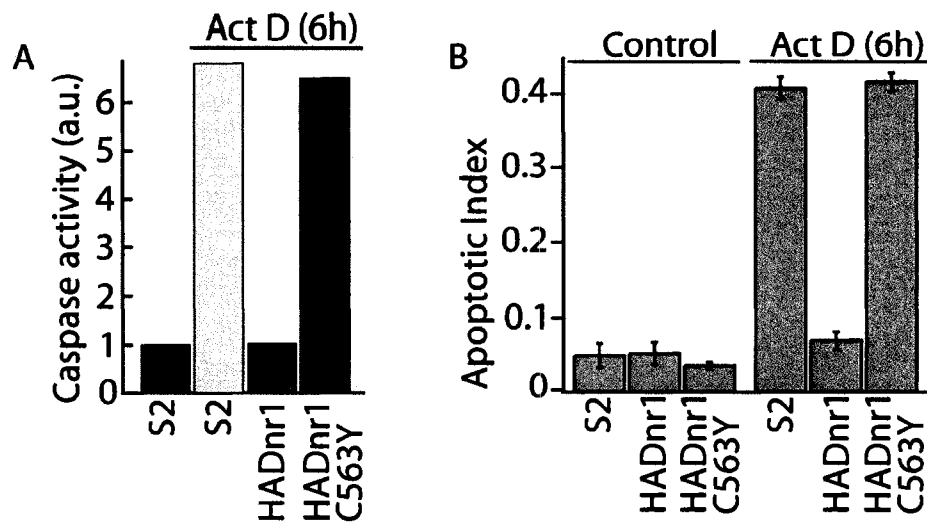
Figure 3.9 Overexpression of Dnr1 inhibits actinomycin D induced caspase activity and apoptosis. (A) DEVDase caspase activity in lysates from S2 cells, S2 cells treated with actinomycin D, S2 cells that stably express HA-Dnr1 treated with actinomycin D and S2 cells that stably express HA-Dnr1C563Y treated with actinomycin D. We detected a significant decrease in DEVDase activity in S2 cells that stably express HA-Dnr1 compared to control S2 cells, whereas the expression of HA-Dnr1C563Y fails to impact actinomycin D induced caspase activity. (B) The apoptotic indexes of S2 cells, S2 cells that stably express HA-Dnr1 or HA-Dnr1C563Y before (columns 1-3) or after exposure to actinomycin D (columns 4-6). We detected a significant decrease in the apoptotic index of S2 cells that stably express HA-Dnr1 compared to control S2 cells, whereas the expression of HA-Dnr1C563Y had no impact on the apoptotic index. Results are the mean of three independent experiments and error bars indicate standard error. (E. Foley contributed panels A and B)

3.2.6 Dnr1 Overexpression Protects the *Drosophila* Eye from HID Induced Apoptosis

To determine if Dnr1 interacts with the apoptotic machinery in the whole organism, I took advantage of the Upstream Activating Sequence (UAS)/GAL4 expression system to monitor Dnr1 regulation of apoptosis in the developing eye. I chose the developing eye as it is a dispensable structure and apoptosis is readily detected by simple visual inspection of the adult eye. The *Drosophila* adult eye is a highly organized structure that consists of approximately 800 ommatidia (Figure 3.10 a). Overexpression of the pro-apoptotic molecule Hid, using the GMR promoter (GMR-Hid), in cells behind the mophogenetic furrow of the developing eye results in a severely reduced adult eye from apoptosis (Figure 3.10 b). To determine if Dnr1 inhibits Hid induced apoptosis in the developing eye, I designed a series of crosses to co-express one or two copies of UAS-HA-Dnr1 with GMR-Hid in the developing eye. An ey-GAL4 driver regulated the expression of UAS-HA-Dnr1 in the developing eye. ey-GAL4 is expressed throughout the eye prior to the activation of the GMR promoter and therefore, the progeny express HA-Dnr1 in the eye prior to induction of Hid expression. Flies that expressed HA-Dnr1 in the absence of GMR-Hid expression had wild-type adult eye in appearance (Figure 3.10 c). In contrast, Flies that expressed one copy of GMR-Hid in a UAS-HA-Dnr1 background, had severely reduced adult eyes due to widespread apoptosis during eye development (fig 2.6 D). Co-expression of one copy of HA-Dnr1 in the presence of one copy of GMR-Hid resulted in a partial restoration of the adult eye (compare Figure 3.10 E to D). Co-expression of two copies of HA-Dnr1 in the presence of one copy of GMR-Hid results in almost a complete restoration of the adult eye (Figure 3.10 F).

Thus, I conclude that, similar to the observations in S2 cells, overexpression of Dnr1 in the developing *Drosophila* eye inhibits the induction of apoptosis by Hid.
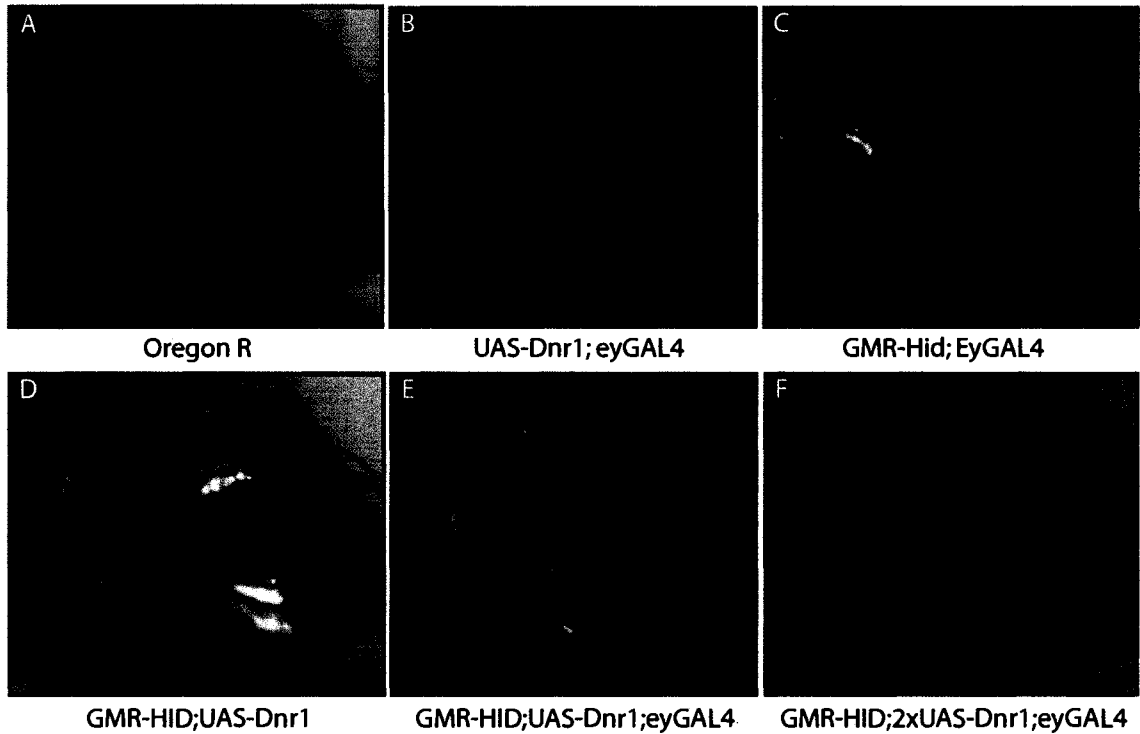
Figure 3.10   Dnr1 blocks Hid induced apoptosis in the developing eye. (A-F) Phenotypic series of *Drosophila* eyes from (A) Oregon R (WT), (B) UAS-Dnr1/+;ey-GAL4, (C) GMR-Hid/GMR-Hid;eyGAL4/+, (D) GMR-HID/+; UAS-Dnr1/+, (E) GMR-HID/+; UAS-Dnr1/+;eyGAL4/+ and (F) GMR-HID/+; UAS-Dnr1/UAS-Dnr1;ey-GAL4/+ flies. Expression of the pro-apoptotic molecule Hid in the eye during development ablates the fly eye (C and D). The prior induction of one copy of Dnr1 (E) partially reverses and two copies of Dnr1 (F) strongly reverses Hid induced eye ablation. The overexpression of Dnr1 in the developing eye inhibits Hid induced apoptosis.

3.3 Analysis of Dnr1 Interactions with Dredd and Dronc

3.3.1 Dnr1 Mediated Depletion of Dredd and Dronc is Pro-Domain Independent

Stable expression of HA-Dnr1 in S2 cells results in depletion of F-H-Dredd-M and myc-Dronc. Additional work in our lab determined that HA-Dnr1 does not affect the protein levels of the effector caspase Drice (Adam Hrdlicka, unpublished). Initiator caspases have large prodomains which contain protein interaction domains, such as CARD in Dronc and the unique DID domain found in Dredd, that are absent from the prodomains of effector caspases. Based on these observations, I hypothesized that Dnr1 recognizes a structural feature of the prodomains of Dredd and Dronc to mediate their depletion. To test this hypothesis, I transfected S2 cells and S2 cells that stably express HA-Dnr1 or HA-Dnr1C563Y with a plasmid that drives the constitutive expression of FLAG-HA-Dredd-myc that lacks a prodomain (F-H-DreddΔPD-myc) (Figure 3.11 a) or an N-terminally 6Xmyc-tagged Dronc that lacks a prodomain (myc-DroncΔPD) (Figure 3.11 b). Twenty-four hours after transfection, I performed a Western blot analysis of cells lysates with an anti-HA antibody for F-H-DreddΔPD-myc lysates and an anti-myc antibody for myc-DroncΔPD lysates. Additionally, I probed the blot with an anti-actin antibody as a loading control for all cells lysates. I detected a single band that corresponds to F-H-DreddΔPD-myc (Figure 3.11 a, lanes 2-4) or a single band that corresponds to myc-DroncΔPD (Figure 3.11 b, lanes 2-4) in the individual transfected cell lines. Interestingly, F-H-DreddΔPD-m and myc-DroncΔPD protein levels appeared diminished in S2 cells that stably express HA-Dnr1, compared to both control S2 cells and S2 cells that stably express HA-Dnr1C563Y.

To confirm this observation, I quantified F-H-DreddΔPD-m or myc-DroncΔPD

protein levels relative to a control protein (actin) in the individual cell lines. The

quantifications revealed that the F-H-DreddΔPD-m:actin ratio was significantly reduced

in S2 cells that stably express HA-Dnr1 compared to control S2 cells (Figure 3.11 a). The

F-H-DreddΔPD-m:actin ratio in control S2 cells was more than double that observed in

S2 cells that stably express HA-Dnr1. Expression of HA-Dnr1C563Y did not affect

F-H-DreddΔPD-m protein levels in S2 cells, as the F-H-DreddΔPD-m:actin ratio was

similar in S2 cells that stably express HA-Dnr1C563Y and control S2. I observed a

similar result after quantification of the myc-DroncΔPD protein levels in the individual

S2 cell lines (Figure 3.11 b). The myc-DroncΔPD:actin ratio was significantly lower in

S2 cells that stably express HA-Dnr1 compared to control S2 cells, whereas

HA-Dnr1C563Y expression had no impact on myc-DroncΔPD protein levels. These data

indicate that the prodomain of Dredd and Dronc is not required for Dnr1-mediated

depletion of Dredd and Dronc. Additionally, the results of the Western blot analysis

confirm the requirement of a functional RING domain in Dnr1 to mediate the depletion

of Dredd and Dronc.

A

F-H-DreddΔPD-M

-S2 +S2 +HA-Dnr1 +HA-Dnr1C563Y

DreddΔPD

Actin

DreddΔPD:
Actin Ratio

10
8
4
0

**

B

MYC-DroncΔPro

-S2 +S2 +HA-Dnr1 +HA-Dnr1C563Y

Myc

Actin

myc:Actin Ratio

10

5

0

**
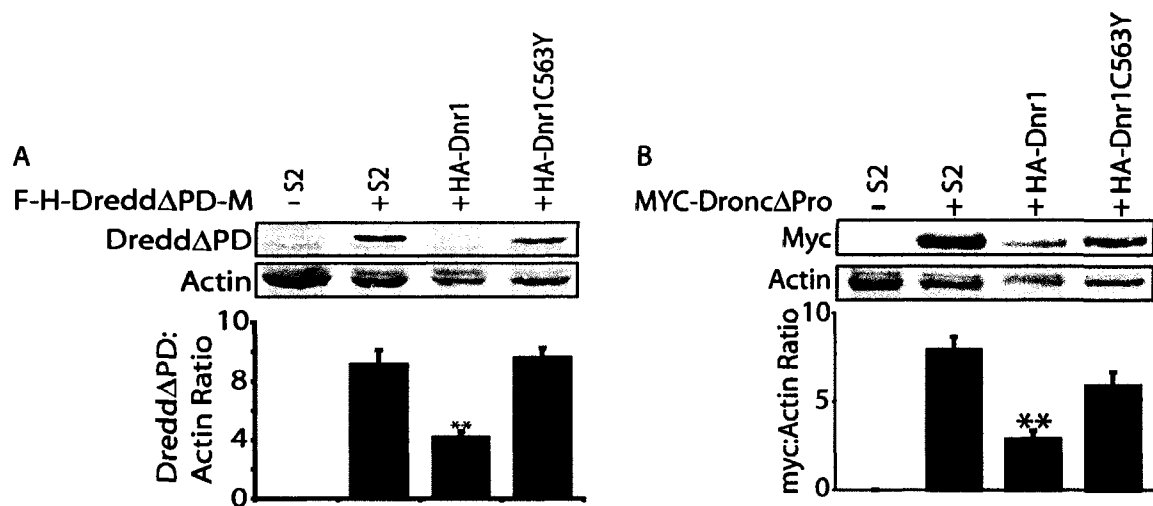
Figure 3.11   Dnr1-dependent destruction of Dredd and Dronc is pro-domain independent. (A) Western blot analysis of S2 cells, S2 cells that stably express HA-Dnr1 and S2 cells that stably express HA-Dnr1C563Y. The individual cell lines were transfected with equal amounts of a plasmid that drives the expression of F-H-Dredd-MΔPD. Twenty-four hours after transfection, cell lysates were probed with an anti-HA antibody (top panel) and an anti-actin antibody (middle panel), which served as a loading control. The level of F-H-Dredd-MΔPD was quantified relative to the level of a control protein (actin) (bottom panel). Results are the mean of three independent experiments and error bars indicate standard error. ** indicates values that differ significantly from S2 cells with a P<0.01. Dnr1 mediates the depletion of F-H-Dredd-MΔPD in S2 cells in a RING domain dependent manner. (B) Western blot analysis of S2 cells, S2 cells that stably express HA-Dnr1 and S2 cells that stably express HA-Dnr1C563Y. The individual cell lines were transfected with equal amounts of a plasmid that drives the expression of 6xmycDroncΔPD. Twenty-four hours after transfection, cell lysates were probed with an anti-myc antibody (top panel) and an anti-actin antibody (middle panel), which served as a loading control. The level of myc-DroncΔPD was quantified relative to the level of a control protein (actin) (bottom panel). Results are the mean of three independent experiments and error bars indicate standard error. ** indicates values that differ significantly from S2 cells with a p<0.01. Dnr1 mediates the depletion of myc-DroncΔPD in S2 cells in a RING domain dependent manner.

3.3.2 Dnr1 Stability in S2 Cells is Dependent on a RING Domain and N-terminal Motifs

I consistently observed that site-directed mutagenesis of the RING domain in Dnr1 results in increased stability of Dnr1 upon expression in S2 cells. In addition to the RING domain, Dnr1 contains an N-terminal FERM domain, a central glutamine/serine-rich region and a FERM_C motif. To determine if additional Dnr1 domains contribute to Dnr1 stability in S2 cells, E. Foley and G. Johnson generated a series of deletion constructs that sequentially remove each domain from Dnr1 (Figure 3.12 a) and I established a series of S2 cells that stably express N-terminally GFP-tagged versions of each construct. I collected cell lysates from each stable cell line and probed them with an anti-GFP antibody by Western blot analysis. Consistent with previous observations, I could barely detect full length Dnr1 on the Western blot (Figure 3.12 b, lane 6), whereas I readily detected a GFP signal from S2 cells that stably express Dnr1 with a RING domain deletion (Figure 3.12 b, lanes 3-5). Interestingly, I consistently observed a more intense GFP signal from S2 cells that stably express $Dnr1^{397-677}$ and $Dnr1^{324-677}$ compared to full length Dnr1 (Figure 3.12 b, lanes 7,8). Both $Dnr1^{397-677}$ and $Dnr1^{324-677}$ have N-terminal deletions, but still retain an intact RING domain. This result indicates that N-terminal motifs within Dnr1 regulate the stability of Dnr1 in S2 cells.

To confirm this observation, I transfected S2 cells with equal amounts of plasmids that drive constitutive expression of N-terminally GFP-tagged full-length Dnr1, $Dnr1^{397-677}$ or $Dnr1^{324-677}$. Twenty-four hours after transfection, I performed a Western blot analysis of cell lysates with an anti-GFP antibody and an anti-actin antibody as a loading control. Consistent with the results from the stable cell lines, S2 cells that express

GFP-Dnr1$^{397\text{-}677}$ and GFP-Dnr1$^{324\text{-}677}$ had a more intense GFP signal compared to the S2

cells that express full-length GFP-Dnr1 (Figure 3.12 c, lanes 2-4). Thus, I conclude that

both N-terminal motifs and the RING domain regulate Dnr1 stability and that deletion of

either motif is sufficient to stabilize Dnr1 in S2 cells.
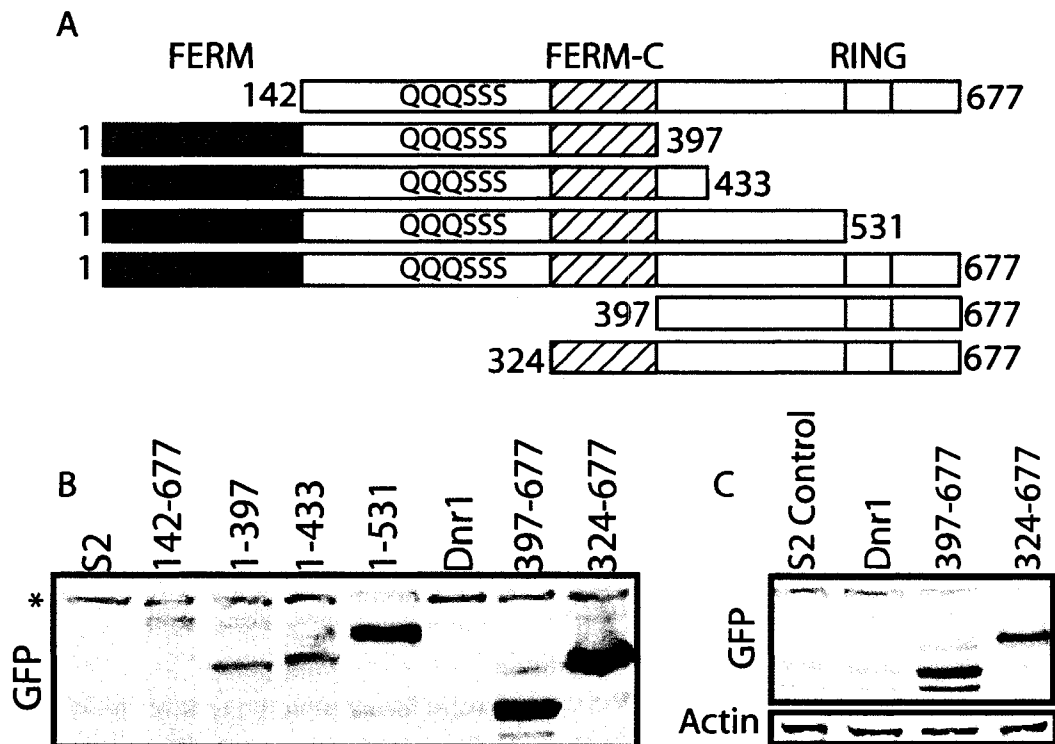
Figure 3.12   Identification of Dnr1 domains that regulate Dnr1 stability. (A) Schematic representation of Dnr1. Dnr1 contains and N-terminal FERM domain (purple), a Glutamine/Serine rich region, a FERM_C motif (hatched) and a RING domain (yellow).The indicated series of GFP-tagged expression constructs were prepared. (B) Anti-GFP Western blot analysis of lysates from S2 cells and S2 cells stably expressing the series of GFP-tagged expression constructs. * indicates a cross reactive band. (C, top panel) Anti-GFP Western blot of lysates from control S2 cells (lane 1) and S2 cells transfected with equal amounts of plasmids that drive the expression of Dnr1(lane 2), Dnr1$^{397\text{-}677}$ (lane 3) and Dnr1$^{324\text{-}677}$ (lane 4). (C, bottom panel) Anti-actin Western blot is shown as a loading control.

3.3.3 Identification of Dnr1 Domains Required to Mediate Dronc Depletion in S2 Cells

To identify the domains of Dnr1 involved in Dronc depletion, I monitored myc-Dronc protein levels in the series of S2 cells that stably express the various Dnr1 deletion constructs (Figure 3.12 a). Specifically, I transfected each S2 cell line with a plasmid that drives constitutive expression of N-terminally 6Xmyc-tagged Dronc (myc-Dronc). Twenty-four hours after transfection, I performed a Western blot analysis of cell lysates with an anti-myc antibody and an anti-actin antibody as a loading control for quantification purposes. I observed three bands that correspond to the full length myc-Dronc (FL) and two Dronc isoforms cleaved at aspartate residue 113 and 135 (D113 and D135, respectively) in the individual transfected cell lines (Figure 3.13 a). I then quantified the full length myc-Dronc protein levels relative to actin (Figure 3.13 a). As expected, S2 cell lines that stably express Dnr1 with C-terminal deletions, which lack the RING domain ($Dnr1^{1-397}$, $Dnr1^{1-433}$ and $Dnr1^{1-531}$) had significantly elevated myc-Dronc protein levels compared to S2 cells that stably express full length Dnr1 (Figure 3.13 a, bottom panel). Surprisingly, I observed significantly elevated levels of myc-Dronc in S2 cells that stably express $Dnr1^{142-677}$ compared to S2 cells that stably express full-length Dnr1.

As the $Dnr1^{142-677}$ construct has an intact RING domain but lacks the N-terminal FERM domain, it is possible the N-terminal FERM domain is also required for Dnr1-mediated myc-Dronc depletion. The FERM domain is a plasma membrane-binding domain, involved in the linkage of cytoplasmic proteins to the membrane. The loss of the FERM domain may alter the subcellular localization of $Dnr1^{142-677}$, and thereby

64

contributes to the inability of $Dnr1^{142-677}$ to deplete myc-Dronc. Two additional Dnr1 deletion constructs, $Dnr1^{324-677}$ and $Dnr1^{397-677}$, that contained an intact RING domain also lacked the N-terminal FERM domain, but retained the ability to deplete Dronc (Figure 3.13 a). The $Dnr1^{324-677}$ and $Dnr1^{397-677}$ constructs lacked the glutamine/serine-rich region in addition to the FERM domain (Figure 3.12). Analysis of the glutamine/serine rich region revealed three putative Nuclear Localization Signals (NLS) (Figure 3.13 b). To determine if the unmasking of the NLS by loss of the FERM domain altered the sub-cellular localization of Dnr1, we compared the sub-cellular localization of $Dnr1^{142-677}$ and $Dnr1^{324-677}$ in S2 cells. Confocal microscopy analysis revealed that $Dnr1^{142-677}$ is a nuclear protein, whereas $Dnr1^{324-677}$ displayed a broad cytoplasmic localization (Figure 3.13 C-M).

The results of the Dnr1 domain analysis indicate that the RING domain of Dnr1 is essential for depletion of the initiator caspase Dronc. However, Dnr1-mediated depletion of Dronc may also depend on the sub-cellular localization of the proteins. Specifically, cytoplasmic localization of Dnr1 and Dronc is required for Dnr1 to mediate Dronc depletion.

A FL→

Actin→

D135→
D113→

B

PMREMRR ELAQQQQQ
QQQQAQQHRLEQQR
KEK E HVLSF KKRR LSK

mycactin ratio

10

8 *
*
6 *
*
4
2
0

142-677
1-397
1-433
1-531
Dnr1
397-677
324-677

Phalloidin   Hoechst   GFP   Merge

C   D   E   F

Dnr1^{142-677}

G   H   I   J

Dnr1^{142-677}

K   L   M

Dnr1^{324-677}
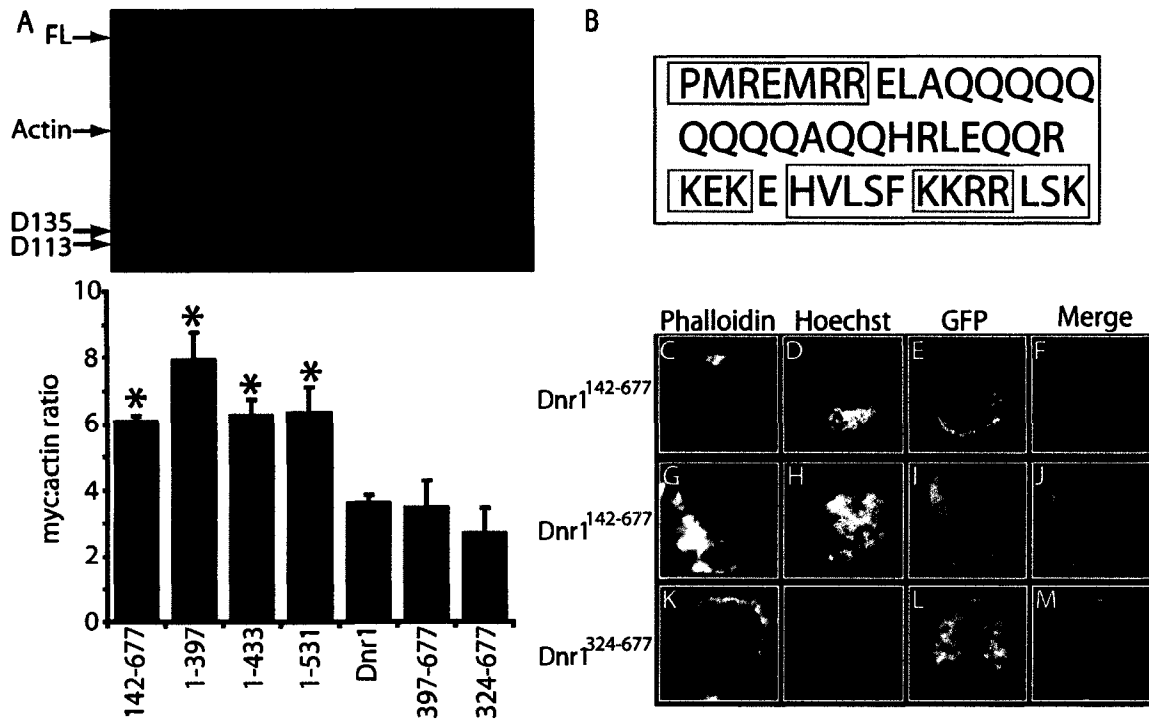
Figure 3.13 Domains of Dnr1 required for Dronc depletion. (A, top panel) Western blot analysis of S2 cells that stably express the series of GFP-tagged Dnr1 expression constructs (fig 3.2A). The individual cell lines were transfected with equal amounts of a plasmid that drives the constitutive expression of 6xmycDronc. Twenty-four hours after transfection, cell lysates were probed with anti-myc and anti-actin antibodies. Three distinct Dronc isoforms were detected corresponding to full-length (FL), D135 and D113 isoforms. (A, bottom panel) myc-Dronc was quantified relative to a control protein (actin). Dnr1$^{324-677}$ and Dnr1$^{397-677}$-expressing cells diminished Dronc levels to a similar extent as wild-type Dnr1. Results are the mean of three independent experiments and error bars indicated standard error. * indicates values that differ significantly from S2 cells that stably express GFP-Dnr1 with a $p<0.05$. (B) Primary sequence of residues 150-193 in Dnr1. Three potential NLS are indicated, two are boxed blue or red boxes, a putative bipartite NLS is boxed green. (C-M) Confocal images of S2 cells transfected with GFPDnr1$^{142-677}$ (C-J) and GFPDnr1$^{324-677}$ (K-M). In the merged images of panels F and M GFP is shown in green, DNA is visualized in blue and filamentous actin is labeled in red. In the merged image of panel J, GFP is shown in green, DNA is visualized in blue and the nuclear envelope is visualized in red with Alexa Fluor-568-labeled wheat germ agglutinin. Whereas GFPDnr1$^{324-677}$ is cytoplasmic GFPDnr1$^{142-677}$ is a nuclear protein. Panels C-F and K-M are shown at 100x magnification and panels G-J are shown at 200x magnification. (G. Johnson contributed panels C-M)

3.3.4 Dnr1 Auto-Ubiquitinates in a RING Domain-Dependent Manner

My analysis indicates that the Dnr1 RING domain is essential to mediate Dronc depletion. In addition, I have observed that loss of the Dnr1 RING domain increases Dnr1 stability in S2 cells. RING-domain proteins can regulate their own stability through auto-ubiquitination. To determine if the Dnr1 RING domain serves as an E3 ubiquitin ligase, I established an *in vitro* ubiquitination assay to monitor Dnr1 self-ubiquitination. To this end, I used commercially available E1, E2, ubiquitin and bacterially purified, recombinant Dnr1 or Dnr1C563Y for an *in vitro* ubiquitination assay. I monitored Dnr1 ubiquitination with an anti-ubiquitin antibody by Western blot analysis. I detected Dnr1 auto-ubiquitination at Dnr1 protein concentrations that ranged from 2μg down to 0.1μg (Figure 3.14 lanes3-8). In contrast to Dnr1, I detected no auto-ubiquitination with 2μg of Dnr1C563Y in the ubiquitination assay (Figure 3.14 lane 2). The results of the ubqiuitination assay indicate that Dnr1 auto-ubiquitinates and that auto-ubiquitiantion requires an intact RING domain on Dnr1, as Dnr1C563Y did not auto-ubiquitinate at concentrations that saw Dnr1 auto-ubiquitination.
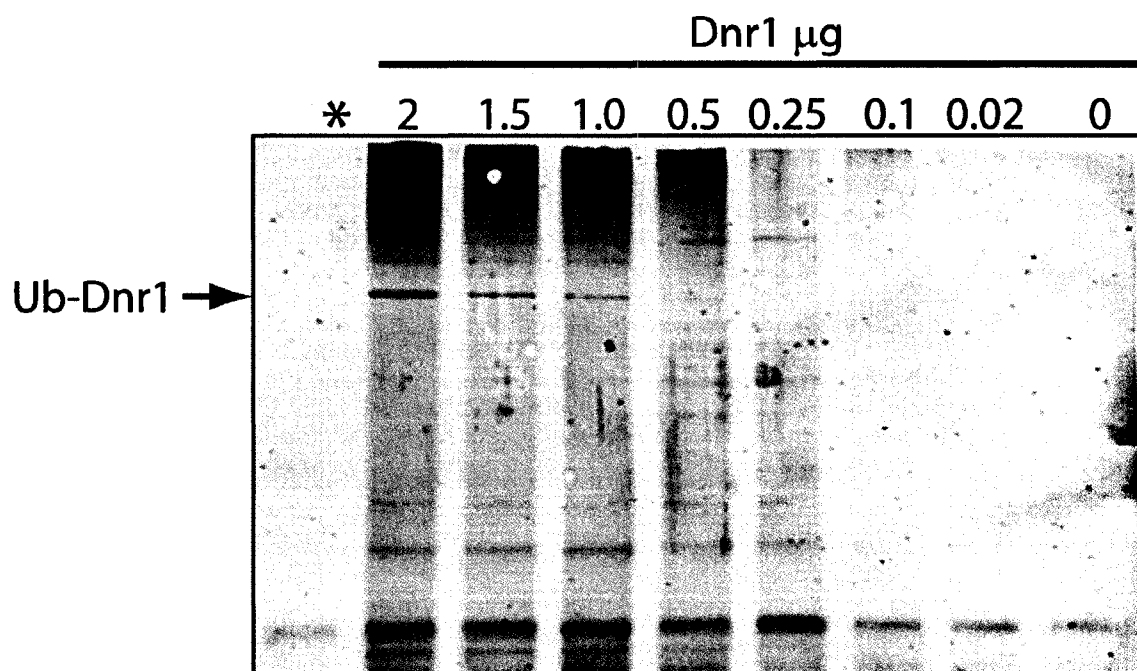
Figure 3.14 Dnr1 auto-ubiquitination in a RING domain-dependent manner. Anti-ubiquitin Western blot of an *in vitro* Dnr1 ubiquitination assay. The ubiquitination assay was performed with commercially available ubiquitin, E1 and E2. 2µg of purified recombinant Dnr1C563Y (lane 1) or various amounts of purified recombinant Dnr1 (as indicated lanes 2-10) served as the E3 ligase and target substrate. Full-length Dnr1 is indicated. Dnr1 auto-ubiquitinates in a RING domain-dependent manner.

Chapter 4

Discussion

4.1 S2 Cell Culture Analysis of Dnr1 Regulation of Imd Signaling

Innate immune signaling plays a critical role in the survival of all organisms. In most metazoans, the innate immune system is the only line of defense against invading microorganism. In higher eukaryotes, the innate immune system is required for an immediate response to an infection and is of critical importance in the progression of adaptive immune responses[5, 6]. Research in the model organism *Drosophila melanogaster* has uncovered the basic mechanisms behind innate immune signaling pathways, which are conserved with higher vertebrates[9]. The initial characterization of the Toll signaling pathway in *Drosophila* resulted in the search for and subsequent identification of the human toll homologs[22, 23]. The Imd signaling pathway responds to gram-negative bacterial infection and bears similarities to the human TNF pathway[48]. The Imd signaling pathway proceeds through NF-κB and JNK modules to initiate a diverse array of physiological responses. The initiator caspase Dredd is required for activation of both the NF-κB and JNK modules[58, 78]. However, we do not fully understand the mechanisms behind the regulation of Dredd activity in the Imd pathway. Recently, Dnr1 was identified as a regulator of Dredd activity in the absence of a microbial insult in *Drosophila* S2 cells[148].

In this study, I characterized the interactions of Dnr1 with Dredd in S2 cell culture assays and monitored the consequence of Dnr1 overexpression in S2 cells on the progression of the Imd immune response. Dnr1 contains a RING domain that is similar to the E3 ubiquitin ligase RING domain of DIAP1. E3 ubiquitin ligases form complexes with their target substrates in order to mark them for proteasomal degradation[137]. Based on these observations, I hypothesized that Dnr1 inhibits Dredd activity by the regulation of Dredd protein levels. Consistent with my hypothesis, I detected the formation of a complex between Dnr1 and Dredd in S2 cell culture (Figure 3.1). Formation of the Dnr1/Dredd complex did not require a catalytically active RING domain on Dnr1, as a Dnr1 variant (Dnr1C563Y) with a point mutation in a cysteine residue critical for RING domain activity also formed a complex with Dredd. A similar mutation (C406Y) has been shown to eliminate ubiquitin ligase function in DIAP1[143]. This result does not exclude the possibility that the RING domain of Dnr1 is required for complex formation with Dredd, as additional residues in the RING domain may mediate Dnr1/Dredd complex formation. While an active RING domain is not required for Dnr1/Dredd complex formation, RING domain activity is required for Dnr1-mediated Dredd depletion (Figure 3.2).These results indicate that Dnr1 regulates Dredd activity, at least partially, by inducing depletion of Dredd protein levels in a RING domain dependent manner, although I cannot rule out additional mechanisms. These mechanisms may include the sequestration of Dredd by Dnr1 or Dnr1 may target additional genes in the Imd pathway to inhibit signaling.

Downstream of Dredd activity, Imd signaling results in the production of the antimicrobial peptides, *att* and *dipt,* and in JNK-phosphorylation. In the initial study that characterized Dnr1 as a regulator Dredd activity in the Imd pathway, Dnr1 depletion

resulted in the ectopic production of a *dipt*-lacZ reporter[148]. Consistent with this finding, overexpression of Dnr1 in S2 cells prior to activation of the Imd signaling pathway resulted in significantly decreased *att* and *dipt* transcription (Figure 3.3). Additionally, I observed a significant reduction of Imd-dependent JNK-phosphorylation upon activation of the Imd pathway (Figure 3.4). Interestingly, overexpression of Dnr1C563Y prior to induction of Imd signaling resulted in a significant reduction in Imd-dependent *att* and *dipt* transcription and JNK-phosphorylation (Figure 3.3 & 3.4). This result may be a consequence of the complex formation observed between the Dnr1 variant and Dredd, which may inhibit Dredd activity in the Imd pathway. Although I have not ruled out the possibility that this result may be an artifact of overexpression of the Dnr1 variant, this observation suggests that Dnr1 may inhibit Dredd activity through a two step process.

The two step process involves the formation of an initial complex between Dnr1 and Dredd, which may contain additional proteins such as an E2 ubiquitin-conjugating enzyme. Although I have not directly shown that Dnr1 ubiquitinates Dredd, the RING domain of Dnr1 is an E3 ubiquitin ligase and as Dnr1 depletes Dredd in a RING domain-dependent manner, it appears likely that Dnr1 ubiquitinates Dredd. Thus I propose that the Dnr1 RING domain mediates the ubiquitination of Dredd thereby marking Dredd for proteasomal degradation. I do not believe the initial binding between Dnr1 and Dredd would be sufficient to inhibit Dredd activity. This is because overexpression of Dnr1C563Y only partially suppressed Dredd activity compared to the almost complete suppression with Dnr1 overexpression, even though I observed substantially higher levels of Dnr1C563Y compared to Dnr1 in S2 cells (Figure 3.1 b). Thus, I propose, the inhibition of Dredd activity observed with Dnr1C563Y overexpression is just an artifact

of the high levels of Dnr1C563Y and to inhibit Dredd activity, Dnr1 must deplete Dredd levels. In this regard, Dnr1 may act in a similar fashion to DIAP1. DIAP1 initially binds Dronc through a BIR domain. This binding is not sufficient to inhibit Dronc activity, but instead DIAP1 promotes Dronc ubiquitination through its C-terminal RING domain[127, 143]. However, the domain of Dnr1 required for Dredd binding remains to be identified and the primary sequence of Dnr1 does not contain a region that shares similarities to the BIR domain of DIAP1, which is required to bind Dronc.

While my research focused on Dnr1 regulation of the Imd pathway in S2 cell culture, additional work in our lab has demonstrated that Dnr1 functions in a similar regard in an *in vivo* setting (S. Guntermann, unpublished). In particular, the depletion of Dnr1 *in vivo* resulted in the ectopic transcription of *att* and *dipt* in the absence of infection. Conversely, overexpression of Dnr1 *in vivo* resulted in reduce *att* and *dipt* transcription in response to *E. coli* infection. The reduced *att* and *dipt* transcription corresponded to a decreased in viability in response to *E. coli* infection, of the *Drosophila* that overexpress Dnr1 compared to wild-type *Drosophila*.

In summary, I have identified a mechanism through which Dnr1 regulates Dredd activity in the Imd pathway. Specifically, Dnr1 complexes with Dredd, which results in the subsequent Dnr1 mediated depletion of Dredd. Accordingly, Dnr1 overexpression results in the downstream loss of *att* and *dipt* transcription and reduced JNK phosphorylation in the Imd pathway.

4.2 Analysis of Dnr1 Regulation of Caspase-Dependent Apoptosis

Caspases are essential mediators of the apoptotic cascade in eukaryotes. In mammals, an intrinsic cell death stimulus results in formation of an apoptosome, which is a large macromolecular complex consisting of the initiator caspase-9, Apaf-1 and cytochrome c and is required for the auto-processing and activation of the initiator caspase-9[86]. In *Drosophila,* activation of the initiator caspase Dronc requires the formation of a complex with the Apaf-1 homolog Dark[128-130]. However, in contrast to mammals, Dronc is normally held in an inactive from through an interaction with DIAP1. Upon receiving a cell death signal, cells up-regulate the expression of the DIAP1 antagonists Rpr, Hid and Grim, which disrupt DIAP1-Dronc interactions, allowing for Dronc auto-processing and activation. Upon activation, the initiator caspases cleave and activate effector caspases, which are responsible for the proteolytic cleavage of a wide range of cellular substrates, thus ushering in apoptosis. A key feature of both mammalian and *Drosophila* caspase-dependent apoptosis is the requirement to regulate caspase activation.

In this study, we characterized the S2 cell culture and *in vivo* role of the putative caspase inhibitor Dnr1. The initial characterization of Dnr1 determined that Dnr1 is involved in the regulation of Dredd activity in the Imd pathway. However, based on the observation that the RING domain of Dnr1 is highly similar to the RING domain of DIAP1, I tested if Dnr1 regulates the *Drosophila* initiator caspase Dronc, which functions in the apoptotic cascade. While it remains to be determined if Dnr1 and Dronc can form a complex similar to the complex between Dnr1 and Dredd, depletion of Dnr1 in S2 cells

resulted in the concomitant increase in full length Dronc levels prior to apoptotic induction. The elevated full length Dronc levels were associated with an increase in the active form of Dronc after apoptotic stimulation (Figure 3.5). Conversely, overexpression of Dnr1 in S2 cells resulted in the depletion of Dronc protein levels. Consistent with the observations for Dredd, an active RING domain was required for Dnr1-mediated depletion of Dronc (Figure 3.8). These data indicated that Dnr1 negatively regulates Dronc in the apoptotic cascade through depletion of Dronc protein.

Downstream of Dronc, apoptotic signaling results in the activation of the effector caspases Drice and Dcp-1 and ultimately cell death. To monitor caspase activation, I used a commercially available anti-active-caspase-3 antibody, which is a reliable indicator of *Drosophila* apoptotic progression. Initially, I determined that the antibody recognizes a Drice-dependent antigen downstream of Dronc in the apoptotic cascade in *Drosophila* S2 cells (Figure 3.6 a). Thus, the anti-active-caspase-3 antibody is a reliable indicator of apoptotic progression downstream of Dronc.

Depletion of Dnr1 in S2 cells prior to the induction of apoptosis resulted in increased caspase activation and activity (Figure 3.6). Correspondingly, Dnr1-depleted S2 cells had an increased apoptotic index compared to control S2 cells (Figure 3.7). Overexpression of Dnr1 in S2 cells had the opposite effect with decreased caspase activity and the protection of S2 cells from apoptotic death (Figure 3.9). These results indicate that Dnr1 negatively regulates caspase-dependent apoptosis in S2 cells. In contrast to DIAP1, Dnr1 does not appear to be essential for caspase inhibition. Instead, Dnr1 appears to partially suppress caspase activity in a similar fashion to DIAP2. Depletion of DIAP2 in S2 cells results in a moderate elevation of caspase activity and a

recent study demonstrated that overexpression of DIAP2 inhibits apoptosis *in vivo*[101, 155].

Additionally, while overexpression of the Dnr1 variant with a point mutation in a cysteine residue critical for RING domain activity inhibits Imd signaling, there was no impact on apoptosis induced by cytotoxic agents. However, overexpression of the RING-domain-inactive Dnr1 variant blocked apoptosis induced by DIAP1 RNAi[156]. This may reflect a fundamental difference in the way Dnr1 interacts with the apoptotic machinery induced by cytotoxic agents or genetic triggers, such as DIAP1 RNAi. The difference in the requirement for an active RING domain to inhibit apoptosis induced by two different triggers is not unique to Dnr1. For example, an active DIAP1 RING domain is required to inhibit Rpr induced apoptosis in S2 cells and *in vivo*, whereas a RING domain-inactive version of DIAP1 inhibits HID-induced apoptosis both in S2 cells and *in vivo*[157, 158].

To determine if Dnr1 interacts with the apoptotic machinery in the whole organism, I determined the impact of Dnr1 overexpression on Hid induced apoptosis in the *Drosophila* eye. Overexpression of Hid in the developing *Drosophila* eye resulted in massive apoptosis and a reduced adult eye (Figure 3.10 C&D). Expression of one copy of a Dnr1 transgene partially rescued the adult eye from Hid induced apoptosis (Figure 3.10 E). Expression of two copies of the Dnr1 transgene completely rescued the adult eye from Hid induced apoptosis (Figure 3.10 F). These data indicate that Dnr1 negative regulation of the *Drosophila* apoptotic apparatus is conserved *in vivo* and is similar to the findings that Hid induced apoptosis is suppressed by the overexpression of DIAP1 in the developing *Drosophila* eye[158]. However, my *in vivo* studies fail to address the mechanism by which Dnr1 inhibits Hid induced apoptosis. Although, the S2 cell culture data suggest that Dnr1 overexpression in the developing eye would deplete Dronc

levels, thus inhibiting Hid induced apoptosis, it remains possible other mechanism may be active. For example, Dnr1 may directly target Hid either through a direct physical interaction or depletion of Hid levels thereby inhibiting apoptosis.

In summary, I have provided evidence both in S2 cell culture and *in vivo* that Dnr1 negatively regulates the *Drosophila* apoptotic cascade. Specifically, Dnr1 regulates the initiator caspase Dronc in a RING domain-dependent manner, which consequently affects downstream caspase activity and apoptosis (Figure 4.1).
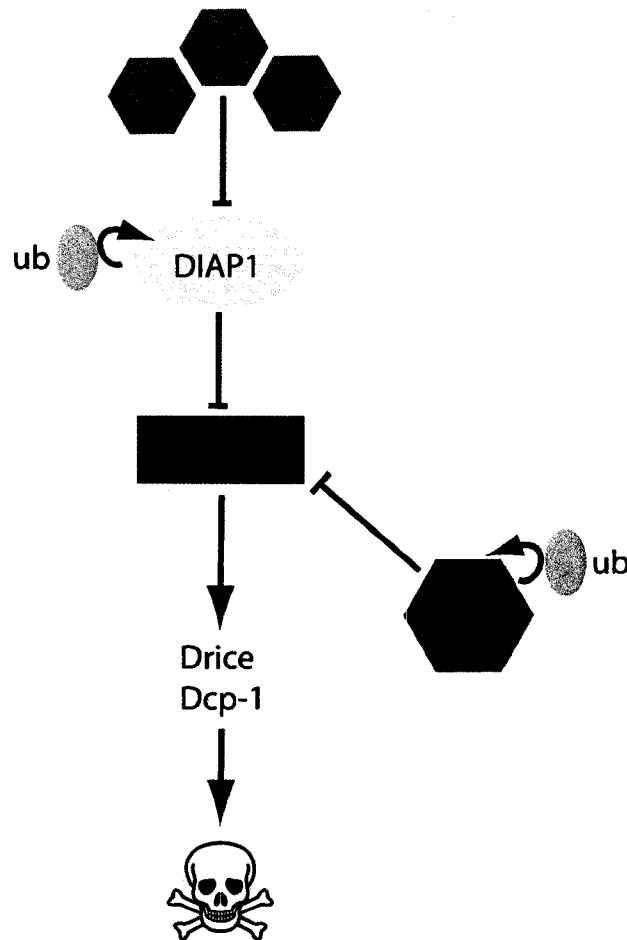

Figure 4.1 Schematic representation of Dnr1 regulation of the *Drosophila* apoptotic pathway. I propose that Dnr1 inhibits the *Drosophila* apoptotic cascade at the level of the initiator caspase Dronc.

76

4.3 Functional Analysis of Dnr1 Regulation of Dnr1, Dredd and Dronc Protein levels.

Dnr1 regulates both the Imd signaling pathway and the apoptotic signaling cascade at the level of the initiator caspases Dredd and Dronc, respectively. I have shown that Dnr1 regulates both its own stability and the activity of Dredd and Dronc in a RING domain-dependent manner. To address the mechanisms behind Dnr1 auto-regulation and the regulation of Dredd and Dronc, I examined the contributions of the various domains of Dnr1, Dredd and Dronc to this process.

Although I have demonstrated that Dnr1 regulates the levels of the initiator caspases Dredd and Dronc in S2 cells, additional work in our lab showed that Dnr1 had no effect on the protein levels of the effector caspase Drice. Thus, I reasoned that Dnr1 is a specific inhibitor of *Drosophila* initiator caspases. As initiator caspases have large N-terminal prodomains which contain protein interaction domains, such as CARD in Dronc and DID in Dredd, that are absent from the prodomains of effector caspases, I hypothesized that Dnr1 recognizes a feature of the prodomain to regulate Dredd and Dronc protein levels. I tested whether Dnr1 could mediate the depletion of variants of Dredd and Dronc that lacked a prodomain. Surprisingly, I showed that Dnr1-mediated the depletion of both the Dredd and Dronc variants that lacked a prodomain (Figure 3.11). This result is further supported by the observation that the Pr2 isoform of Dronc, which lacks a prodomain, is more stable in Dnr1-depleted S2 cells. Thus, I conclude that Dnr1 recognizes a feature within the large or small catalytic subunits to mediated Dredd and Dronc depletion.

To determine the domains of Dnr1 required for its own stability, I examined the stability of a series of Dnr1 deletion constructs in S2 cell culture. Consistent with my other observations, the RING domain has a large impact on the stability of Dnr1. Deletions of Dnr1 that eliminated the RING domain resulted in considerable stabilization of the protein (Figure 3.12). This observation is similar to previous reports that demonstrated DIAP1 regulates its own stability through auto-ubiquitination in a RING domain-dependent manner[159, 160]. However, in addition to the RING domain, N-terminal regions of Dnr1 contribute to the stability of Dnr1 in S2 cells. Deletion of the N-terminal FERM domain and the adjacent glutamine/serine rich region greatly stabilize Dnr1, despite the presence of an intact C-terminal RING domain. This observation suggests that the RING domain of Dnr1 targets the N-terminal region of Dnr1 to mediate self-destruction.

In addition to Dnr1 auto-regulation, the RING domain is essential for Dnr1 mediated depletion of Dredd and Dronc. To determine if additional domains of Dnr1 are involved in initiator caspase depletion, I examined the ability of the various Dnr1 deletion constructs to deplete Dronc protein levels in S2 cell culture. As expected, the Dnr1 constructs that lack the RING domain failed to mediate the depletion of Dronc in S2 cells (Figure 3.13). This observation is similar to reports that demonstrate DIAP1 regulates Dronc through ubiquitination, marking Dronc for proteasomal degradation[143]. Interestingly, in addition to the RING domain, the subcellular localization of Dnr1 contributes to the ability of Dnr1 to mediate Dronc depletion. Dnr1 deletion constructs that localizes to the nucleus, failed to impact on Dronc protein levels despite the presence of an intact C-terminal RING domain. This result is supported by the observation that

Dronc localizes to the cytoplasmic fraction of cells[89]. Thus, nuclear Dnr1 would not have access to Dronc and would fail to deplete Dronc protein levels.

While I have demonstrated that the RING domain is essential for Dnr1 to regulate its own stability and the stability of Dredd and Dronc, I wanted to determine if the RING domain functioned as an E3 ubiquitin ligase similar to the RING domain of DIAP1. To this end, I tested the ability of Dnr1 to auto-ubiquitinate *in vitro*. Consistent with the Dnr1 RING domain functioning as an E3 ubiquitin ligase, I detected Dnr1 auto-ubiquitination (Figure 3.14). Auto-ubiquitination depended on a functional RING domain, as a Dnr1 variant with a point mutation in a cysteine residue critical for RING domain activity failed to auto-ubiquitinate. Thus, Dnr1 appears to regulate its own stability through auto-ubiquitination, targeting it for proteasomal degradation similar to the RING domain containing IAP family members – although there remains the possibility that other E3 ubiquitin ligases participate in Dnr1 ubiquitination or the possibility the pro-apoptotic molecules Hid, Rpr and Grim can bind to and suppress Dnr1 activity.

In summary, both the RING domain and N-terminal motifs of Dnr1 are required to regulate the stability of Dnr1 and the depletion of Dredd and Dronc. Interestingly, it appears that the N-terminal motifs serve different purposes in Dnr1 auto-regulation and Dredd and Dronc regulation. In the case of Dnr1 auto-regulation, the N-terminal motifs are required for the depletion of Dnr1, however the localization of Dnr1 is not important as a nuclear Dnr1 variant, Dnr1$^{142-677}$, is depleted in S2 cells (Figure 3.12) In the case of Dronc regulation, the N-terminal motifs of Dnr1 are required for cytoplasmic localization of Dnr1. The cytoplasmic localization of Dnr1 is probably critical for Dronc depletion,

because Dronc localizes to the cytoplasm[89]. Nuclear Dnr1 would therefore not have access to Dronc and hence would not be able to mediate Dronc depletion.

4.4 Summary

I have demonstrated that Dnr1 contributes to regulation of both the Imd signaling pathway and the apoptotic cascade *in Drosophila*. Dnr1 appears to regulate the activity of Dredd and Dronc, respectively, in these two pathways by mediating their destruction in a RING domain dependent manner. This study is the first to describe the mechanism behind Dnr1 regulation of Dredd in the Imd pathway. Additionally, this is the first study to ascribe a role to Dnr1 in the regulation of the apoptotic pathway, both in an S2 cell culture and *in vivo* setting. Thus, I conclude that Dnr1 is an inhibitor of the *Drosophila* initiator caspases, Dredd and Dronc.

4.5 Future Experiments

While I have started to uncover the mechanisms behind Dnr1-dependent regulation of the *Drosophila* initiator caspases Dredd and Dronc, a number of issues remain to be addressed. Dnr1 appears to regulate Dredd and Dronc activity in S2 cell culture through depletion of their protein levels and although it seems likely this mechanism will be conserved *in vivo,* this issue still remains to be explored. Additionally, the exact mechanism involved in Dnr1 mediated-depletion of Dredd and Dronc remains an open question. I have shown that Dnr1 auto-ubiquitinates in a RING domain-dependent manner and it would seem likely that Dnr1 ubiquitinates Dredd and Dronc to

mark them for proteasomal degradation. An *in vitro* ubiquitination assay may help to answer this question and give us further insight into Dnr1 regulation of Dredd and Dronc. Furthermore, while I have shown that Dnr1 over-expression in the developing eye can inhibit Hid induced apoptosis, additional studies could determine if Dnr1 can inhibit apoptosis induced by Rpr and Grim. These studies will give us further information into the role of Dnr1 in apoptotic regulation *in vivo*. Additionally, as Hid, Rpr and Grim bind to DIAP1 to induce apoptosis; it would be interesting to determine if Hid, Rpr, and Grim bind to Dnr1 in a similar fashion. This result may give us insight into the mechanism used to relieve Dnr1 repression of Dronc inhibition in *Drosophila*.

Furthermore, I have identified some of the domains of Dnr1, Dredd and Dronc involved in Dnr1 regulation of Dredd and Dronc. However, an issue that still remains open is the domains and/or motifs that allow Dnr1 and Dredd to complex and if Dnr1 binds Dronc directly. A series of immunoprecipitation assays with the available Dnr1 deletion constructs may help to narrow in on the region involved in Dnr1/Dredd complex formation and allow us to identify the motifs involved in this complex formation. Additionally, immunoprecipitation assays with catalytically inactive Dronc constructs may allow us to determine if Dnr1 forms a complex with Dronc. Lastly, Dnr1 appears to regulate Dredd and Dronc levels by targeting a region in the large or small catalytic subunit of Dredd and Dronc. An immunopreciptation assay could determine if Dnr1 forms a complex with variants of Dredd and Dronc that lack a prodomain and provide insight into Dnr1 regulation of Dredd and Dronc.

I have demonstrated that Dnr1 regulates Imd signaling and apoptosis. Dnr1 impinges on these two pathways at the level of the initiator caspase and mediates their

destruction, which appears to require the activity of the Dnr1 E3 ubiquitin ligase RING domain. Based on these observations, I hypothesize that Dnr1 is part of a larger macromolecular complex required for the regulation of Dronc-dependent apoptotic signaling. To identify additional components that make up the macromolecular complex, I proposed to perform a genome wide RNAi screen in S2 cells that overexpress Dnr1. Our lab possesses a *Drosophila* whole genome dsRNA library and we have protocols for the systematic depletion of each individual *Drosophila* gene.

To perform the screen, I will deplete each *Drosophila* gene in S2 cells that overexpress Dnr1. I will then induce apoptosis with actinomycin D and monitor apoptotic progression with the anti-active caspase-3 antibody. I will induce apoptosis with actinomycin D in S2 cells that overexpress Dnr1 incubated with GFP dsRNA to serve as a control level for the active caspase-3 signal. I predict that the depletion of genes required for Dnr1-mediated inhibition of apoptosis will results in an increased active caspase-3 signal compared to control cells. Conversely, I predict the depletion of negative regulators of Dnr1-mediated apoptotic inhibition will result in a decreased active caspase-3 signal compared to control cells. The completion of the full genome RNAi screen will allow me to identify both positive and negative regulators of Dnr1 activity and provide valuable insight into the Dnr1-dependent regulation of apoptosis in *Drosophila*.

To validate the use of the anti-active caspase-3 antibody to monitor apoptosis, I performed a preliminary trial screen in S2 cells with Dcp-1, DIAP1, and Dronc dsRNA, all known components of the apoptotic cascade. I incubated S2 cells with Dcp-1, DIAP1 or Dronc dsRNA to deplete the respective transcripts. Seventy-two hours later, I treated

the cells with actinomycin D for four hours and monitored apoptosis with the anti-active caspase-3 antibody. As expected, loss of DIAP1 resulted in mass apoptosis even prior to actinomycin D treatment and loss of Dronc inhibited the induction of apoptosis by actinomycin D. Furthermore, depletion of Dcp-1 had no impact on the active-caspase-3 signal, which is consistent with the observation that Drice and Dcp-1 are highly similar and may have functional redundancies (Figure 4.2).

Finally, our lab has done preliminary studies on the human Dnr1 homolog, Myosin Regulatory Light Chain Interacting protein (MIR). MIR appears to function as a negative regulator of caspase-dependent apoptosis in human HeLa cells. Additionally, overexpression of MIR in *Drosophila* S2 cells results in a similar phenotype to that of Dnr1 overexpression (A. Schindler, unpublished). The work on Dnr1 in *Drosophila* can act as a springboard to the studies of MIR, which will provide valuable new information into the regulation of critical signaling pathways in humans.
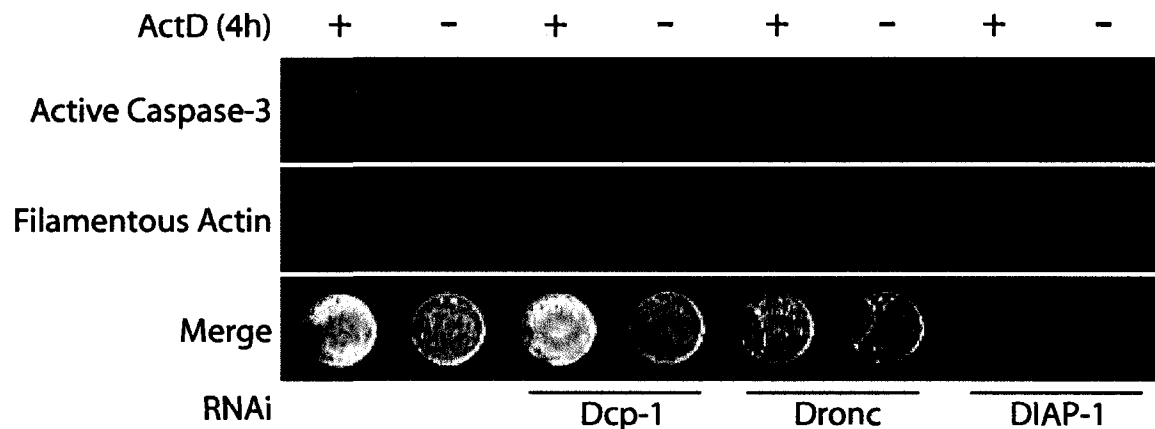
Figure 4.2 Trial screen for genes involved in actinomycin D induced apoptosis. In Cell Western analysis of control S2 cells (Columns 1&2), S2 cells incubated with Dcp-1 dsRNA (Columns 3&4), S2 cells incubated with Dronc dsRNA (Columns 5&6), S2 cells incubated with DIAP1 dsRNA (Columns 7&8). Cells were incubated with actinomycin D for 4 hours where indicated. Cells were fixed, permeabilized and probed with an anti-active-caspase-3 antibody (top panel) and stained with Alexa-Fluor-680-phallodin (to visualize actin) (middle panel). The top and middle panels are false colored and merged in the bottom panel with Anti-Active-Caspase-3 in green and Alexa-Fluor-680-phallodin in red. An anti-active-caspase-3 signal was detected after actinomycin D in control S2 cells and S2 cells treated with Dcp-1 dsRNA, whereas the signal is abrogated in S2 cells treated with Dronc dsRNA after actinomycin D exposure. Cells treated with DIAP1 dsRNA underwent rampant apoptosis prior to actinomycin D treatment.

5 Bibliography

1. Beutler, B. Innate immunity: an overview. *Mol Immunol* **40**, 845-859 (2004).
2. Kimbrell, D.A. & Beutler, B. The evolution and genetics of innate immunity. *Nat Rev Genet* **2**, 256-267 (2001).
3. Medzhitov, R. & Janeway, C., Jr. Innate immunity. *N Engl J Med* **343**, 338-344 (2000).
4. Hoffmann, J.A. & Reichhart, J.M. Drosophila innate immunity: an evolutionary perspective. *Nat Immunol* **3**, 121-126 (2002).
5. Schnare, M., Barton, G.M., Holt, A.C., Takeda, K., Akira, S. & Medzhitov, R. Toll-like receptors control activation of adaptive immune responses. *Nat Immunol* **2**, 947-950 (2001).
6. Fearon, D.T. & Locksley, R.M. The instructive role of innate immunity in the acquired immune response. *Science* **272**, 50-53 (1996).
7. Medzhitov, R. & Janeway, C.A., Jr. Decoding the patterns of self and nonself by the innate immune system. *Science* **296**, 298-300 (2002).
8. Kurata, S., Ariki, S. & Kawabata, S. Recognition of pathogens and activation of immune responses in Drosophila and horseshoe crab innate immunity. *Immunobiology* **211**, 237-249 (2006).
9. Hoffmann, J.A. The immune response of Drosophila. *Nature* **426**, 33-38 (2003).
10. Hoffmann, J.A., Kafatos, F.C., Janeway, C.A. & Ezekowitz, R.A. Phylogenetic perspectives in innate immunity. *Science* **284**, 1313-1318 (1999).
11. Bulet, P., Hetru, C., Dimarcq, J.L. & Hoffmann, D. Antimicrobial peptides in insects; structure and function. *Dev Comp Immunol* **23**, 329-344 (1999).
12. Gutierrez, E., Wiggins, D., Fielding, B. & Gould, A.P. Specialized hepatocyte-like cells regulate Drosophila lipid metabolism. *Nature* **445**, 275-280 (2007).
13. Colombani, J., Raisin, S., Pantalacci, S., Radimerski, T., Montagne, J. & Leopold, P. A nutrient sensor mechanism controls Drosophila growth. *Cell* **114**, 739-749 (2003).
14. Grewal, S.S. & Saucedo, L.J. Chewing the fat; regulating autophagy in Drosophila. *Dev Cell* **7**, 148-150 (2004).
15. Sondergaard, L. Homology between the mammalian liver and the Drosophila fat body. *Trends Genet* **9**, 193 (1993).
16. De Gregorio, E., Spellman, P.T., Tzou, P., Rubin, G.M. & Lemaitre, B. The Toll and Imd pathways are the major regulators of the immune response in Drosophila. *Embo J* **21**, 2568-2579 (2002).
17. Michel, T., Reichhart, J.M., Hoffmann, J.A. & Royet, J. Drosophila Toll is activated by Gram-positive bacteria through a circulating peptidoglycan recognition protein. *Nature* **414**, 756-759 (2001).
18. Anderson, K.V., Jurgens, G. & Nusslein-Volhard, C. Establishment of dorsal-ventral polarity in the Drosophila embryo: genetic studies on the role of the Toll gene product. *Cell* **42**, 779-789 (1985).
19. Ip, Y.T., Reach, M., Engstrom, Y., Kadalayil, L., Cai, H., Gonzalez-Crespo, S., Tatei, K. & Levine, M. Dif, a dorsal-related gene that mediates an immune response in Drosophila. *Cell* **75**, 753-763 (1993).

20. Lemaitre, B., Nicolas, E., Michaut, L., Reichhart, J.M. & Hoffmann, J.A. The dorsoventral regulatory gene cassette spatzle/Toll/cactus controls the potent antifungal response in Drosophila adults. *Cell* **86**, 973-983 (1996).

21. Lemaitre, B., Meister, M., Govind, S., Georgel, P., Steward, R., Reichhart, J.M. & Hoffmann, J.A. Functional analysis and regulation of nuclear import of dorsal during the immune response in Drosophila. *Embo J* **14**, 536-545 (1995).

22. Medzhitov, R., Preston-Hurlburt, P. & Janeway, C.A., Jr. A human homologue of the Drosophila Toll protein signals activation of adaptive immunity. *Nature* **388**, 394-397 (1997).

23. Rock, F.L., Hardiman, G., Timans, J.C., Kastelein, R.A. & Bazan, J.F. A family of human receptors structurally related to Drosophila Toll. *Proc Natl Acad Sci U S A* **95**, 588-593 (1998).

24. Aderem, A. & Ulevitch, R.J. Toll-like receptors in the induction of the innate immune response. *Nature* **406**, 782-787 (2000).

25. Weber, A.N., Tauszig-Delamasure, S., Hoffmann, J.A., Lelievre, E., Gascan, H., Ray, K.P., Morse, M.A., Imler, J.L. & Gay, N.J. Binding of the Drosophila cytokine Spatzle to Toll is direct and establishes signaling. *Nat Immunol* **4**, 794-800 (2003).

26. Gobert, V., Gottar, M., Matskevich, A.A., Rutschmann, S., Royet, J., Belvin, M., Hoffmann, J.A. & Ferrandon, D. Dual activation of the Drosophila toll pathway by two pattern recognition receptors. *Science* **302**, 2126-2130 (2003).

27. Lemaitre, B., Kromer-Metzger, E., Michaut, L., Nicolas, E., Meister, M., Georgel, P., Reichhart, J.M. & Hoffmann, J.A. A recessive mutation, immune deficiency (imd), defines two distinct control pathways in the Drosophila host defense. *Proc Natl Acad Sci U S A* **92**, 9465-9469 (1995).

28. Varfolomeev, E.E. & Ashkenazi, A. Tumor necrosis factor: an apoptosis JuNKie? *Cell* **116**, 491-497 (2004).

29. Baldwin, A.S., Jr. The NF-kappa B and I kappa B proteins: new discoveries and insights. *Annu Rev Immunol* **14**, 649-683 (1996).

30. Beg, A.A., Finco, T.S., Nantermet, P.V. & Baldwin, A.S., Jr. Tumor necrosis factor and interleukin-1 lead to phosphorylation and loss of I kappa B alpha: a mechanism for NF-kappa B activation. *Mol Cell Biol* **13**, 3301-3310 (1993).

31. Finco, T.S., Beg, A.A. & Baldwin, A.S., Jr. Inducible phosphorylation of I kappa B alpha is not sufficient for its dissociation from NF-kappa B and is inhibited by protease inhibitors. *Proc Natl Acad Sci U S A* **91**, 11884-11888 (1994).

32. Chung, J.Y., Park, Y.C., Ye, H. & Wu, H. All TRAFs are not created equal: common and distinct molecular mechanisms of TRAF-mediated signal transduction. *J Cell Sci* **115**, 679-688 (2002).

33. Vanden Berghe, T., van Loo, G., Saelens, X., Van Gurp, M., Brouckaert, G., Kalai, M., Declercq, W. & Vandenabeele, P. Differential signaling to apoptotic and necrotic cell death by Fas-associated death domain protein FADD. *J Biol Chem* **279**, 7925-7933 (2004).

34. Baker, S.J. & Reddy, E.P. Transducers of life and death: TNF receptor superfamily and associated proteins. *Oncogene* **12**, 1-9 (1996).

35. Thakar, J., Schleinkofer, K., Borner, C. & Dandekar, T. RIP death domain structural interactions implicated in TNF-mediated proliferation and survival. *Proteins* **63**, 413-423 (2006).

36. Liu, J. & Lin, A. Role of JNK activation in apoptosis: a double-edged sword. *Cell Res* **15**, 36-42 (2005).

37. Micheau, O. & Tschopp, J. Induction of TNF receptor I-mediated apoptosis via two sequential signaling complexes. *Cell* **114**, 181-190 (2003).

38. Baud, V. & Karin, M. Signal transduction by tumor necrosis factor and its relatives. *Trends Cell Biol* **11**, 372-377 (2001).

39. Wajant, H., Pfizenmaier, K. & Scheurich, P. Tumor necrosis factor signaling. *Cell Death Differ* **10**, 45-65 (2003).

40. Thorburn, A. Death receptor-induced cell killing. *Cell Signal* **16**, 139-144 (2004).

41. Leulier, F., Parquet, C., Pili-Floury, S., Ryu, J.H., Caroff, M., Lee, W.J., Mengin-Lecreulx, D. & Lemaitre, B. The Drosophila immune system detects bacteria through specific peptidoglycan recognition. *Nat Immunol* **4**, 478-484 (2003).

42. Choe, K.M., Werner, T., Stoven, S., Hultmark, D. & Anderson, K.V. Requirement for a peptidoglycan recognition protein (PGRP) in Relish activation and antibacterial immune responses in Drosophila. *Science* **296**, 359-362 (2002).

43. Gottar, M., Gobert, V., Michel, T., Belvin, M., Duyk, G., Hoffmann, J.A., Ferrandon, D. & Royet, J. The Drosophila immune response against Gram-negative bacteria is mediated by a peptidoglycan recognition protein. *Nature* **416**, 640-644 (2002).

44. Kaneko, T., Goldman, W.E., Mellroth, P., Steiner, H., Fukase, K., Kusumoto, S., Harley, W., Fox, A., Golenbock, D. & Silverman, N. Monomeric and polymeric gram-negative peptidoglycan but not purified LPS stimulate the Drosophila IMD pathway. *Immunity* **20**, 637-649 (2004).

45. Ramet, M., Manfruelli, P., Pearson, A., Mathey-Prevot, B. & Ezekowitz, R.A. Functional genomic analysis of phagocytosis and identification of a Drosophila receptor for E. coli. *Nature* **416**, 644-648 (2002).

46. Mellroth, P., Karlsson, J., Hakansson, J., Schultz, N., Goldman, W.E. & Steiner, H. Ligand-induced dimerization of Drosophila peptidoglycan recognition proteins in vitro. *Proc Natl Acad Sci U S A* **102**, 6455-6460 (2005).

47. Lim, J.H., Kim, M.S., Kim, H.E., Yano, T., Oshima, Y., Aggarwal, K., Goldman, W.E., Silverman, N., Kurata, S. & Oh, B.H. Structural basis for preferential recognition of diaminopimelic acid-type peptidoglycan by a subset of peptidoglycan recognition proteins. *J Biol Chem* **281**, 8286-8295 (2006).

48. Kaneko, T. & Silverman, N. Bacterial recognition and signalling by the Drosophila IMD pathway. *Cell Microbiol* **7**, 461-469 (2005).

49. Takehana, A., Katsuyama, T., Yano, T., Oshima, Y., Takada, H., Aigaki, T. & Kurata, S. Overexpression of a pattern-recognition receptor, peptidoglycan-recognition protein-LE, activates imd/relish-mediated antibacterial defense and the prophenoloxidase cascade in Drosophila larvae. *Proc Natl Acad Sci U S A* **99**, 13705-13710 (2002).

50. Werner, T., Liu, G., Kang, D., Ekengren, S., Steiner, H. & Hultmark, D. A family of peptidoglycan recognition proteins in the fruit fly Drosophila melanogaster. *Proc Natl Acad Sci U S A* **97**, 13772-13777 (2000).

51.   Kaneko, T., Yano, T., Aggarwal, K., Lim, J.H., Ueda, K., Oshima, Y., Peach, C., Erturk-Hasdemir, D., Goldman, W.E., Oh, B.H., Kurata, S. & Silverman, N. PGRP-LC and PGRP-LE have essential yet distinct functions in the drosophila immune response to monomeric DAP-type peptidoglycan. *Nat Immunol* **7**, 715-723 (2006).

52.   Takehana, A., Yano, T., Mita, S., Kotani, A., Oshima, Y. & Kurata, S. Peptidoglycan recognition protein (PGRP)-LE and PGRP-LC act synergistically in Drosophila immunity. *Embo J* **23**, 4690-4700 (2004).

53.   Choe, K.M., Lee, H. & Anderson, K.V. Drosophila peptidoglycan recognition protein LC (PGRP-LC) acts as a signal-transducing innate immune receptor. *Proc Natl Acad Sci U S A* **102**, 1122-1126 (2005).

54.   Georgel, P., Naitza, S., Kappler, C., Ferrandon, D., Zachary, D., Swimmer, C., Kopczynski, C., Duyk, G., Reichhart, J.M. & Hoffmann, J.A. Drosophila immune deficiency (IMD) is a death domain protein that activates antibacterial defense and can promote apoptosis. *Dev Cell* **1**, 503-514 (2001).

55.   Leulier, F., Vidal, S., Saigo, K., Ueda, R. & Lemaitre, B. Inducible expression of double-stranded RNA reveals a role for dFADD in the regulation of the antibacterial response in Drosophila adults. *Curr Biol* **12**, 996-1000 (2002).

56.   Hu, S. & Yang, X. dFADD, a novel death domain-containing adapter protein for the Drosophila caspase DREDD. *J Biol Chem* **275**, 30761-30764 (2000).

57.   Naitza, S., Rosse, C., Kappler, C., Georgel, P., Belvin, M., Gubb, D., Camonis, J., Hoffmann, J.A. & Reichhart, J.M. The Drosophila immune defense against gram-negative infection requires the death protein dFADD. *Immunity* **17**, 575-581 (2002).

58.   Leulier, F., Rodriguez, A., Khush, R.S., Abrams, J.M. & Lemaitre, B. The Drosophila caspase Dredd is required to resist gram-negative bacterial infection. *EMBO Rep* **1**, 353-358 (2000).

59.   Vidal, S., Khush, R.S., Leulier, F., Tzou, P., Nakamura, M. & Lemaitre, B. Mutations in the Drosophila dTAK1 gene reveal a conserved function for MAPKKKs in the control of rel/NF-kappaB-dependent innate immune responses. *Genes Dev* **15**, 1900-1912 (2001).

60.   Giot, L., Bader, J.S., Brouwer, C., Chaudhuri, A., Kuang, B., Li, Y., Hao, Y.L., Ooi, C.E., Godwin, B., Vitols, E., Vijayadamodar, G., Pochart, P., Machineni, H., Welsh, M., Kong, Y., Zerhusen, B., Malcolm, R., Varrone, Z., Collis, A., Minto, M., Burgess, S., McDaniel, L., Stimpson, E., Spriggs, F., Williams, J., Neurath, K., Ioime, N., Agee, M., Voss, E., Furtak, K., Renzulli, R., Aanensen, N., Carrolla, S., Bickelhaupt, E., Lazovatsky, Y., DaSilva, A., Zhong, J., Stanyon, C.A., Finley, R.L., Jr., White, K.P., Braverman, M., Jarvie, T., Gold, S., Leach, M., Knight, J., Shimkets, R.A., McKenna, M.P., Chant, J. & Rothberg, J.M. A protein interaction map of Drosophila melanogaster. *Science* **302**, 1727-1736 (2003).

61.   Kleino, A., Valanne, S., Ulvila, J., Kallio, J., Myllymaki, H., Enwald, H., Stoven, S., Poidevin, M., Ueda, R., Hultmark, D., Lemaitre, B. & Ramet, M. Inhibitor of apoptosis 2 and TAK1-binding protein are components of the Drosophila Imd pathway. *Embo J* **24**, 3423-3434 (2005).

62.	Zhuang, Z.H., Sun, L., Kong, L., Hu, J.H., Yu, M.C., Reinach, P., Zang, J.W. & Ge, B.X. Drosophila TAB2 is required for the immune activation of JNK and NF-kappaB. *Cell Signal* **18**, 964-970 (2006).

63.	Gesellchen, V., Kuttenkeuler, D., Steckel, M., Pelte, N. & Boutros, M. An RNA interference screen identifies Inhibitor of Apoptosis Protein 2 as a regulator of innate immune signalling in Drosophila. *EMBO Rep* **6**, 979-984 (2005).

64.	Valanne, S., Kleino, A., Myllymaki, H., Vuoristo, J. & Ramet, M. Iap2 is required for a sustained response in the Drosophila Imd pathway. *Dev Comp Immunol* **31**, 991-1001 (2007).

65.	Boutros, M., Agaisse, H. & Perrimon, N. Sequential activation of signaling pathways during innate immune responses in Drosophila. *Dev Cell* **3**, 711-722 (2002).

66.	Silverman, N., Zhou, R., Erlich, R.L., Hunter, M., Bernstein, E., Schneider, D. & Maniatis, T. Immune activation of NF-kappaB and JNK requires Drosophila TAK1. *J Biol Chem* **278**, 48928-48934 (2003).

67.	Chen, W., White, M.A. & Cobb, M.H. Stimulus-specific requirements for MAP3 kinases in activating the JNK pathway. *J Biol Chem* **277**, 49105-49110 (2002).

68.	Park, J.M., Brady, H., Ruocco, M.G., Sun, H., Williams, D., Lee, S.J., Kato, T., Jr., Richards, N., Chan, K., Mercurio, F., Karin, M. & Wasserman, S.A. Targeting of TAK1 by the NF-kappa B protein Relish regulates the JNK-mediated immune response in Drosophila. *Genes Dev* **18**, 584-594 (2004).

69.	Kockel, L., Homsy, J.G. & Bohmann, D. Drosophila AP-1: lessons from an invertebrate. *Oncogene* **20**, 2347-2364 (2001).

70.	Ramet, M., Lanot, R., Zachary, D. & Manfruelli, P. JNK signaling pathway is required for efficient wound healing in Drosophila. *Dev Biol* **241**, 145-156 (2002).

71.	Sluss, H.K., Han, Z., Barrett, T., Goberdhan, D.C., Wilson, C., Davis, R.J. & Ip, Y.T. A JNK signal transduction pathway that mediates morphogenesis and an immune response in Drosophila. *Genes Dev* **10**, 2745-2758 (1996).

72.	Lu, Y., Wu, L.P. & Anderson, K.V. The antibacterial arm of the drosophila innate immune response requires an IkappaB kinase. *Genes Dev* **15**, 104-110 (2001).

73.	Rutschmann, S., Jung, A.C., Zhou, R., Silverman, N., Hoffmann, J.A. & Ferrandon, D. Role of Drosophila IKK gamma in a toll-independent antibacterial immune response. *Nat Immunol* **1**, 342-347 (2000).

74.	Silverman, N., Zhou, R., Stoven, S., Pandey, N., Hultmark, D. & Maniatis, T. A Drosophila IkappaB kinase complex required for Relish cleavage and antibacterial immunity. *Genes Dev* **14**, 2461-2471 (2000).

75.	Stoven, S., Silverman, N., Junell, A., Hedengren-Olcott, M., Erturk, D., Engstrom, Y., Maniatis, T. & Hultmark, D. Caspase-mediated processing of the Drosophila NF-kappaB factor Relish. *Proc Natl Acad Sci U S A* **100**, 5991-5996 (2003).

76.	Dushay, M.S., Asling, B. & Hultmark, D. Origins of immunity: Relish, a compound Rel-like gene in the antibacterial defense of Drosophila. *Proc Natl Acad Sci U S A* **93**, 10343-10347 (1996).

77.	Stoven, S., Ando, I., Kadalayil, L., Engstrom, Y. & Hultmark, D. Activation of the Drosophila NF-kappaB factor Relish by rapid endoproteolytic cleavage. *EMBO Rep* **1**, 347-352 (2000).

78. Zhou, R., Silverman, N., Hong, M., Liao, D.S., Chung, Y., Chen, Z.J. & Maniatis, T. The role of ubiquitination in Drosophila innate immunity. *J Biol Chem* **280**, 34048-34055 (2005).

79. Chun, H.J., Zheng, L., Ahmad, M., Wang, J., Speirs, C.K., Siegel, R.M., Dale, J.K., Puck, J., Davis, J., Hall, C.G., Skoda-Smith, S., Atkinson, T.P., Straus, S.E. & Lenardo, M.J. Pleiotropic defects in lymphocyte activation caused by caspase-8 mutations lead to human immunodeficiency. *Nature* **419**, 395-399 (2002).

80. Salmena, L., Lemmers, B., Hakem, A., Matysiak-Zablocki, E., Murakami, K., Au, P.Y., Berry, D.M., Tamblyn, L., Shehabeldin, A., Migon, E., Wakeham, A., Bouchard, D., Yeh, W.C., McGlade, J.C., Ohashi, P.S. & Hakem, R. Essential role for caspase 8 in T-cell homeostasis and T-cell-mediated immunity. *Genes Dev* **17**, 883-895 (2003).

81. Margolin, N., Raybuck, S.A., Wilson, K.P., Chen, W., Fox, T., Gu, Y. & Livingston, D.J. Substrate and inhibitor specificity of interleukin-1 beta-converting enzyme and related caspases. *J Biol Chem* **272**, 7223-7228 (1997).

82. Alnemri, E.S., Livingston, D.J., Nicholson, D.W., Salvesen, G., Thornberry, N.A., Wong, W.W. & Yuan, J. Human ICE/CED-3 protease nomenclature. *Cell* **87**, 171 (1996).

83. Thornberry, N.A., Bull, H.G., Calaycay, J.R., Chapman, K.T., Howard, A.D., Kostura, M.J., Miller, D.K., Molineaux, S.M., Weidner, J.R., Aunins, J. & et al. A novel heterodimeric cysteine protease is required for interleukin-1 beta processing in monocytes. *Nature* **356**, 768-774 (1992).

84. Yuan, J., Shaham, S., Ledoux, S., Ellis, H.M. & Horvitz, H.R. The C. elegans cell death gene ced-3 encodes a protein similar to mammalian interleukin-1 beta-converting enzyme. *Cell* **75**, 641-652 (1993).

85. Degterev, A., Boyce, M. & Yuan, J. A decade of caspases. *Oncogene* **22**, 8543-8567 (2003).

86. Shi, Y. Mechanisms of caspase activation and inhibition during apoptosis. *Mol Cell* **9**, 459-470 (2002).

87. Fuentes-Prior, P. & Salvesen, G.S. The protein structures that shape caspase activity, specificity, activation and inhibition. *Biochem J* **384**, 201-232 (2004).

88. Fischer, U., Janicke, R.U. & Schulze-Osthoff, K. Many cuts to ruin: a comprehensive update of caspase substrates. *Cell Death Differ* **10**, 76-100 (2003).

89. Dorstyn, L., Colussi, P.A., Quinn, L.M., Richardson, H. & Kumar, S. DRONC, an ecdysone-inducible Drosophila caspase. *Proc Natl Acad Sci U S A* **96**, 4307-4312 (1999).

90. Doumanis, J., Quinn, L., Richardson, H. & Kumar, S. STRICA, a novel Drosophila melanogaster caspase with an unusual serine/threonine-rich prodomain, interacts with DIAP1 and DIAP2. *Cell Death Differ* **8**, 387-394 (2001).

91. Chen, P., Rodriguez, A., Erskine, R., Thach, T. & Abrams, J.M. Dredd, a novel effector of the apoptosis activators reaper, grim, and hid in Drosophila. *Dev Biol* **201**, 202-216 (1998).

92. Fraser, A.G. & Evan, G.I. Identification of a Drosophila melanogaster ICE/CED-3-related protease, drICE. *Embo J* **16**, 2805-2813 (1997).

93.   Song, Z., McCall, K. & Steller, H. DCP-1, a Drosophila cell death protease essential for development. *Science* **275**, 536-540 (1997).

94.   Dorstyn, L., Read, S.H., Quinn, L.M., Richardson, H. & Kumar, S. DECAY, a novel Drosophila caspase related to mammalian caspase-3 and caspase-7. *J Biol Chem* **274**, 30778-30783 (1999).

95.   Harvey, N.L., Daish, T., Mills, K., Dorstyn, L., Quinn, L.M., Read, S.H., Richardson, H. & Kumar, S. Characterization of the Drosophila caspase, DAMM. *J Biol Chem* **276**, 25342-25350 (2001).

96.   Tibbetts, M.D., Zheng, L. & Lenardo, M.J. The death effector domain protein family: regulators of cellular homeostasis. *Nat Immunol* **4**, 404-409 (2003).

97.   Hay, B.A. & Guo, M. Caspase-dependent cell death in Drosophila. *Annu Rev Cell Dev Biol* **22**, 623-650 (2006).

98.   Hultmark, D. Drosophila immunity: paths and patterns. *Curr Opin Immunol* **15**, 12-19 (2003).

99.   Lamkanfi, M., Declercq, W., Kalai, M., Saelens, X. & Vandenabeele, P. Alice in caspase land. A phylogenetic analysis of caspases from worm to man. *Cell Death Differ* **9**, 358-361 (2002).

100.   Baum, J.S., Arama, E., Steller, H. & McCall, K. The Drosophila caspases Strica and Dronc function redundantly in programmed cell death during oogenesis. *Cell Death Differ* **14**, 1508-1517 (2007).

101.   Leulier, F., Ribeiro, P.S., Palmer, E., Tenev, T., Takahashi, K., Robertson, D., Zachariou, A., Pichaud, F., Ueda, R. & Meier, P. Systematic in vivo RNAi analysis of putative components of the Drosophila cell death machinery. *Cell Death Differ* **13**, 1663-1674 (2006).

102.   Quinn, L.M., Dorstyn, L., Mills, K., Colussi, P.A., Chen, P., Coombe, M., Abrams, J., Kumar, S. & Richardson, H. An essential role for the caspase dronc in developmentally programmed cell death in Drosophila. *J Biol Chem* **275**, 40416-40424 (2000).

103.   Xu, D., Li, Y., Arcaro, M., Lackey, M. & Bergmann, A. The CARD-carrying caspase Dronc is essential for most, but not all, developmental cell death in Drosophila. *Development* **132**, 2125-2134 (2005).

104.   Muro, I., Monser, K. & Clem, R.J. Mechanism of Dronc activation in Drosophila cells. *J Cell Sci* **117**, 5035-5041 (2004).

105.   Yan, N., Huh, J.R., Schirf, V., Demeler, B., Hay, B.A. & Shi, Y. Structure and activation mechanism of the Drosophila initiator caspase Dronc. *J Biol Chem* **281**, 8667-8674 (2006).

106.   Hawkins, C.J., Yoo, S.J., Peterson, E.P., Wang, S.L., Vernooy, S.Y. & Hay, B.A. The Drosophila caspase DRONC cleaves following glutamate or aspartate and is regulated by DIAP1, HID, and GRIM. *J Biol Chem* **275**, 27084-27093 (2000).

107.   Meier, P., Silke, J., Leevers, S.J. & Evan, G.I. The Drosophila caspase DRONC is regulated by DIAP1. *Embo J* **19**, 598-611 (2000).

108.   Kumar, S. & Doumanis, J. The fly caspases. *Cell Death Differ* **7**, 1039-1044 (2000).

109.   Jacobson, M.D., Weil, M. & Raff, M.C. Programmed cell death in animal development. *Cell* **88**, 347-354 (1997).

110. Baehrecke, E.H. How death shapes life during development. *Nat Rev Mol Cell Biol* **3**, 779-787 (2002).
111. Opferman, J.T. & Korsmeyer, S.J. Apoptosis in the development and maintenance of the immune system. *Nat Immunol* **4**, 410-415 (2003).
112. Wang, P., Zhang, J., Bellail, A., Jiang, W., Hugh, J., Kneteman, N.M. & Hao, C. Inhibition of RIP and c-FLIP enhances TRAIL-induced apoptosis in pancreatic cancer cells. *Cell Signal* **19**, 2237-2246 (2007).
113. Blanchard, B.J., Chen, A., Rozeboom, L.M., Stafford, K.A., Weigele, P. & Ingram, V.M. Efficient reversal of Alzheimer's disease fibril formation and elimination of neurotoxicity by a small molecule. *Proc Natl Acad Sci U S A* **101**, 14326-14332 (2004).
114. Zou, H., Henzel, W.J., Liu, X., Lutschg, A. & Wang, X. Apaf-1, a human protein homologous to C. elegans CED-4, participates in cytochrome c-dependent activation of caspase-3. *Cell* **90**, 405-413 (1997).
115. Acehan, D., Jiang, X., Morgan, D.G., Heuser, J.E., Wang, X. & Akey, C.W. Three-dimensional structure of the apoptosome: implications for assembly, procaspase-9 binding, and activation. *Mol Cell* **9**, 423-432 (2002).
116. Boatright, K.M., Renatus, M., Scott, F.L., Sperandio, S., Shin, H., Pedersen, I.M., Ricci, J.E., Edris, W.A., Sutherlin, D.P., Green, D.R. & Salvesen, G.S. A unified model for apical caspase activation. *Mol Cell* **11**, 529-541 (2003).
117. Hill, M.M., Adrain, C. & Martin, S.J. Portrait of a killer: the mitochondrial apoptosome emerges from the shadows. *Mol Interv* **3**, 19-26 (2003).
118. Li, P., Nijhawan, D., Budihardjo, I., Srinivasula, S.M., Ahmad, M., Alnemri, E.S. & Wang, X. Cytochrome c and dATP-dependent formation of Apaf-1/caspase-9 complex initiates an apoptotic protease cascade. *Cell* **91**, 479-489 (1997).
119. Earnshaw, W.C., Martins, L.M. & Kaufmann, S.H. Mammalian caspases: structure, activation, substrates, and functions during apoptosis. *Annu Rev Biochem* **68**, 383-424 (1999).
120. White, K., Grether, M.E., Abrams, J.M., Young, L., Farrell, K. & Steller, H. Genetic control of programmed cell death in Drosophila. *Science* **264**, 677-683 (1994).
121. Hay, B.A., Wassarman, D.A. & Rubin, G.M. Drosophila homologs of baculovirus inhibitor of apoptosis proteins function to block cell death. *Cell* **83**, 1253-1262 (1995).
122. Grether, M.E., Abrams, J.M., Agapite, J., White, K. & Steller, H. The head involution defective gene of Drosophila melanogaster functions in programmed cell death. *Genes Dev* **9**, 1694-1708 (1995).
123. Chen, P., Nordstrom, W., Gish, B. & Abrams, J.M. grim, a novel cell death gene in Drosophila. *Genes Dev* **10**, 1773-1782 (1996).
124. Peterson, C., Carney, G.E., Taylor, B.J. & White, K. reaper is required for neuroblast apoptosis during Drosophila development. *Development* **129**, 1467-1476 (2002).
125. Zachariou, A., Tenev, T., Goyal, L., Agapite, J., Steller, H. & Meier, P. IAP-antagonists exhibit non-redundant modes of action through differential DIAP1 binding. *Embo J* **22**, 6642-6652 (2003).

126. Lee, C.Y. & Baehrecke, E.H. Genetic regulation of programmed cell death in Drosophila. *Cell Res* **10**, 193-204 (2000).

127. Chai, J., Yan, N., Huh, J.R., Wu, J.W., Li, W., Hay, B.A. & Shi, Y. Molecular mechanism of Reaper-Grim-Hid-mediated suppression of DIAP1-dependent Dronc ubiquitination. *Nat Struct Biol* **10**, 892-898 (2003).

128. Zhou, L., Song, Z., Tittel, J. & Steller, H. HAC-1, a Drosophila homolog of APAF-1 and CED-4 functions in developmental and radiation-induced apoptosis. *Mol Cell* **4**, 745-755 (1999).

129. Rodriguez, A., Oliver, H., Zou, H., Chen, P., Wang, X. & Abrams, J.M. Dark is a Drosophila homologue of Apaf-1/CED-4 and functions in an evolutionarily conserved death pathway. *Nat Cell Biol* **1**, 272-279 (1999).

130. Yu, X., Wang, L., Acehan, D., Wang, X. & Akey, C.W. Three-dimensional structure of a double apoptosome formed by the Drosophila Apaf-1 related killer. *J Mol Biol* **355**, 577-589 (2006).

131. Enari, M., Sakahira, H., Yokoyama, H., Okawa, K., Iwamatsu, A. & Nagata, S. A caspase-activated DNase that degrades DNA during apoptosis, and its inhibitor ICAD. *Nature* **391**, 43-50 (1998).

132. Liu, X., Zou, H., Slaughter, C. & Wang, X. DFF, a heterodimeric protein that functions downstream of caspase-3 to trigger DNA fragmentation during apoptosis. *Cell* **89**, 175-184 (1997).

133. Clem, R.J. & Miller, L.K. Control of programmed cell death by the baculovirus genes p35 and iap. *Mol Cell Biol* **14**, 5212-5222 (1994).

134. Uren, A.G., Coulson, E.J. & Vaux, D.L. Conservation of baculovirus inhibitor of apoptosis repeat proteins (BIRPs) in viruses, nematodes, vertebrates and yeasts. *Trends Biochem Sci* **23**, 159-162 (1998).

135. Deveraux, Q.L. & Reed, J.C. IAP family proteins--suppressors of apoptosis. *Genes Dev* **13**, 239-252 (1999).

136. Salvesen, G.S. & Duckett, C.S. IAP proteins: blocking the road to death's door. *Nat Rev Mol Cell Biol* **3**, 401-410 (2002).

137. Vaux, D.L. & Silke, J. IAPs, RINGs and ubiquitylation. *Nat Rev Mol Cell Biol* **6**, 287-297 (2005).

138. Hay, B.A. Understanding IAP function and regulation: a view from Drosophila. *Cell Death Differ* **7**, 1045-1056 (2000).

139. Wang, S.L., Hawkins, C.J., Yoo, S.J., Muller, H.A. & Hay, B.A. The Drosophila caspase inhibitor DIAP1 is essential for cell survival and is negatively regulated by HID. *Cell* **98**, 453-463 (1999).

140. Kaiser, W.J., Vucic, D. & Miller, L.K. The Drosophila inhibitor of apoptosis D-IAP1 suppresses cell death induced by the caspase drICE. *FEBS Lett* **440**, 243-248 (1998).

141. Muro, I., Hay, B.A. & Clem, R.J. The Drosophila DIAP1 protein is required to prevent accumulation of a continuously generated, processed form of the apical caspase DRONC. *J Biol Chem* **277**, 49644-49650 (2002).

142. Rodriguez, A., Chen, P., Oliver, H. & Abrams, J.M. Unrestrained caspase-dependent cell death caused by loss of Diap1 function requires the Drosophila Apaf-1 homolog, Dark. *Embo J* **21**, 2189-2197 (2002).

143. Wilson, R., Goyal, L., Ditzel, M., Zachariou, A., Baker, D.A., Agapite, J., Steller, H. & Meier, P. The DIAP1 RING finger mediates ubiquitination of Dronc and is indispensable for regulating apoptosis. *Nat Cell Biol* **4**, 445-450 (2002).

144. Jones, G., Jones, D., Zhou, L., Steller, H. & Chu, Y. Deterin, a new inhibitor of apoptosis from Drosophila melanogaster. *J Biol Chem* **275**, 22157-22165 (2000).

145. Hauser, H.P., Bardroff, M., Pyrowolakis, G. & Jentsch, S. A giant ubiquitin-conjugating enzyme related to IAP apoptosis inhibitors. *J Cell Biol* **141**, 1415-1422 (1998).

146. Vernooy, S.Y., Chow, V., Su, J., Verbrugghe, K., Yang, J., Cole, S., Olson, M.R. & Hay, B.A. Drosophila Bruce can potently suppress Rpr- and Grim-dependent but not Hid-dependent cell death. *Curr Biol* **12**, 1164-1168 (2002).

147. Leulier, F., Lhocine, N., Lemaitre, B. & Meier, P. The Drosophila inhibitor of apoptosis protein DIAP2 functions in innate immunity and is essential to resist gram-negative bacterial infection. *Mol Cell Biol* **26**, 7821-7831 (2006).

148. Foley, E. & O'Farrell, P.H. Functional dissection of an innate immune response by a genome-wide RNAi screen. *PLoS Biol* **2**, E203 (2004).

149. Chishti, A.H., Kim, A.C., Marfatia, S.M., Lutchman, M., Hanspal, M., Jindal, H., Liu, S.C., Low, P.S., Rouleau, G.A., Mohandas, N., Chasis, J.A., Conboy, J.G., Gascard, P., Takakuwa, Y., Huang, S.C., Benz, E.J., Jr., Bretscher, A., Fehon, R.G., Gusella, J.F., Ramesh, V., Solomon, F., Marchesi, V.T., Tsukita, S., Tsukita, S., Hoover, K.B. & et al. The FERM domain: a unique module involved in the linkage of cytoplasmic proteins to the membrane. *Trends Biochem Sci* **23**, 281-282 (1998).

150. Borden, K.L. & Freemont, P.S. The RING finger domain: a recent example of a sequence-structure family. *Curr Opin Struct Biol* **6**, 395-401 (1996).

151. Pickart, C.M. Mechanisms underlying ubiquitination. *Annu Rev Biochem* **70**, 503-533 (2001).

152. Livak, K.J. & Schmittgen, T.D. Analysis of relative gene expression data using real-time quantitative PCR and the 2(-Delta Delta C(T)) Method. *Methods* **25**, 402-408 (2001).

153. Mimnaugh, E.G., Bonvini, P. & Neckers, L. The measurement of ubiquitin and ubiquitinated proteins. *Electrophoresis* **20**, 418-428 (1999).

154. Lemaitre, B., Reichhart, J.M. & Hoffmann, J.A. Drosophila host defense: differential induction of antimicrobial peptide genes after infection by various classes of microorganisms. *Proc Natl Acad Sci U S A* **94**, 14614-14619 (1997).

155. Zimmermann, K.C., Ricci, J.E., Droin, N.M. & Green, D.R. The role of ARK in stress-induced apoptosis in Drosophila cells. *J Cell Biol* **156**, 1077-1087 (2002).

156. Primrose, D.A., Chaudhry, S., Johnson, A.G., Hrdlicka, A., Schindler, A., Tran, D. & Foley, E. Interactions of DNR1 with the apoptotic machinery of Drosophila melanogaster. *J Cell Sci* **120**, 1189-1199 (2007).

157. Yokokura, T., Dresnek, D., Huseinovic, N., Lisi, S., Abdelwahid, E., Bangs, P. & White, K. Dissection of DIAP1 functional domains via a mutant replacement strategy. *J Biol Chem* **279**, 52603-52612 (2004).

158. Lisi, S., Mazzon, I. & White, K. Diverse domains of THREAD/DIAP1 are required to inhibit apoptosis induced by REAPER and HID in Drosophila. *Genetics* **154**, 669-678 (2000).

159. Holley, C.L., Olson, M.R., Colon-Ramos, D.A. & Kornbluth, S. Reaper eliminates IAP proteins through stimulated IAP degradation and generalized translational inhibition. *Nat Cell Biol* **4**, 439-444 (2002).
160. Yoo, S.J., Huh, J.R., Muro, I., Yu, H., Wang, L., Wang, S.L., Feldman, R.M., Clem, R.J., Muller, H.A. & Hay, B.A. Hid, Rpr and Grim negatively regulate DIAP1 levels through distinct mechanisms. *Nat Cell Biol* **4**, 416-424 (2002).